Neurotechnology for Brain Repair : Imaging, Enhancing and Restoring Human Motor Function

THÈSE N^O 6397 (2014)

PAR

Andrea BIASIUCCI

EPFL

ÉCOLE POLYTECHNIQUE
FÉDÉRALE DE LAUSANNE

Suisse
2014

"E quindi uscimmo a riveder le stelle."
Dante, Inferno, c. XXXIV, v. 139

Acknowledgements

Abstract

Neurotechnology is the application of scientific knowledge to the practical purpose of under-standing, interacting and/or repairing the brain or, in a broader sense, the nervous system. The development of novel approaches to decode functional information from the brain, to enhance specific properties of neural tissue and to restore motor output in real end-users is a fundamental challenge to translate these novel solutions into clinical practice. In this Thesis, I introduce i) a novel imaging method to characterize movement-related electroen-cephalographic (EEG) potentials; ii) a brain stimulation strategy to improve brain-computer interface (BCI) control; iii) and a therapy for motor recovery involving a neuroprosthesis. Overall, results show i) that stable EEG topographies present a subject-independent orga-nization that can be used to robustly decode actual or attempted movements in sub-acute stroke patients and healthy controls, with minimal a-priori information; ii) that transcranial direct-current stimulation (tDCS) enhances the modulability of sensorimotor rhythms used for brain-computer interaction in chronic Spinal Cord Injured (SCI) individuals and healthy controls; iii) that neuromuscular electrical stimulation (NMES) controlled via closed-loop neural activity induces significantly stronger upper limb functional recovery in chronic stroke patients than sham NMES therapy, and that these changes are clinically relevant. These results have or might have important implications in i) disease diagnostics and monitoring through EEG; ii) assistive technology and reduction of permanent disability following SCI; iii) rehabilitation and recovery of upper limb function following a stroke, also after several years of complete paralysis. Briefly, this Thesis provides the conceptual framework, scientific rationale, technical details and clinical evidence supporting translational Neurotechnology that improves, optimizes and disrupts current medical practice in monitoring, substituting and recovering lost upper limb function.

Key words: neuroimaging, EEG topographic analysis, non invasive brain stimulation, transcra-nial direct current stimulation, neuroprosthetics, neuromuscular electrical stimulation, brain computer interfaces

Sommario

La Neurotecnologia è l'applicazione del sapere scientifico allo scopo pratico di capire, interagire e/o riparare il cervello o, in senso più ampio, il sistema nervoso. Lo sviluppo di nuovi approcci atti a decodificare informazioni funzionali dal cervello, ad aumentare specifiche proprietà del tessuto neurale, o a ripristinare l'output motorio in veri utenti finali è una sfida fondamentale per la traslazione di queste nuove soluzioni alla pratica clinica. In questa tesi, introduco i) un nuovo metodo di imaging in grado di caratterizzare potenziali motori dall'elettroencefalogramma (EEG); ii) una strategia di stimolazione cerebrale finalizzata al miglioramento del controllo di una interfaccia cervello-macchina (BCI); iii) ed una terapia finalizzata al recupero motorio basata su una neuroprotesi. Complessivamente, i risultati mostrano i) che topografie EEG stabili presentano un'organizzazione indipendente dal soggetto che può essere utilizzata per decodificare in maniera robusta movimenti reali o tentati in pazienti sub-acuti aventi ictus o in contolli sani, utilizzando minima informazione a-priori; che la stimolazione transcranica in corrente continua (tDCS) aumenta la modulabilità dei ritmi sensorimotori utilizzati per l'interazione cervello-macchina in pazienti con lesioni spinali (SCI) e controlli sani; iii) che la stimolazione elettrica neuromuscolare (NMES), controllata dall'attività neurale ad anello chiuso, induce un recupero funzionale dell'arto superiore significativamente più forte rispetto ad elettroterapia sham, e che questo recupero è rilevante clinicamente. Questi risultati hanno o sono in grado di avere importanti implicazioni per i) la diagnostica ed il monitoraggio clinico mediante EEG; ii) la tecnologia assistiva e la riduzione della disabilità permanente derivante da lesioni spinali; iii) la riabilitazione della funzione del membro superiore a seguito di uno stroke, anche dopo molti anni di paralisi completa. In breve, questa Tesi riporta l'apparato concettuale, il razionale scientifico, i dettagli tecnici e l'evidenza clinica atta a supportare una Neurotecnologia traslazionale che migliora, ottimizza e sovverte la pratica clinica attuale nel monitoraggio, nella sostituzione e nel recupero della funzionalità motoria dell'arto superiore.

Key words: diagnostica neurologica per immagini, analisi topografica EEG, stimolazione cerebrale non invasiva, stimolazione transcranica in corrente continua, neuroprotesi, stimolazione elettrica neuromuscolare, interfacce cervello macchina

Résumé

La Neurotechnologie caractérise l'application de connaissances scientifiques à des fins pratiques de compréhension, d'interaction, et/ou de rétablissement des mécanismes cérébraux. Elle comprend ainsi le développement de nouvelles approches assurant un décodage des informations fonctionnelles provenant du cerveau, renforçant les propriétés spécifiques du tissu neural, et restaurant l'activité motrice chez des utilisateurs véritables. Transposer ces solutions novatrices à la pratique clinique représente un défi fondamental. Dans cette thèse, j'introduis i) une nouvelle méthode d'imagerie identifiant des potentiels électro-encéphalographiques (EEG) relatifs au mouvement ; ii) une stratégie de stimulation cérébrale afin d'améliorer le contrôle par interface cerveau-ordinateur (BCI) ; iii) et une thérapie de récupération motrice impliquant une neuroprothèse. Dans l'ensemble, les résultats démontrent i) que des topographies EEG stables présentent une organisation indépendante des sujets, et que celle-ci peut être exploitée pour décoder de manière robuste des mouvements réels ou amorcés chez des patients subaigus (victimes d'accidents vasculaires cérébraux, AVC) comme chez des témoins sains, et cela avec une information induite minimale ; ii) que la stimulation transcrânienne en courant direct (tDCS) améliore la modulabilité des rythmes sensori-moteurs employés dans l'interaction cerveau-ordinateur chez des patients chroniques atteints d'une lésion médullaire (SCI), comme chez des témoins sains ; iii) qu'une thérapie par stimulation électrique neuro-musculaire (NMES) contrôlée en circuit fermé, conduit à une récupération fonctionnelle du membre supérieur significativement et cliniquement plus importante chez des patients chroniques victimes d'AVC, comparée à une thérapie NMES fictive. D'importantes implications de ces résultats pourraient être considérées en matière de i) diagnostics de maladies et contrôle par EEG ; ii) technologie d'assistance et atténuation d'invalidité permanente suite à SCI ; iii) rééducation et récupération fonctionnelle du membre supérieur post-AVC, et ceci également après plusieurs années de paralysie complète. En résumé, cette thèse offre un cadre conceptuel combiné à des arguments scientifiques, des détails techniques, et des données cliniques, qui soutiennent une Neurotechnologie translationnelle cherchant à améliorer et optimiser le contrôle, la substitution et la récupération de la fonction lésé du membre supérieur.

Mots clefs : neuro-imagerie, analyse topographique EEG, stimulation cérébrale non invasive, stimulation transcrânienne à courant direct, neuroprothèse, stimulation électrique neuro-musculaire, interfaces cerveau-ordinateur

Contents

Contents

List of Figures

List of Tables

1 Introduction

> Any sufficiently advanced technology is
> indistinguishable from magic.
>
> Arthur C. Clarke

In recent years, greater attention has been given to public health aspects of neurological disorders, as it has become evident that many priority health problems, in both developing and developed regions, affect the brain and the entire nervous system [94]. The Global Burden of Disease Study, a report conducted by the World Health Organization, the World Bank and Harvard School of Public Health to estimate the total burden of illness globally, demonstrated that between 1990 and 2020 there will be a remarkable change in the rank order of diseases [105]. Neurology is at the focal point of these modifications (**Table 1.1**), and consensus has been reached on relative weight of different disabilities (**Table 1.2**). The paralysis of two limbs (i.e. paraplegia and hemiplegia) and the paralysis of the four limbs (i.e. quadriplegia) ranked among the most devastating conditions [105], requiring immediate action by health ministries worldwide.

Recent history can be seen as a sequence of techno-economic waves inducing substantial economic, political, and social change [90] (**Tab. 1.3**). Neurotechnology, the application of scientific knowledge to the practical purpose of understanding, interacting and/or repairing the brain or, in a broader sense, the nervous system, will play an important role in preventing neurological diseases, in reducing the economic and social impact of disability, and in promoting the recovery of lost motor function.

The future of neurotechnology and its impact on human welfare, with regard to motor disability, will strongly depend on advances in these three areas: *imaging, enhancing, restoring*. This triad will accompany the reader throughout this Thesis, whose intent is to capitalize on current state-of-the-art in neuroimaging, transcranial stimulation and neural interfaces to demonstrate how neurotechnology might disrupt the future of restorative medicine. The translational studies presented in this document share the use of low health risk, low cost

Table 1. The 15 Leading Causes of Disease Burden, 1990 and 2020

Ranking	1990	2020
1	Lower respiratory tract infections	Ischemic heart disease
2	Diarrheal diseases	Unipolar major depression
3	Perinatal conditions	Road traffic accidents
4	Unipolar major depression	Cerebrovascular disease
5	Ischemic heart disease	Chronic obstructive pulmonary disease
6	Cerebrovascular disease	Lower respiratory tract infections
7	Tuberculosis	Tuberculosis
8	Measles	War
9	Road traffic accidents	Diarrheal diseases
10	Congenital anomalies	Human immunodeficiency virus
11	Malaria	Perinatal conditions
12	Chronic obstructive pulmonary disease	Violence
13	Falls	Congenital anomalies
14	Iron-deficiency anemia	Self-inflicted injuries
15	Protein-energy malnutrition	Trachea, bronchus, and lung cancers

Table 1.1: **Global burden of Disease 1990-2020.** The Global Burden of Disease study [105] demonstrates that, between 1990 and 2020, there will be a remarkable change in the rank order of disease burden globally. The 15 leading causes of disease burden in 2020 for developed regions are shown here.

Table 2. Severity of Disability for 22 Indicator Conditions

Disability Class	Severity Weights	Indicator Conditions
1	0.00-0.02	Vitiligo of face, weight for height less than 2 SDs
2	0.02-0.12	Watery diarrhea, severe sore throat, severe anemia
3	0.12-0.24	Radius fracture in a stiff cast, infertility, erectile dysfunction, rheumatoid arthritis, angina
4	0.24-0.36	Below-the-knee amputation, deafness
5	0.36-0.50	Rectovaginal fistula, mild mental retardation, Down syndrome
6	0.50-0.70	Unipolar major depression, blindness, paraplegia
7	0.70-1.00	Active psychosis, dementia, severe migraine, quadriplegia

Table 1.2: **Severity of disability.** Relative severity of 22 "indicator conditions" selected to represent distinct severities of disability, weighted between 0.00 (perfect health) and 1.00 (equivalent to death). The disorders selected as indicator conditions were identified by the readily achieved consensus on weights among health workers from all regions of the world, despite diverse cultural backgrounds. Data from [105].

procedures and devices – namely electroencephalography (EEG), transcranial direct-current stimulation (tDCS), brain-computer interfaces (BCI), neuromuscular electrical stimulation (NMES, often called functional electrical stimulation, FES) – on real end-users, and they were designed as to meet the requirements of current clinical practice.

The document is articulated in three core chapters on *imaging, enhancing,* and *restoring* human motor function: **Chapter 2** presents the use of single-trial decoding of motor tasks from stable EEG topographies as an imaging modality, with a methodological validation on healthy subjects and an exploratory pilot sub-acute stroke patients; **Chapter 3** introduces a pilot study on the effect of tDCS on electroencephalographic (EEG) features normally used to control a BCI system in chronic spinal cord injured and able-bodied individuals; **Chapter 4** presents a sham-controlled phase 1 clinical trial evaluating the effects of brain-controlled neuromuscular electrical stimulation (NMES) for upper limb motor recovery in chronic stroke patients. Finally, results presented in each of the chapters are framed and discussed under the broader perspective of neurotechnology in the **Discussion & Conclusions Chapter**.

Below, a short description introduces each of the core Chapters.

Functional EEG imaging

The development of body imaging techniques is one of the most relevant achievements in medicine [4], and recent advances in EEG indicate that its insights into neural networks and

	1	2	3	4	5	6
Long Wave	Mechanization	Railroadization	Electrification	Motorization	Information	Neurotechnology
Time period	1770–1830	1820–1880	1870–1920	1910–1970	1960–2020	2010–2060
New inputs	Canals, water power	Coal, iron, steam power	Electricity, steel, copper	Oil	Microprocessor	Biochip, brain imaging,???
Driving sector	Agriculture, cotton spinning	Railroads, locomotives, machine tools	Steel products, electricity	Automobile, oil refining	Microchips, computers	Biotechnology, nanotechnology
New sectors	Iron tools, canal transportation	Steam shipping, telegraphy	Construction, precision machine tools	Aircraft, construction, services	Networking, global finance, e-commerce	Neuroceuticals, bio-education

Table 1.3: **Six long waves of techno-economic development.** Recent history can be seen as a sequence of techno-economic waves inducing substantial economic, political, and social change . Neurotechnology, the set of tools that influence the human brain, will allow people to experience life in ways that are currently unattainable. As people begin to experience life less constrained by the mere evolution of brain chemistry, neurotechnology will give rise to a new type of human society, a post-industrial, post-informational, neurosociety. Reproduced from [90].
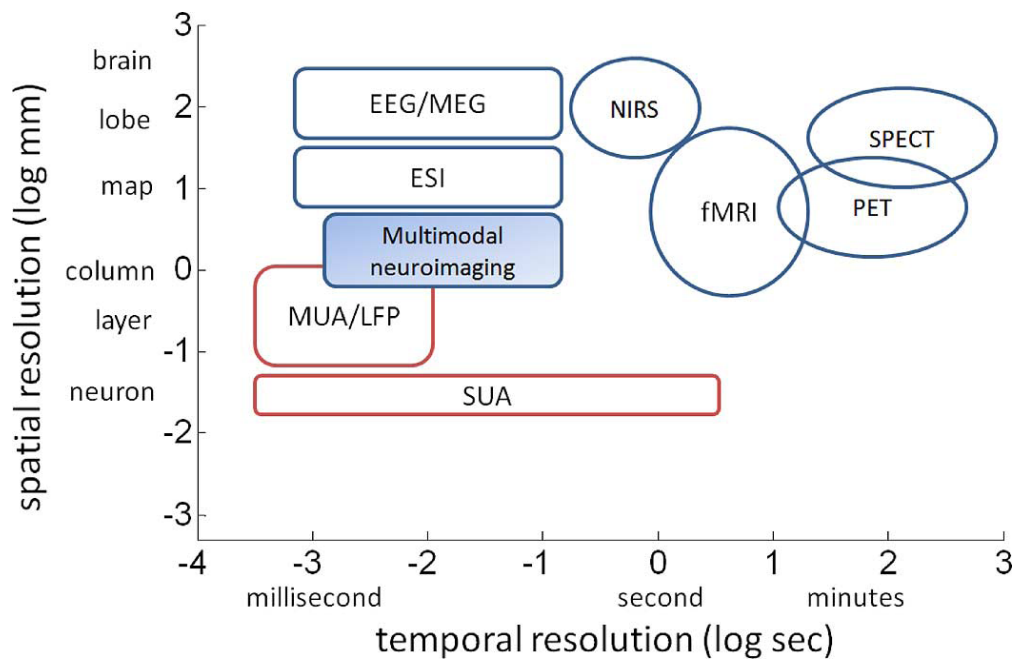
Figure 1.1: **Brain imaging modalities.** Schematic illustration of the ranges of spatial and temporal resolution of various noninvasive (in blue) imaging techniques and invasive (in red) experimental techniques. electroencephalography (EEG), magnetoencephalography (MEG), electromagnetic source imaging (ESI), multi-unit activity (MUA), local field potential (LFP), single-unit activity (SUA), near infra red spectroscopy (NIRS), functional magnetic resonance imaging (fMRI), positron emitting tomography (PET), single-photon emission computed tomography (SPECT). Reproduced from [62].

brain function will have an increasingly important role in medical diagnosis and treatment in the near future [101]. EEG measures electrical potentials and magnetic fluxes propagated in a virtually instantaneous time from activated neuronal tissues to the scalp. The instantaneous nature of EEG indicates an intrinsically high temporal resolution and precision, which make them well suited for studying brain functions on the neuronal time scale, even though the collective nature suggests low spatial resolution and specificity, which impede mapping brain functions in great regional details [62]. **Fig. 1.1** clusters available brain imaging modalities by spatial and temporal resolution.

Efforts to decode neural activity from EEG fostered the naissance of BCI technology [152], even though the idea of decoding brain function from electrical currents recorded from the scalp has accompanied EEG since its discovery [8]. BCI systems widely demonstrated the potential of EEG, especially as a new communication and control channel for disabled people [12, 82].

Current BCI algorithms overcame several limitations coming from the fact that the EEG is an ever-changing, complex signal with statistical properties which depend on both time and space [89]. These developments were made possible by a growing interest in single-trial analyses of event-related potentials (ERP) in neuroscience [64, 88, 28] and by consistent

advances in machine learning [98, 96, 56, 103].

Time-locked changes in the activity of neuronal populations, such as those induced by the execution of a motor action, were traditionally described in terms of average event-related potentials (ERPs) or by means of single-trial analyses of frequency-specific event-related synchronization (ERS) and desynchronization (ERD) patterns at specific scalp locations [118]. However, these a-priori assumptions and ambiguous single channels waveform analyses limit the physiological interpretability of the results [95], especially for pathologies where assumptions on EEG analyses drawn from healthy individuals, such as space and time-frequency localization of events, might not be valid [69].

Topographic EEG analysis, based upon the interesting property of the EEG to maintain stability of voltage topographies for short time periods typically spanning between 50 and 150ms [83], is inherently neurophysiologically interpretable (a change in topographic is indicative of a change in the configuration of the underlying sources) and overcomes the limitations of single waveform analyses by treating entire electrode montage data as a multivariate vector without any a-priori bias [106]. Topographic EEG information has been used to characterize different developmental stages during wakeful rest [75] and several neurological disorders including schizophrenia [86] and stroke [78].

Methodologically, recent studies demonstrated that single-trial EEG topographic analysis can be used to describe fine temporal aspects of time-locked [143] and non-locked [144] brain activity, extending the applicability of this technique beyond averaged potentials.

These findings might be especially suited for the monitoring of brain patterns produced by an impaired brain. Despite recent advances in science and prevention, stroke is the first cause of disability, involving around 20 million people worldwide per year and represents the third most common cause of death. 75% of this population will survive the vascular accident, but approximately 5 million individuals will be disabled by their stroke [91]. Consequently, the development of new techniques to support efficient functional rehabilitation as well as to monitor the progression of the disease ranks among the primary interests of current research. A growing body of literature suggests that similarities exist in terms of neural activity between the state in which a motor action is imagined and the state of execution, resulting in the benefits seen in mental practice for rehabilitation[68]. Indeed, several studies provide hints on the positive effects of mental practice in adjunction to physical practice [109].

BCI protocols involving executed or attempted movements or motor imagery might in fact be used to monitor and encourage plasticity phenomena occurring after stroke (or more generally after brain injury) [97]. Several factors affecting the production of EEG patterns need to be taken into account, including: the extent to which patients have detectable brain signals that can support training strategies; which brain signal features are best suited for use in monitoring and restoring motor functions and how these features can be used most effectively; and what are the most effective approaches for BCI aimed at improving motor functions (for instance, what guidance should be provided to the patient to maximize training

that produces beneficial changes in brain signals). Preliminary findings suggested that event-related EEG activity time-frequency maps of event-related EEG activity and their classification are proper tools to monitor MI related brain activity in stroke patients and to contribute to quantify the effectiveness of MI [133]. Pilot studies and case reports on stroke patients using a BCI system found that the best signals appear over the ipsilateral (unaffected) hemisphere [19]. Finally, the idea that BCI technology can induce neuroplasticity has received remarkable support from the community based on invasive detection of brain electrical signals [97].

BCIs normally monitor variations in specific frequency bands of spectral power associated with different tasks, such as motor imagery or attempted movements, to generate an output that can be used for communication and control of devices such as a virtual keyboard, a telepresence robot or a powered wheelchair [96, 23]. The use of non-parametric methods, such as FFT, restricts the frequency analysis of EEG patterns in the time scale of seconds, losing the good temporal resolution of this recording modality [74]. The use of EEG-Microstates [85], i.e. stable voltage topographies produced during a certain task, represents an alternative imaging analysis method that preserves the superb time resolution of EEG down to tens or hundreds of ms.

Chapter 2 is articulated in two main sections: the first explores the use of stable EEG topographic maps for single-trial decoding of motor-related potentials; the second presents a pilot study on chronic stroke patients that evaluates the possibility to use these EEG signatures of motor tasks for rehabilitation. **Section 2.1** provides evidence that comprehensive scalp potential field analysis is suitable to decode and describe single-trial single-subject motor function from EEG data with minimal a-priori information and high temporal resolution by applying a classification procedure normally used in closed-loop BCI systems. **Section 2.2** addresses the issue of tracking brain patterns for BCI–aided stroke rehabilitation by combining standard EEG time-frequency analysis [119, 55] to EEG topographic analysis. Extracted information could be used to provide feedback about relevant task–related mental patterns to patients, practitioners, or clinicians during the therapeutic cycle.

Neuroenhancement and electroceuticals

Neuroenhancement describes the use of neuroscience-based techniques for enhancing cognitive function by directly acting on the human brain and nervous system, altering its properties to increase performance for a specific cognitive task or set of tasks [30]. Recent studies on the use of non-invasive transcranial direct-current stimulation (tDCS) to enhance attention, learning, and memory demonstrated that tDCS guided by neuroimaging can produce large increases in task performance during behavioral tasks and other signal detection measures that lasts at least 24 h after stimulation is ended [29, 31, 45]. This appealing concept has been further extended by a recent statement from a multinational pharmaceutical corporation (GlaxoSmithKline) on a growing interest in the so-called "electroceuticals" – electrical impulses

that target individual nerve fibers or specific brain circuits to treat an array of conditions, modulating the neural impulses controlling the body, repairing lost function and restoring health [46]. In addition, tDCS has been proposed as a technique for studying motor processes and as a tool for treating neurological disorders or neurorehabilitation [145, 65, 130]. This technique modifies neuronal excitability, by shifting the resting potential of cortical neurons [145] (see **Fig. 1.2** for an overview on electrodes montage and resulting cortical areas engaged by the stimulation), and its effects have been reported to last between 40 and 90 min depending on the length of the stimulation [110]. Previous experiments suggest that stimulation of brain area M1 results in a selective increase or decrease of cortical excitability and motor evoked potentials [100, 125]. Consistently, there is evidence that tDCS also modulates event-related desynchronization during Motor Imagery (MI) tasks [93].

This is in agreement with previous studies that shows that tDCS modifies neuronal excitability so as to increase ipsilateral motor-evoked potentials after anodal stimulation of the left M1, and a decrease after cathodal stimulation [80, 125]. In some cases the effect lasted for about 40 min after the stimulation, although other studies have reported effects lasting up to 90 min [110]. Bilateral stimulation of motor cortices (i.e. anodal tDCS over the motor cortex and cathodal stimulation over the contralateral hemisphere) produces selective increase/decrease of excitability, respectively [100]. Moreover, DC stimulation has also been reported as influencing long-term skills motor learning [129]. Consequently, tDCS has been proposed as non-invasive, low-cost and easy-to use technique for studying motor processes in healthy subjects and as a facilitating technique for treating neurological disorders [145] or neural rehabilitation [65, 130]. Moreover, influencing the ability of people to produce patterns that can be recognized by a BCI system might simplify the interaction and augment system reliability, providing a more effective tool for assistive technology.

Chapter 3 presents a study on 12 spinal cord injured individuals and 13 able bodied controls whose goal is to quantify the effects of anodal tDCS on the EEG features that are normally used during brain-computer interaction. We find a shift in discriminable EEG activity in a two-tasks motor imagery protocol on the stimulated hemisphere, for both groups. Interestingly, anodal tDCS also has a carry-over effect with respect to sham-tDCS, allowing people to sustain the production of discriminable patterns for longer periods of time.

The neuroprosthetic era

Despite considerable efforts over the last decades, the quest for novel treatments for arm functional recovery after stroke remains a top priority [122], as current interventions yield limited gains [36, 155, 73]. This makes the pursuit of novel principles, devices and interventions aiming at functional recovery a top research priority relating to life after stroke [122].

In recent years, synergistic efforts in neural engineering and restoration medicine are demonstrating how neuroprosthetic approaches can control devices and ultimately restore body function [16]. In particular, after two decades of research, non-invasive brain-computer inter-
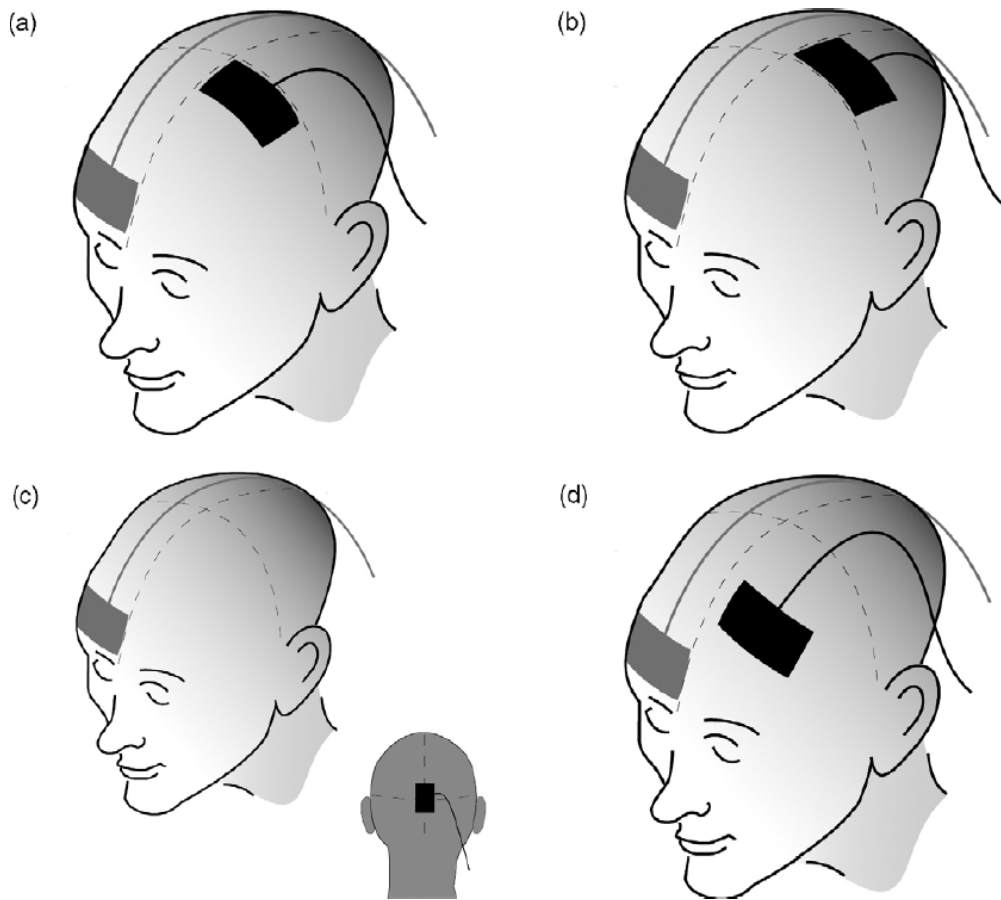
Figure 1.2: **Typical electrodes montage on scalp surface for tDCS.** The four figures illustrate the typical placement of anode and cathode during stimulation of the primary motor cortex (A), somatosensory cortex (B), primary visual cortex (C), anterior language cortex (D). Note that in Fig. 1(C) one electrode is placed at the back of the head (see small image of the head), while the other electrode is placed at the right supra-orbital area. One electrode is placed on the area of the scalp covering the target structure and the other electrode is typically placed either over the supraorbital area of the other hemisphere or over the corresponding area of the contralateral hemisphere. Reproduced from [145].

face (BCI) systems are reaching their technological maturity [97], and might be used to reliably translate neural activity into meaningful outputs driving activity-dependent neuroplasticity and functional motor recovery [33] (see **Fig. 1.3**). Real-time BCI control consists in learning to modify the efficacy of spared neural ensembles (representing movement, sensation, and cognition) through progressive practice with contingent feedback and reward —sharing its neurobiological basis with rehabilitation [40]. Although invasive BCIs based on neuronal spike patterns recorded with implanted arrays of microelectrodes may represent the strategy of choice for most severe cases [13], issues related to safety, low-power and wireless systems, long-term recording stability, and robust performance without daily retraining still need to be extensively addressed before they may become therapeutic reality [33, 32].

Preliminary attempts to use non-invasive BCI systems for upper limb rehabilitation after stroke have illustrated a variety of ways to couple them with other interventions, although not all trials reported clinical benefits. Most studies involved a few patients who operated a BCI to control either rehabilitation robots [19, 18, 124, 22, 147] or neuromuscular electrical stimulation (NMES) [34, 153]. A few works have described changes in functional magnetic resonance imaging (fMRI) that correlates with eventual motor improvements [22, 147, 153]. Recent randomized controlled trials showed that BCI-aided robotic therapies provided significantly greater motor gains than robotic therapies alone [126, 3], although the absolute difference between the two therapies was moderate. In the former study, involving 30 chronic patients [126], only the BCI group exhibited a functional improvement, although moderate (3.4 points in the upper extremity section of the Fugl-Meyer assessment, FMA-UE). In the latter case, involving a mixture of 14 subacute and chronic patients [3], both groups achieved a higher improvement (above 7.0 FMA-UE points), probably due to the shorter time after the stroke and less severity of patients' motor impairments.

The results of these randomized controlled trials are somehow discouraging. Does this mean that, despite its promises, BCI interventions will not change the landscape of motor stroke rehabilitation as they cannot provide clinically relevant improvements to patients as compared to the therapies they are combined to? We hypothesize that, for BCI to drive activity-dependent plasticity of spared neural circuits, the associated contingent feedback must not only be functionally meaningful (e.g., passive movement of the lesioned limb by a robot), but must also be tailored to reorganize the targeted neural circuits by providing rich sensory inputs via the natural afferent pathways [140] so as to activate all spare components of the central nervous system involved in motor control —from the cortex to subcortical areas to spinal cord. NMES fulfills these two properties of feedback contingent to appropriate patterns of neural activity: it elicits functional movement and conveys proprioceptive information via the peripheral nerves it stimulates to contract the target muscles.

To test this hypothesis, the study presented in **Chapter 4** aimed at assessing whether five weeks of therapy BCI-aided NMES (BCI-NMES for short, could yield stronger and clinically relevant functional recovery than sham-NMES therapy, and whether signatures of neuroplasticity would be associated to motor improvement. To probe the limits of our hypothesis, we
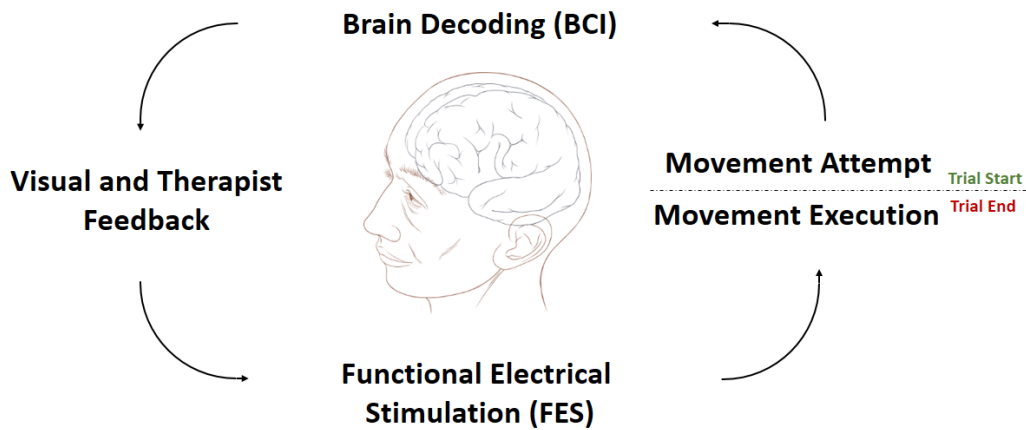
Figure 1.3: **The BCI loop for rehabilitation.** A Brain-Computer Interface (BCI) systems can translate spared EEG signatures of a motor task, such as an attempted movements resulting in μ and β rhythms modulations, into meaningful rewarding functional electrical stimulation (FES) of the affected limb. The repetition of this schema might be used to drive beneficial cortical plasticity by increased sensorimotor drive.

enrolled chronic patients in their plateau phase of recovery with moderate-to-severe arm paresis and minimal exclusion criteria. The BCI was calibrated for each subject in order to monitor individual spatial-frequency EEG features —i.e., sensorimotor μ and β EEG rhythms— representing movement attempts as encoded in the activity of spared motor networks. Whenever a hand-extension attempt was decoded from the EEG, the BCI activated NMES of the extensor digitorum communis muscle. Surprisingly high and clinically relevant improvements of affected arm functions were found for subjects in the BCI-NMES group, with signs of retention after 36 weeks. Also, EEG neuromarkers suggest that the functional recovery is promoted by changes in cortical excitability and in interhemispheric connectivity.

2 Imaging Motor Function

> A rock pile ceases to be a rock pile the moment a single man contemplates it, bearing within him the image of a cathedral.
>
> Antoine de Saint-Exupery

This Chapter explores the use of stable EEG topographic information and single trial decoding of motor tasks as a novel tool for brain imaging and rehabilitation. In particular, **Section 2.1** presents a study on stable EEG decoding involving 11 able-bodied individuals performing an actual movement of the hand or resting. **Section 2.2** presents an exploratory study on the combined use of time-frequency and topographic EEG analyses in order to describe fine temporal aspects of brain engagement in an imagined motor tasks involving 6 chronic stroke patients.

2.1 Decoding motor attempts from single-trial stable topographic EEG[1]

Outlook. *Electroencephalography (EEG) offers new insights into neural networks and brain function, gaining an increasingly important role in medical diagnosis and treatment. Time-locked changes in the activity of neuronal populations, such as those induced by the execution of a motor action, were traditionally described in terms of average event-related potentials (ERPs) or by means of single-trial analyses of frequency-specific event-related synchronization (ERS) and desynchronization (ERD) at specific scalp locations. However, these a-priori assumptions*

---

[1]This section was adapted from Biasiucci, A., Chavarriaga, R., Leeb, R., Murray, M.M., Mattia, D., Millán, J.d.R. (2014) **"Decoding single-trial topographic EEG correlates of motor engagement and rest reveals subject-independent organization"**, in preparation [10]. **Contributions:** D.M. designed the protocol and coordinated data recordings, A.B., R.C., R.L., M.M.M., J.d.R.M. designed the analyses, A.B. developed the methods, A.B., M.M.M., J.d.R.M. analyzed the data.

and ambiguous single channels waveform analyses constrain the physiological interpretability of the results, thus limiting the adoption of EEG as a brain imaging tool in clinical applications. Here we use state-of-the-art algorithms used in the field of brain computer interfaces (BCI) to show that comprehensive scalp potential field analysis is suitable to decode and describe single-trial single-subject motor function from EEG data with minimal a-priori information. We found that the strength of the potential field across the whole scalp can be used to predict whether unseen trials contain motor or resting activity with high temporal resolution both during preparatory and execution phases of single trials. We also found that stable potential field topographies extracted during preparatory phases resemble those extracted during execution phases of single trials, and that these patterns are extremely consistent across subjects. Our results demonstrate that motor function can be accurately decoded from scalp voltage potential field with superb temporal resolution and that a subject independent structure of stable voltage topographies emerges from the data. We anticipate these findings to be a starting point for more sophisticated brain imaging and rehabilitation applications for pathologies where assumptions on EEG analyses drawn from healthy individuals such as space and time-frequency localization of events might not be valid.

Experimental protocol

Eleven unpaid volunteers provided written, informed consent to participate in the experiment. EEG was recorded at the Fondazione Santa Lucia, Rome, Italy. The subjects (five men, six women, aged 30±7 years) had no current or prior neurological or psychiatric illnesses.

The study was approved by the local Ethics Committee of the Fondazione Santa Lucia and was conducted according to the Declaration of Helsinki. The data used in this study were previously published in a study concerning cortical responsiveness in healthy subjects while operating a sensorimotor rhythm-based BCI [120].

Briefly, subjects sat in front of a screen in a dimly lit room with their arms on a desk. Each session was divided into runs consisting of 30 trials each. Each trial lasted 9s; with an inter-trial interval of 1.5s. During rest trials (**Fig. 2.1**, top) the subject was instructed to watch the cursors moving on screen. During movement trials (**Fig. 2.1** , bottom) a green rectangle appeared on top of the screen and the subject was asked to start performing the motor task during the 4s while the cursor crossed the green area of the screen. A recording session was composed of 8 runs; each run included 15 resting trials and 15 motor trials. The motor task consisted in a tonic complete finger grasping. Trial and run sequences were randomized.
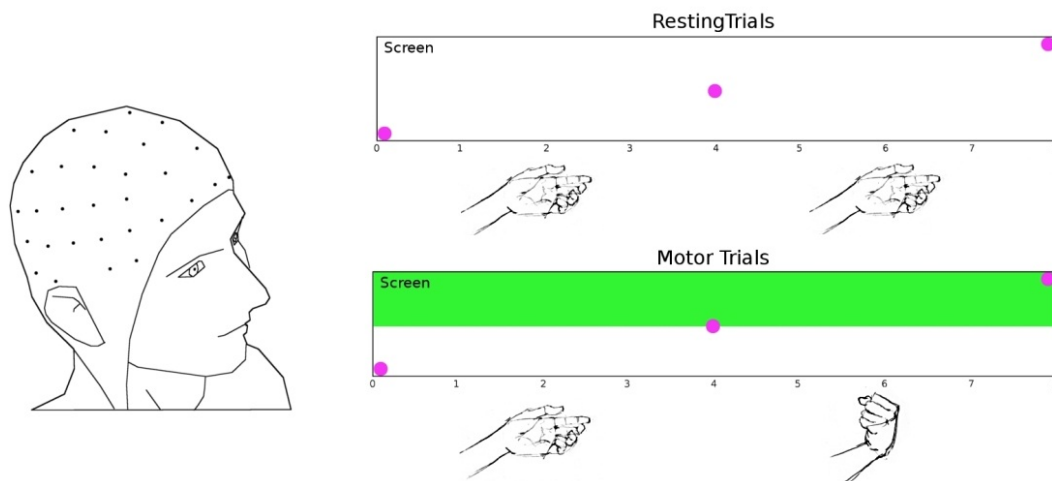
Figure 2.1: **Experimental protocol timeline.** Subjects sat in front of a screen, providing visual instructions about the task to perform. During resting trials (top), a cursor appeared on the bottom of the screen and started moving vertically towards the top of the screen, at a constant speed. During movement trials (bottom), a green rectangle appeared on the top half of the screen, and was displayed for the entire length of the trial, 8s. Then, a cursor appeared on the bottom of the screen and started moving vertically towards the top of the screen, at a constant speed. Subjects were instructed to get ready to perform the motor task during the 4s where the cursor moved on the white part of the screen, and to start executing the motor task with one of their upper limbs as soon as the cursor reached the green rectangle, sustaining the movement for the remaining 4s of the trial, until the cursor reached the top of the screen. Subjects were instructed to watch the cursor without speaking or producing facial movements, blinks or other types of muscular activity not directly required by the motor task.

2.1.1   Methods

2.1.2   General Analyses Structure

This aim of this study is to test whether comprehensive scalp potential field analysis can reliably differentiate the execution of a motor task from rest on single-trials with minimal a-priori information.

First, the time window yielding most relevant information about the motor task is extracted, for each subject, by single-trial classification of the global field power (GFP), a reference-free measure of topographic electric field strength [84]. Second, stable voltage topographies are extracted in an unsupervised manner from concatenated motor task and rest trials, independently for each subject and data fold. Finally, sets of stable topographies are compared across subjects to quantify their similarity.

We quantify classification performance in terms of single-sample and single-trial classification accuracy and compare it to the average performance obtained on the same data by repeated shuffling of task labels, i.e. by a permutation test. Then, we quantify the similarity of stable topographies extracted across different folds of data to ensure stability of the results. The same procedure is applied to stable topographies extracted during preparation and action phases of concatenated single-trials – i.e. concatenating the first or last 4s following the trial-start cue, independently of the task. Finally we quantify the topographic similarity of stable topographies extracted during action phases across different subjects.

The use of single-trial analyses of EEG information is suitable to understand the contribution of individual subjects to a group-analysis and to investigate single subjects' mechanisms [64, 119, 143]. In this regard, the use of machine learning methods is essential to highlight single-subject modulations in the appearance of specific stable topographies across time, depending on the currently performed task.

Several caveats were considered when designing the classification techniques on EEG data presented in this section, as to avoid experimental biases and overoptimistic results [87]. To this purpose, we did not use any global statistic to perform artifact rejection and EEG pre-processing, and we tested our model in a 5-fold cross-validation procedure, estimating all parameters solely on training sets.

EEG recordings and pre-processing

Scalp EEG potentials were collected from 61 positions (according to an extension of the 10-20 International System), digitized at 200 Hz and amplified by a BrainAmp, Brainproducts GmbH, Germany. We discarded the 20 outermost EEG channels (namely FP1, FP2, FPz, AF7, AF8, F7, F8, FT7, FT8, T7, T8, TP7, TP8, P7, P8, PO7, PO8, O1, O2, Oz) from any further analysis as they were more likely to carry muscular and other types of artifacts. EEG epochs affected by artifacts were manually rejected whenever the raw EEG values or the bipolar EOG signals,

representing horizontal and vertical eye movements, exceeded a threshold of $\pm\,100\mu$V. In addition, noisy channels were manually identified and spline interpolated [115]. Prior to any analysis, the EEG was band-pass filtered in 1-40 Hz and re-referenced to the common average reference (CAR).

2.1.3 Single-trial classification

Single-trial classification was performed by Bayesian filtering, a statistical model that takes into account the task-specific temporal structure of GFP – i.e. spatial variance across whole-scalp electrodes montage. Bayesian filtering is a recursive Bayesian estimation method [67] computing state probabilities at each sampling time step, according to the observations and the previous state estimations. This method was previously introduced for single- trial classification of error-related potentials from EEG waveforms recorded at specific electrode locations [51].

The state to be decoded is a time series S_t with $t = 0..T$. We assumed that there were two possible states at each time t:

$$S_t = \begin{cases} 1 & \textit{Movement} \\ 0 & \textit{Resting} \end{cases}$$

At each time t, observations O_t were given by the instantaneous GFP, extracted from single-trials of data.

In order to model its temporal dynamics, we specified a transition model by a first order Markov hypothesis for states over time:

$$P(S_t|S_{0:t-1}) = P(S_t|S_{t-1}) = \mathbb{1}, \qquad t = 0..T \tag{2.1}$$

where T is a generic time point. The transition model of **Eq.** (2.1) is equal to the identity matrix since no state change is allowed within the same trial.
Probability distribution $P(O_t|S_t)$, predicts the GFP observations given the state. The two expressions yield the joint probability:

$$P(S_{0:T}, O_{0:T}) = P(S_0)P(O_0|S_0)\prod_{t=1}^{T}(P(S_t|S_{t-1})P(O_t|S_t)) \tag{2.2}$$

This distribution can be solved recursively through a prediction-estimation procedure [42]. In the first step, a prediction of the state is calculated with respect to the transition model:

$$P(S_t, O_{0:t-1}) = \sum_{t-1}^{T} (P(S_t|S_{t-1})P(S_{t-1}|O_{0:t-1})) \qquad (2.3)$$

then, we computed the following estimation based on the GFP observations model:

$$P(S_t, O_{0:t}) \propto P(O_t, S_t)P(S_t, O_{0:t-1}) \qquad (2.4)$$

The recursive prediction-estimation formula could then be simplified, given the identity transition matrix of **Eq.** (2.1):

$$P(S_t = 1, O_{0:t-1}) \propto P(O_t, S_t)P(S_t = 1, O_{1:t-1}) \qquad (2.5)$$

and correspondingly for $P(S_t = 0, O_{0:t-1})$. A trial is then assigned to the class with the highest probability, for instance to "movement" ($S_t = 1$) whenever the logarithm of quotient Q_t is positive:

$$\ln(Q_t) = \ln(Q_{t+1}) + \ln(P(O_t|S_t = 1)) - \ln(P(O_t|S_t = 0)) \qquad (2.6)$$

The model of GFP occurrences across time was chosen to be Gaussian with mean μ and variance σ, i.e. two parameters had to be estimated for each time point. Mean and variance were learnt with usual estimators within each fold of the data.

2.1.4 Identification of stable topographies

To extract stable topographies, the EEG was band-pass filtered EEG was further normalized it by the instantaneous GFP. Given the fact that GFP tells the researcher how strong a recorded potential is on average across the electrode montage, normalizing the EEG signal by its instantaneous value is a way to make the analysis independent of the response strength, only focusing the analysis on topographic changes [106].

Stable EEG topographies were extracted unsupervisedly from concatenated pre-processed
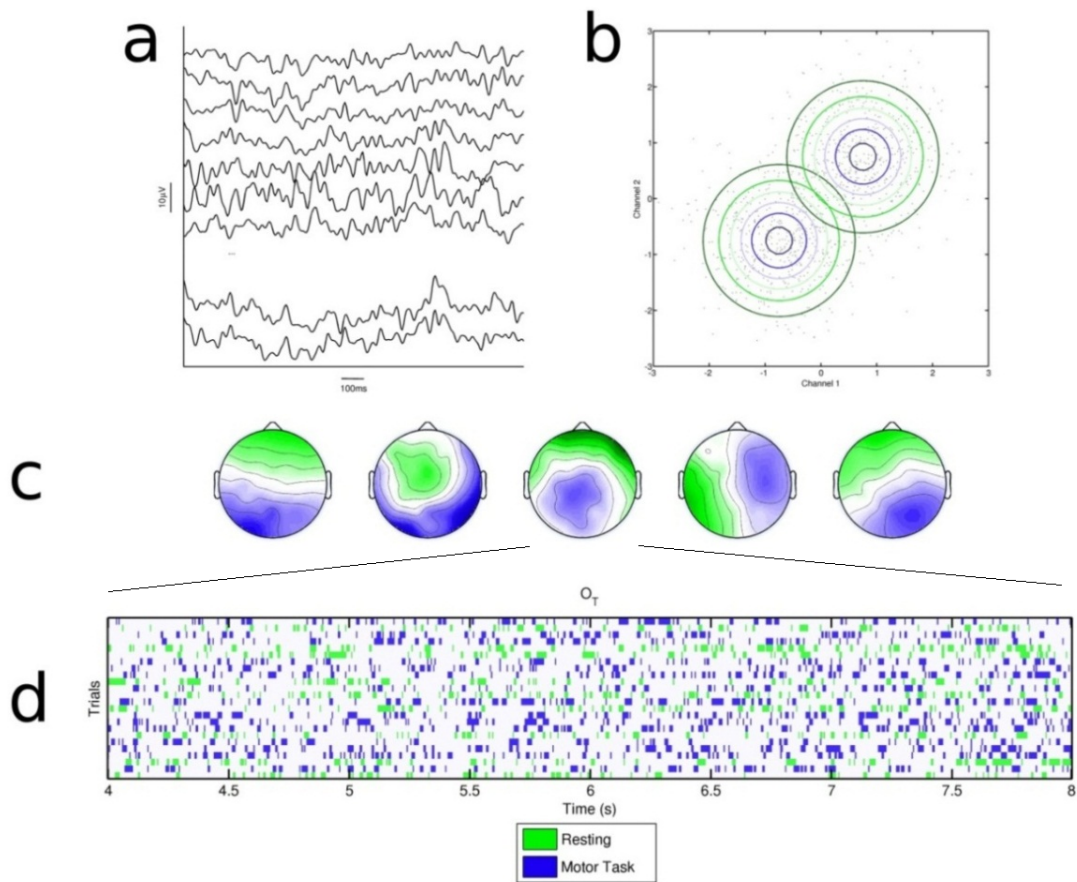
Figure 2.2: **Stable topographies identification procedure.** First, raw EEG is band-pass filtered in the 1-40Hz frequency band (a). The identification of stable voltage topographies in the data is achieved by means of an unsupervised clustering procedure, for example by a Gaussian Mixture Model: in this example, the temporal observations of two channels are scattered on a plane disregarding the temporal order of their appearance, and two Gaussian models are fit to the data (b). For each of the N_μ clusters in the model, an expectation-maximization procedure computes the parameter of the Gaussian models that best describe the data. In the case of concatenated single-trials of EEG data having five stable clusters, means of each Gaussian model are shown in (c). Each of the prototypes can be associated by any distance measure to each time instant of EEG values, a procedure called "segmentation". Segmented single trials during rest (green) or the motor task (blue), with respect to the third template map in (c), are shown in (d).

resting and movement trials. We only considered the 8s per trial during which subjects were instructed to fixate the moving cursor and not to produce any muscle activity (either in preparation to perform, i.e. 0-4s, or during task execution, i.e. 4-8s). The stable topographies extraction process consists in applying a clustering method to the concatenated signal of individual subjects so that each stable topography represents one of the N_μ natural clusters of the data, where $N_\mu = 5$ is chosen a-priori. **Fig. 2.7** provides a justification of this choice based on decoding performance, i.e. N_μ is chosen according to the model that yields the highest single-trial accuracy in discriminating the two types of tasks. Even though any data clustering technique could be used to extract these features, literature focused on three core methods: k-means clustering [113], hierarchical agglomerative clustering [142] and Gaussian Mixture Models (GMM) [143]. Here, we choose a GMM, whose parameters are estimated through an expectation-maximization (EM) procedure [99]. This choice is justified by the fact that GMM has been already validated in the context of single-trial topographic analysis, as initially proposed in [143].

2.1.5 Topographic correlations

Similarities between two sets $\mathcal{M}_1$ and $\mathcal{M}_2$ containing an equal number of stable topographies were quantified by means of a pair-wise correlation coefficients $\boldsymbol{R}_{i,j}$ between the stable topography i belonging to $\mathcal{M}_1$, $i = 1..5$, and the stable topography j belonging to $\mathcal{M}_2$, $j = 1..5$. In this study, where five stable topographies were extracted, $\boldsymbol{R}$ is a 5 by 5 matrix of correlation coefficients (shown in **Fig. 2.4**). The matrix $\boldsymbol{R}$ can be collapsed in a single value γ_s by considering, for each row of $\boldsymbol{R}$, the highest correlation value between two stable topographies belonging to $\mathcal{M}_1$ and $\mathcal{M}_2$, respectively. In the case of two stable topographies belonging to $\mathcal{M}_1$ having their maximum correlation with the same stable topography of $\mathcal{M}_2$, the second maximum value is considered, so that no repetition is allowed - i.e. each stable topography belonging to $\mathcal{M}_1$ is uniquely associated to a stable topography in $\mathcal{M}_2$ depending on their mutual correlation. Finally, these unique values for each of the five stable topographies can be averaged to provide a measure γ_s of similarity between the two sets $\mathcal{M}_1$ and $\mathcal{M}_2$. Correlation coefficients $\boldsymbol{R}_{i,j}$ and γ_s can be compared to the values computed with randomly shuffled topographies as to identify the likelihood of getting a certain correlation value by chance [20].

2.1.6 Results

GFP is consistently modulated on single trials

Here, we test whether GFP - i.e. the spatial variance across the electrodes montage - conveys task-specific information. In other words, we exploit the fact that during a movement we expect a more ordered topographic organization, resulting in a more stable variance across electrode montages, than in rest. The classification performance of each is compared to

chance level estimated from data repeating the classification procedure 100 per fold with randomly shuffled task labels, and statistical differences are tested by means of two tails, unpaired ttest. This type of randomization test has been previously applied to brain imaging in EEG and fMRI and it represents a conservative and rigorous assessment of statistical properties of observed data [20]. **Fig. 2.3a** and **b** show the average classification performance across time in preparation and action time periods of single trials. Single trial classification results are computed within a 5-fold cross-validation procedure – i.e. 80% of the data is used to train the model and 20% to compute performance, iteratively for all data partitions. The performance is calculated as the average accuracy across folds of stable topographies, further averaged across subjects. Eight of the subjects present a classification accuracy significantly above chance in the same time frame of movement execution, but not during the preparation.

These results provide strong evidence that subjects consistently modulate GFP during movement, with respect to resting. This modulation happens on single trials and can be used to decode whether an unobserved trial belongs to the motor or rest ensemble. Interestingly, statistically significant changes occur at a similar timing with respect to well known μ and β rhythms synchronization and desynchronization accompanying movement generation [24]. Interestingly, the fact that some spatial patterns identified during resting can also be found during the execution of a movement, where they become prominent has been already extensively documented in functional magnetic resonance imaging resting state networks (fMRI-RSN) [35].

Stable topographies are consistent across same-subject data folds

To ensure that stable topographies are consistently representing cortical engagement in the motor task, we quantified the similarity of those extracted from independent folds of same subject's data. This property is crucial both from a machine perspective and for the inherent physiological interpretability of the patterns [87]. In general, being the number of rest and movement trials in the training set not necessarily equal across different folds, and given the intrinsic non-stationarity and variability of EEG [71], one might expect to see slightly different stable topographies extracted from different data partitions, but nonetheless these differences should be very limited. **Fig. 2.4a** shows the correlation coefficients computed on stable topographies belonging to two different folds.

Table 2.1 reports the average topographic correlation value across folds, for each subject. All subjects show a significant correlation with respect to values obtained by correlating randomly shuffled topographies, with extremely consistent stable topographies extracted from different data folds (AVG $\gamma_s = 0.88$). Importantly, these results imply that classification on different folds refers to nearly identical stable topographies.
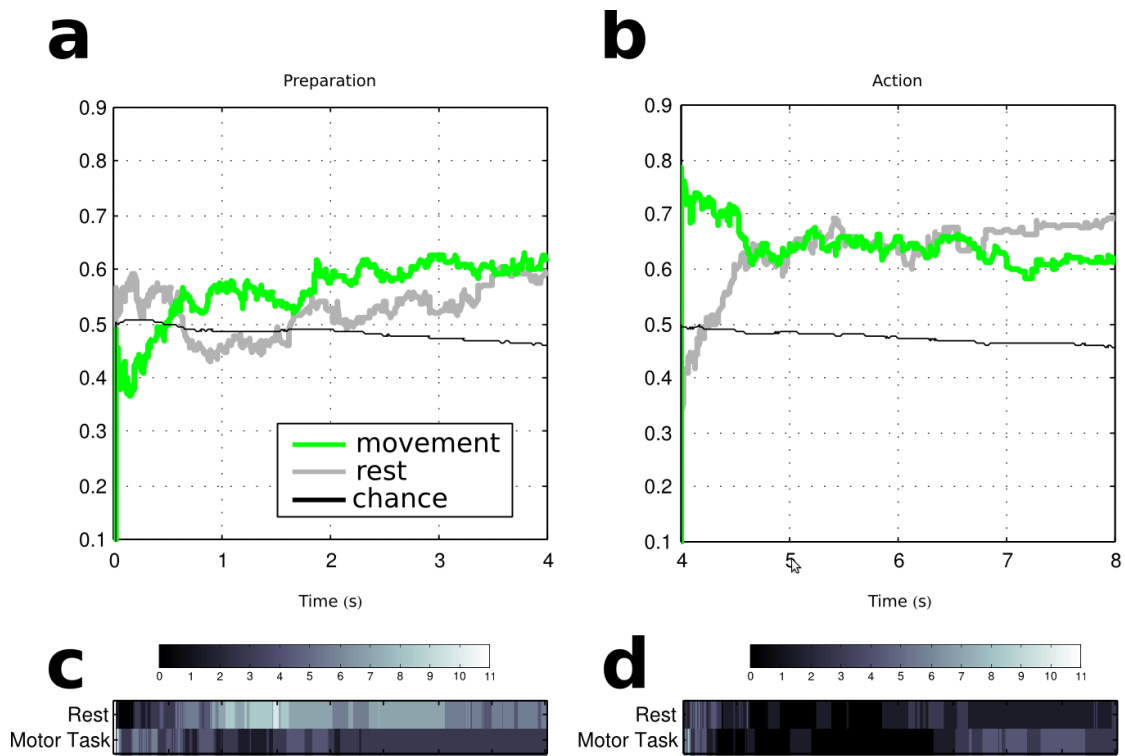
Figure 2.3: **Classification performance.** For each time point, the curve shows the average single-trial decoding performance averaged across subjects for data belonging to the preparation of the movement (a) or to the execution of the movement (b). Accuracy value of 1 would imply that, at a certain time point t, 100% of trials could be decoded by the Bayesian filter. The filer uses stable topographies occurrences up to time t, for all the subjects. Panels (c) and (d) show the amount of subjects that present a statistically significant classification accuracy across time, assessed by uncorrected repeated wilcoxon tests. Classification performance at a certain time point across folds is considered to be significantly different from chance resulting $p < 0.05$.
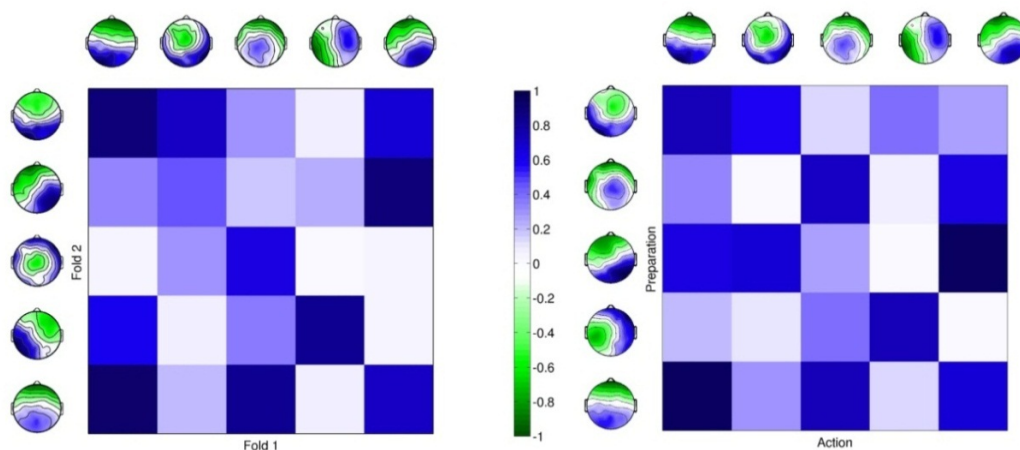
Figure 2.4: **Topographic correlation analysis.** Correlation of stable topographies extracted from different data folds (a) and different phases of trials, i.e. preparation vs action (b). Correlation between topographies is quantified in terms of a matrix R of $R_{i,j}$ correlation coefficients. For each line of R, the highest, unique, correlation value between two templates is selected, and the set of five correlation values is then averaged, providing the topographic similarity coefficient γ_s.

Table 2.1: **Topographic correlation across folds and phases of single trials (i.e. preparation, action).**γ_s values comparing the similarity of the set of stable topographies extracted during the action period of fold 1 against all other folds (column 2) and action and preparation periods of each fold (column 3). The average correlation coefficient is compared to the average correlation value obtained correlating random shuffles of the stable topographies scalp locations 100 times per fold.

Subject	Action Fold 1 vs Action Fold N	Action Fold N vs Preparation Fold N
1	0.93 (0.04)	0.75 (0.04)
2	0.83 (0.03)	0.74 (0.04)
3	0.87 (0.04)	0.92 (0.03)
4	0.94 (0.04)	0.87 (0.04)
5	0.84 (0.04)	0.69 (0.04)
6	0.91 (0.04)	0.80 (0.04)
7	0.86 (0.04)	0.83 (0.04)
8	0.92 (0.03)	0.97 (0.04)
9	0.78 (0.04)	0.68 (0.04)
10	0.95 (0.02)	0.86 (0.03)
11	0.91 (0.04)	0.84 (0.04)
AVG	0.88 (0.03)	0.81 (0.03)

Stable topographies during preparation and action yield very high correlation

In addition to the consistency test across folds, we quantified, for each fold of subjects' data, the topographic similarity between sets of stable topographies extracted during the 4s of sustained movement or resting (i.e. "action periods") and the 4s prior to the cue indicating the beginning of a motor trial and the respective first 4s of rest trials (i.e. "preparation periods"). Results of this analysis are reported in **Table 2.1**. An example of stable topographies extracted during action and preparation periods of single trials is shown in **Fig. 2.4b**. Results show that stable topographies extracted during preparation periods highly resemble those extracted during action periods (AVG $\gamma_s = 0.81$). All subjects show a significant correlation with respect to values obtained by correlating randomly shuffled topographies. Furthermore, we tested whether the distribution of topographic correlation indexes extracted by comparing the action periods of fold 1 against the action periods of all other folds was statistically different from the distribution of topographic correlation indexes extracted by comparing the action periods and preparation periods of each (**Table 2.1**). We find that these distributions are statistically different (two-tailed unpaired ttest, p<0.01).

These findings can be explained by the fact that nearly identical stable topographies appear during action periods of different data folds and by the fact that stable topographies extracted during preparation and action periods might reflect the sequential activations of spatially different brain areas. In this regard, prior neurophysiological investigation demonstrated the activation of separate cortical areas – i.e. the supplementary motor area (SMA) and the primary motor area (M1) – during the preparation to perform a motor task up to 2s before task onset [116, 117]. Summarizing, these results show that preparation and action periods present a very similar set of stable topographies, even though these patterns are not as similar as we found by comparing action periods of different data folds.

Stable topographies are shared among subjects

In addition to previous analyses, we tested whether the stable topographies extracted from single trials are shared among different subjects. To do so, we correlated stable topographies extracted during action periods across different subjects, fold by fold. **Fig. 2.5** shows the average γ_s across subjects. Even though all subjects show a significant correlation with at least one other subject (two tailed unpaired ttest, p<0.01), seven of them show an average $\gamma_s > 0.85$, implying a very consistent set of stable topographies across different data folds and subjects.

In our knowledge, this is the first time that shared stable topographic patterns are characterized on single-trial and single-subject movement-related EEG data. Our results show that a basic stable topographic codebase is shared across subjects. Interestingly, the scalp distributions we found in our experiment are consistent with stable topographies previously characterized for group-averaged data during wakeful rest in a normative study [75] (shown in **Fig. 2.6**. Besides, the subject independent structure of stable topographies during the exe-
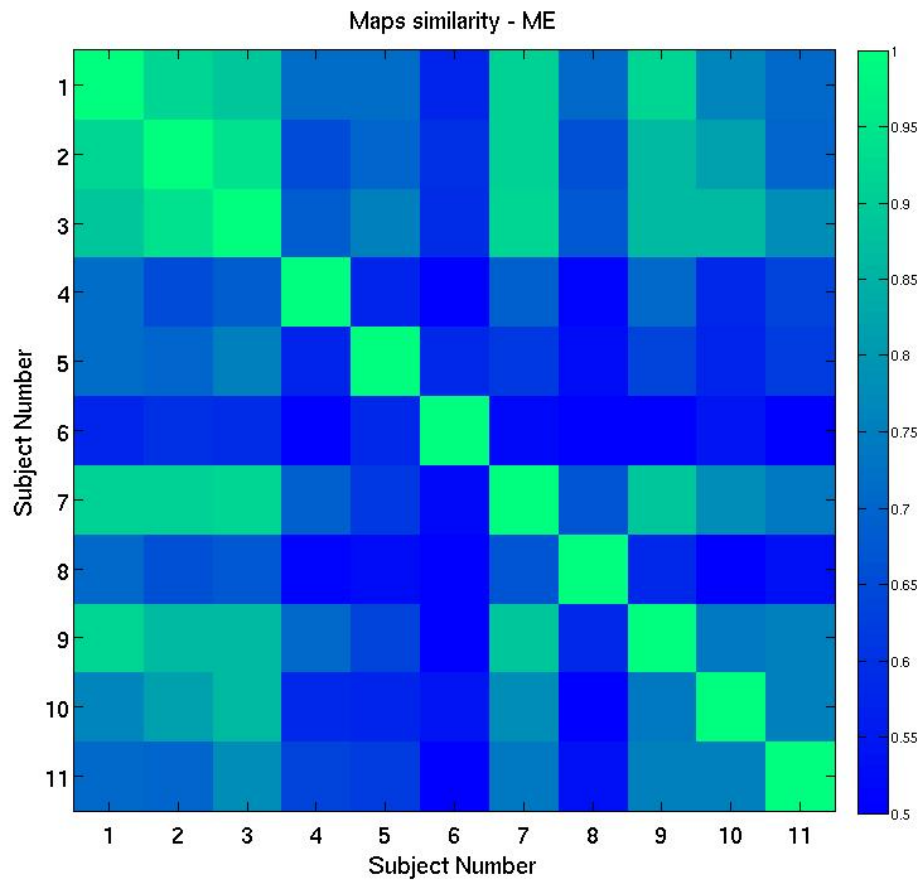
Figure 2.5: **Subject-independent structure of stable topographies.** Stable topographies extracted during action periods across different subjects were correlated, fold by fold. This figure shows that average γ_s values above 0.85 for 7 subjects, representing very similar sets of stable EEG topographies.
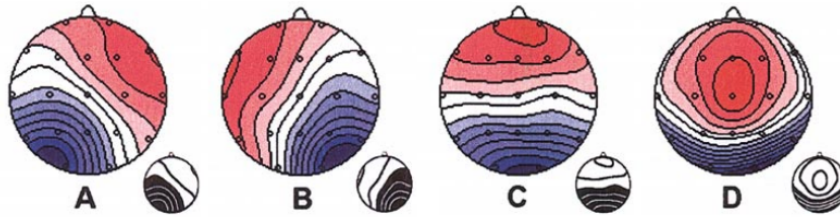
Figure 2.6: **Stable EEG topographies extracted from average resting data.** Stable topographies extracted from 2-s eyes closed resting average data collected from 496 healthy subjects. Map areas of opposite polarity are arbitrarily coded in red and blue using a linear color scale, left ear is left, nose is up. Note that the four topographies extend over wide scalp areas and are likely to represent global brain electric events. Reproduced from [75].

cution of a movement and resting recalls the well documented spatially consistent structure of fMRI-RSN [35], highlighting the fact that not only similar spatial activation over the cortex is found for active tasks and wakeful rest, but that these patterns are also well spread across subjects.

2.1.7 Discussion

In this study, we demonstrate that GFP can be used to discriminate a motor task from rest on single-subject and single-trial data and that a subject-independent topographic structure emerges from the EEG through single-trial analysis of stable topographies generated during the execution of a movement or resting. This evidence is further supported by consistence in the stable topographies extracted across independent same-subject data partitions. Our results also demonstrate that the set of stable topographies isolated during action periods of single trials is essentially preserved, for each subject, during preparatory phases. In other words, we find that sets of stable topographies extracted from action periods of single trials are shared among different subjects. The use of multivariate topographic analysis techniques allowed us to characterize the motor task with no a-priori information concerning the spatial-spectral location of EEG signatures.

The classification framework we used in this study expands current state of the art methods in single-trial topographic analysis [143, 144]. In particular, with respect to the method proposed in [143], few important differences have to be highlighted: first, we use a one-dimensional signal, the GFP, to classify single trials, assuming that during a motor task a more ordered topographic structure will timely appear with respect to rest. The hypotheses that drove us to do so is that stable topographies represent spatially segregated cortical networks, and that given the high temporal resolution of EEG more information about the task would be encoded in the temporal appearance of certain topographic patterns, rather than in small changes in voltage distribution across the scalp. The former of these hypotheses is strongly supported by multimodal fMRI-EEG research showing that not only rapid fluctuations of

stable EEG topographies are correlated with some fMRI-RSN, but that networks associated to stable topographies correspond to a range of previously described RSNs [154]. The latter of our hypotheses is supported by the classification results shown in **Fig. 2.3**, showing that we are able to decode single-trial information from GFP in eight of the subjects with strong statistical evidence, but even in those where we were not able to achieve a classification result above chance, we find a single-trial classification accuracy, on average, above 65%. Furthermore, using GFP has the advantage of not requiring any additional delay due to signal processing, and it appears suitable for novel BCI applications that might require a reliable yet fast classification of EEG potentials.

The second difference with respect to state-of-the-art methods concerns the number of stable topographies extracted from data. As previously mentioned, the number of stable topographies is chosen a-priori in GMM clustering. The choice of the optimal number of states to consider is highly dependent on the application of interest. Different approaches have been proposed, normally by either maximizing signal reconstruction (i.e. the global explained variance of the reconstructed signal as compared to the original) [113] or by maximizing the classification accuracy in the case of single-trial topographic analysis [143]. It is important to highlight a fundamental difference between group average and single-trial analysis procedures: dealing with individual subjects and trials waveforms instead of averages, grand-averages or even mean grand-averages introduces a substantial variability in the data that needs to be taken into account when we look for stable EEG topographies. For these reasons, rather than looking for the optimal number of clusters for each subjects and condition, we select N_μ a-priori and justify this choice by post-hoc analysis. Furthermore, the choice of imposing the same number of stable topographies across subjects simplifies comparability and reduces the number of free parameters to discuss. We quantified the effects of different number of patterns N_{mu} by repeating the whole classification procedure with the occurrences of each stable template map, instead of GFP. Classification results like the ones presented in **Fig. 2.7** are further averaged across subjects as to have a single number to quantify group performance and a single number obtained by iteratively repeating the classification procedure on data having randomly permuted condition labels. **Fig. 2.7** shows that models with $N_\mu = 4, 5, 6$ pass the permutation test. An absolute maximum is obtained for $N_\mu = 5$, justifying our choice of $N_\mu = 5$ for each individual in this study. We also highlight the fact that the overall performance is very similar for $N_\mu = 4, 5, 6$. Finally, the methodology we propose in this study tends to disadvantage high numbers of clusters, as the appearance across time is affected by the absolute number of considered stable topographies.

The use of a 5-fold cross-validation procedure was essential to establish the predictive power of GFP occurrence across time. The choice of 5 equal folds of data is arbitrary but reasonable, iteratively using 80% of the data as training set and 20% as test set, as often done in single-trial brain imaging studies [127, 87]. Still, given the limited amount of available data, it is not obvious to show consistent results across data partitions both in terms of classification accuracy and of stable EEG topography. Indeed, one criticism that might arise is that classification
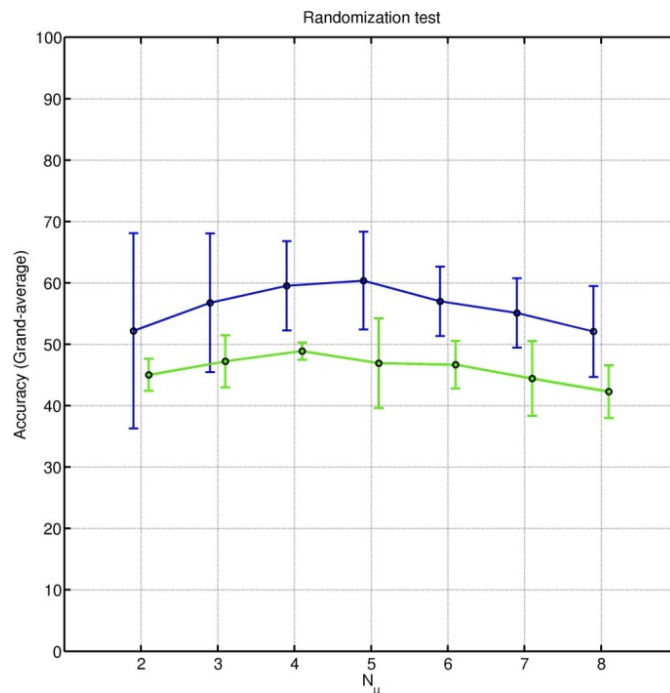
Figure 2.7: **Number of states.** Effect of the number of states N_u on the predictive power of stable EEG topographies occurrences (blue line); this performance is compared to random shuffling of the data (green line).

performance shown in **Fig. 2.3** does not always refer to the same stable topographies and that repeating the extraction procedure, model training and testing across different fold of data would lead to arbitrary results. The consistency check reported in **Fig. 2.4a** and **Table 2.1** clears this doubt showing that nearly identical topographies are extracted across different data folds.

An interesting point of discussion arising from the results reported in **Fig. 2.4b** and **Table 2.1** is that stable topographies extracted during preparation periods of single trials are very similar to those extracted during action periods. In our opinion, these results might reflect the sequential activations of spatially different brain areas – i.e. activations of the supplementary motor area (SMA) and of the primary motor area (M1) – during the preparation to perform a movement up to 2s before task onset [116, 117]. This type of activation, in other words, would still differentiate the preparation of a movement from the first 4s of resting trials.

We find worth mentioning that the 5 stable topographies we identified for each of our subjects consistently appear in several studies about resting EEG, including a seminal multi-center study involving 496 subjects between 6 and 80 years determining 4 stable EEG topographies extracted from group-averaged data as the most representative of eyes-closed resting, specifying their average duration and latency of appearance [75]; the choice of 4 stable topographies, is mostly related to signal reconstruction considerations, and no single-trial analysis is performed. This, observation, together with the topographic consistency during preparation and

action periods shown in **Fig. 2.4b** and **Table 2.1**, supports the idea that a similar topographic codebase is shared across subjects and task, and that the appearance across time of some of the members of the codebase is modulated depending on the task, as reported in **Fig. 2.3**.

On top of the similarity between stable topographies we isolated for each subject and the four traditional stable topographies isolated during resting [75], reported in **Fig. 2.6**, we find that all our subjects present a stable topography having its spatial configuration consistent with the "motor map" identified through EMG aligned-averaged EEG, described in [21], both appearing during preparation and action periods of their experiment.

Another interesting discussion point is the fact that the topographic patterns we identified during action periods of single trials are very consistent with more recent studies concerning the link between topographic EEG patterns and fMRI-RSNs, greatly speaking about their physiological meaning. Indeed, an important property of stable EEG topographies suitable to understand the link with fMRI-RSN is the fact that they have statically self-similar, scale-free (fractal) dynamics – explaining why statistical correlations between fMRI-RSNs and two order of magnitude faster stable topographies are preserved [146]. Concerning our study, shared topographies (reported in **Fig. 2.5** greatly resemble those found in [154], reproduced in **Fig. 2.8a**: qualitatively, our results resemble the patterns presented in their study, having the patterns of 2 of our subjects consistent with stable topography associated to Sensorimotor2 and Attention fMRI-RSNs (i.e. topographic template 4), and the remaining 9 subjects having patterns consistent with the topographic template associated to Sensorimotor1 fMRI-RSNs (i.e. topographies 10, 11, 12). Considered at a group level, many of the topographies of **Fig. 2.2c** and their average greatly resemble topographic distributions that were related to structures playing a critical switching role between default mode and central-executive function [139], see for example Map 3 described in [17], reproduced in **Fig. 2.8b**.
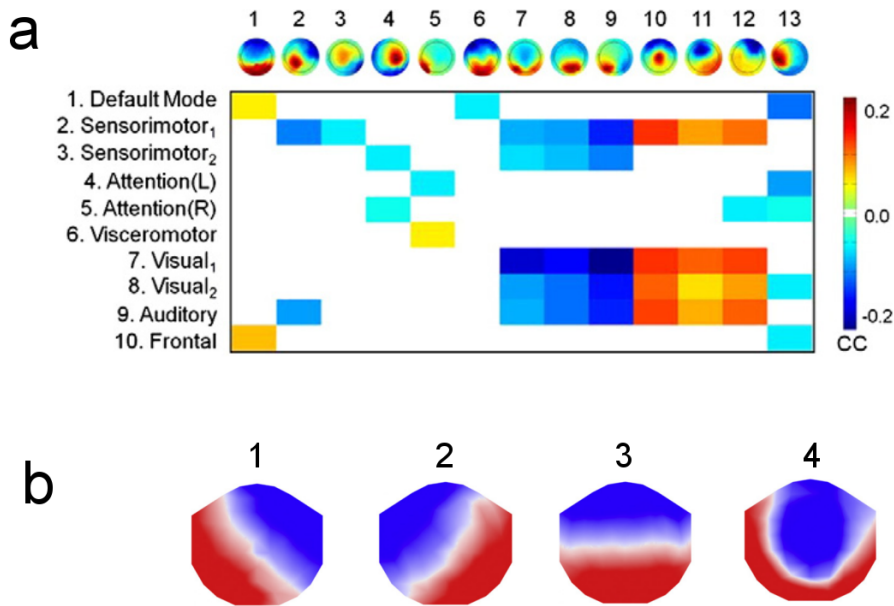
Figure 2.8: **Stable topographies as electrophysiological signatures of fMRI-RSN.** a) Pair-wise correlation coefficient (CC) between the time courses of thirteen temporal independent EEG stable topographies and ten fMRI-RSNs. Note that the relationship between microstates and RSNs falls into three categories. Topographies 1–6 each correlated with only one or two RSNs. In contrast, topographies 7–12 are similarly correlated to sensorimotor, visual and auditory networks. Topography 13 was correlated to several RSNs. Reproduced from [154]. b) EEG stable topographies identified at the group level and BOLD activations revealed by GLM and ICA. Stable topography 1 group-level template map, BOLD activations revealed by GLM regression of its time course and the corresponding correlated IC spatial map were located in bilateral temporal areas. Stable topography 2 group-level template map, BOLD activations revealed by GLM regression of its time course and correlated IC spatial map were located in bilateral extrastriate visual areas. Stable topography 3 group-level template map, BOLD activations revealed by GLM regression of its time course and correlated IC spatial map were located in the ACC and bilateral inferior frontal areas. Stable topography 4 group-level template map, BOLD activations revealed by GLM regression of its time course and correlated IC spatial map were located in right superior and middle frontal gyri as well as the right superior and inferior parietal lobules. Reproduced from [17].

2.2 Stable EEG topographies sequencing in stroke survivors[2]

Outlook. *Non–Invasive BCI systems convey a great potential in the field of stroke rehabilitation, where the continuous monitoring of mental tasks execution could support the positive effects of standard therapies. In this study, we combine time-frequency analysis of EEG with the topographic analysis to identify and track task–related patterns of brain activity emerging during a single BCI session. Six Stroke patients executed Motor Imagery of the affected and unaffected hands: EEG sites were ranked depending on their discriminant power (DP) at different time instants and the resulting discriminant periods were used as a prior to extract the stable EEG topographies. Results show that the combination of these two techniques can provide insights about specific motor–related processes happening at a fine grain temporal resolution. Such events, represented by stable EEG topographies, can be tracked and used both to quantify changes of underlying neural structures and to provide feedback to patients and therapists.*

2.2.1 Experimental protocol

Six Stroke patients suffering from left or right hemisphere lesions participated in the experiment at Fondazione Santa Lucia, Rome, Italy. The subject was comfortably seated in an armchair placed in a dimly lit room with her/his upper limbs on a desk, visible to her/him, with hand posture on a side view. A screen is positioned on the desk in front of the patient and she/he is provided with a visual feedback. Scalp EEG potentials are collected from 61 positions (according to an extension of the 10- 20 International System), bandpass filtered between 0.1 and 70 Hz, digitized at 200 Hz and amplified by a commercial EEG system. Each session is divided in runs consisting of 30 trials, temporally determined by a cursor appearing in the low center of the screen and moving towards the top at constant velocity on a straight trajectory. Total trial duration is 9 s; inter-trial interval is 1.5 s.

During rest trials (**Fig. 2.9**; rest trial timeline), the patient is simply asked to watch the cursor's trajectory on screen. During motor task trials (**Fig. 2.9**; "Movement" trial timeline), a green rectangle appears on top of the screen (rectangle's width is 100% of screen width, rectangle height equals to 57% approximately of screen length, occupying the last 4 s of cursor trajectory) and the patient is asked to start performing the cued motor task (motor execution/motor imagery, unaffected/affected hand) when cursor reached the green rectangle and to continue until the end of trajectory. Each run is dedicated to a different motor task. Two different motor tasks (A and B) are examined. Task A consists of tonic grasping movement, Task B is a tonic complete finger extension.Command sequence is randomized. Runs of the the EEG session include 15 ± 1 rest trials and 15 ± 1 motor trials (total 30). The EEG session starts with the unaffected hand: in the first run the patient is asked to move his hand (first run - Task A, second

---

[2]This section was adapted from Biasiucci, A., Chavarriaga, R., Hamner, B., Leeb, R., Pichiorri, F., De Vico Fallani, F., Mattia,D., Millán, J.d.R. (2011) **"Combining discriminant and topographic information in BCI: preliminary results on stroke patients."**, 5th International IEEE/EMBS Conference on Neural Engineering (NER) [9]. **Contributions:** D.M. designed the protocol, D.M., F.P., F.d.V.F. coordinated and executed clinical data recordings, A.B., R.C., R.L., J.d.R.M. designed the analyses, A.B., B.H. developed the methods, A.B., J.d.R.M. analyzed the data.

run - Task B); in the following 2 runs the patient is asked to imagine the same movements (1 run - Task A, 1 run - Task B). The second part of the session involved the affected hand: in this case, if execution is not possible at all, patient is just asked to attempt the movement. In the remaining of this study we focus only in the motor imagery tasks.

––––––––––––– Rest trial timeline –––––––––––––––––>

Phase	ITI	Cue	Cursor		Post
Patient's screen	Blank screen	Target on	Cursor moves through the screen		Still
Instructions	Rest	Rest	Watch the cursor		Stop

←— 1.5 s —→←— 1 s —→←——— 3 s ———→←——— 4 s ———→←— 1 s —→

––––––––– "Movement" trial timeline –––––––––––––>

Phase	ITI	Cue	Preparation	Task	Post
Patient's screen	Blank screen	Target on	Cursor moves towards the "go" area	Cursor moves inside the "go" area	Still
Instructions	Rest	Rest	Get ready	Go	Stop

←— 1.5 s —→←— 1 s —→←——— 3 s ———→←——— 4 s ———→←— 1 s —→

Figure 2.9: **Single-trial description.** Analysis for this study was constrained to the first 2 seconds of the "Go" window. "rest" trials were analyzed in the same time window.

2.2.2 Methods

The techniques provided in this section aim at combining a discriminant analysis with the topographic analysis of EEG signals. Briefly, discriminant analysis was used to select time windows within each run when EEG task-specific activity was localized over motor areas. Then, topographic analysis was performed on the selected window to assess whether the discriminant activity was reflected on changes in the duration or occurrence of the obtained stable EEG topographies.

To do so, we first computed EEG Power Spectral Densities (PSD) for all electrodes and then ranked the contributions of all channels in all frequency bands through Canonical Variate Analysis (CVA) [55]. Furthermore, we considered different intervals of the spectrogram to characterize changes of discriminability in time. Then, the most informative time window was selected for further topographic analysis; we defined this procedure "time–constrained topographic analysis". EEG signals extracted from the informative window were clustered in topographic maps whose number of occurrences per second and average durations were then compared for every task (i.e. MI of the unaffected and affected hands movements – UH and AH respectively) against rest condition.

2.2.3 Power spectral density estimation & canonical variate analysis

As a first step the 16 most external electrodes were discarded to avoid muscular contamination on the data (i.e. electrodes FPZ, AF7, AF8, F7, F8, FT7, FT8, T7, T8, TP7, TP8, P7, P8, PO7, PO8, Oz), then EEG signals were down-sampled to 128 Hz and referenced to the Common Average Reference (CAR) before estimating their power spectral density (PSD) in the band 4–28 Hz with 4 Hz resolution over a window of 2 seconds from trigger onset. The PSD was computed every 50 ms using the Welch method with 5 overlapped (25 %) Hanning windows of 500 ms.

Following previous studies, we computed the Discriminant Power (DP) of each feature using Canonical Variate Analysis [55]. For this study, we were interested in using this frequency analysis to determine when salient motor–related EEG features were more likely to appear in time. Consequently, we extracted the DP information of non–overlapping spectrogram blocks lasting 500ms. For every block, we computed the most discriminant electrodes for all frequency bands as the ones having a value equal or greater than 70% of the DP maximum and checked whether activity in the motor areas (i.e. electrodes FC5, FC3, FC1, FCz, FC2, FC4, FC6, C5, C3, C1, Cz, C2, C4, C6, CP5, CP3, CP1, CPZ, CP2, CP4, CP6) was highly discriminant. We then picked the most discriminant electrodes covering motor areas from every time frame and we compared which of those showed the highest DP value. The time window associated with this most discriminant activity was finally selected for the topographic analysis.

2.2.4 Stable EEG topographies

Epochs were extracted from each subject depending on the salient time window selected through the discriminant analysis described above. In the case of no discriminant pattern covering motor areas epochs were extracted in the interval from 0 to 2s after trigger onset. Stable topographies were computed from concatenated epochs of MI condition and resting with a modified version of the k-means clustering algorithm [113]. To extract k stable EEG topographies, this algorithm used the time-domain EEG signal, took each time instant as a 64-dimensional vector, and then clustered the time instances based on their vector orientations. It is initialized with k 61-dimensional unit vectors of random orientation, and then alternates between a cluster-assignment phase and a dictionary-update phase until convergence is reached. In the cluster-assignment phase, each time instance was assigned to the dictionary element with the maximal magnitude cosine similarity. In the dictionary-update phase, for each dictionary element, the sum of the self-outer products of the associated time signals was taken, and the dictionary element was updated to the normalized dominant eigenvector of this matrix. We extracted a number of $k = 5$ maps per subject and condition.

Once the set of stable topographies was learned, the time-domain signal was clustered with an additional penalty to encourage smoothness of the resulting signal. Following previous studies[113], we used values of the window size $b = 3$ and smoothness penalty $\lambda = 5$. The smooth signal allowed for measurements of the occurrences and duration of the stable topographies that were not corrupted by random fluctuations in the EEG signal.

The number of map occurrences per second and mean duration (ms) of each topographic template were calculated and compared to the occurrences and duration of those from the respective rest trials. Percentage variations (MI vs rest), were computed as follows:

$$(\Lambda_{Map,MI} - \Lambda_{Map,rest})/\Lambda_{Map,rest} \cdot 100, \tag{2.7}$$

where Λ represents either map occurrences or mean duration.

Obtained maps for one of the subjects are shown on **Fig. 2.10**. EEG Stable EEG topographies provide physiologically relevant maps [106] that range from a motor–related lateralization (**Fig. 2.10** - map 3) to muscular artifacts such as eye blinks (**Fig. 2.10** - map 4).
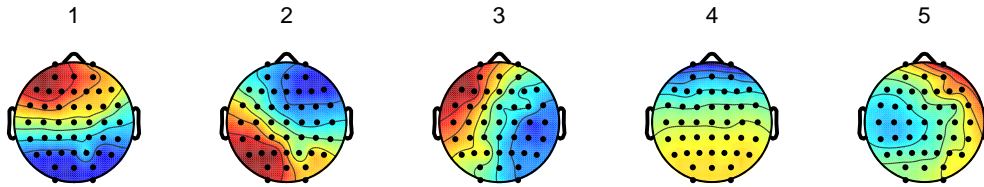
Figure 2.10: **Exemplary topographic template in a Stroke Patient.** Extracted topographic templates for chronic stroke patient S6 (lesion on left hemisphere) performing MI of grasping movements (Task A) of the affected hand.

2.2.5 Results

The discriminant analysis identified different combinations of electrode locations and frequencies as the peak of most discriminant activity in the four considered time frames from 0 to 2s. **Table 2.2** provides, for every subject and condition, the electrode, frequency and time frame containing the most discriminant information. Reported spatial locations and frequency are compatible with current BCI literature for MI tasks. In four of the analyzed conditions (namely S1 - AH A, S4 - AH B, S6 - AH A, S6 UH B), no discriminant activity was found over motor areas. It is worth noticing that three of these cases correspond to motor imagery of the affected hand.

Concerning the time–constrained topographic analysis, **Table 2.3** provides the percentage variation in terms of occurrences per second and average map durations, for every subject and condition. Note that, since stable topographies are extracted independently for every condition, no comparison can be made column-wise. Variations in map occurrence were consistently larger than changes in average map duration. The maps associated with the two strongest variations in occurrence for every conditions are highlighted on **Table 2.3**. Remarkably, maps that exhibit the largest occurrence variation show a common lateralized trend in at least one of the two selected with this simple rule, and this was observed for most of the subjects. Values "N/A" refer to maps that, after the smoothing described in Section 2.2.2,

Table 2.2: **Discriminant analysis results (Affected and Unaffected Hand: AH, UH respectively)**

Sub.(Lesion Site)	Task	Electrode	Freq. [Hz]	Time Win. [s]
S1(L)	AH – B	-	-	-
	AH – A	CPz	16	0.5-1
	UH – B	CP2	16	0.5-1
	UH – A	C3	12	0-0.5
S2(R)	AH – B	CPz	12	0-0.5
	AH – A	C6	28	1-1.5
	UH – B	C2	24	0-0.5
	UH – A	FC6	28	0-0.5
S3(L)	AH – B	C5	4	0-0.5
	AH – A	FC6	16	0-0.5
	UH – B	CPz	4	1.5-2
	UH – A	C3	20	0-0.5
S4(R)	AH – B	-	-	-
	AH – A	FC4	16	0-0.5
	UH – B	FC2	4	0.5-1
	UH – A	C2	28	0.5-1
S5(R)	AH – B	FCz	8	0-0.5
	AH – A	Cz	16	0.5-1
	UH – B	C1	12	0-0.5
	UH – A	CPz	16	1-1.5
S6(L)	AH – B	C1	4	0.5-1
	AH – A	-	-	-
	UH – B	-	-	-
	UH – A	C3	28	0-0.5

do not occur at all in the selected window.

Since the topographic analysis was performed on the time windows obtained from the discriminant analysis, this suggests that the maps that exhibit large variations are related to task-specific EEG topographies. This is particularly important for the case of stroke rehabilitation, since it is possible to continuously monitor the generation of topographic maps with a fine temporal resolution.

2.2.6 Discussion

This study aims at combining standard BCI discriminant analysis with stable topographies extraction in order to identify potential EEG topographies related to motor imagery. The use of a discriminant framework allows us to constrain the analysis on a relevant time window related to motor imagery only. Furthermore, the use of stable EEG topographies can capture short, transient and stable voltage configurations on the scalp, thus providing insights on

Table 2.3: **Topographic analysis - Occurrences (Duration)**

	Task	% Variation, MI vs rest				
		Map 1	Map 2	Map 3	Map 4	Map 5
S1(L)	AH – B	41 (34)	-11 (-23)	**81 (30)**	**-77 (-29)**	N/A
	AH – A	0 (-8)	**-24 (-5)**	18 (10)	**35 (14)**	N/A
	UH – B	-6 (-17)	**-88 (-48)**	**417 (191)**	33 (-7)	N/A
	UH – A	1 (-49)	15 (21)	**404 (42)**	**100 (11)**	N/A
S2(R)	AH – B	**45 (66)**	-32 (-19)	16 (-3)	22 (50)	**-38 (-35)**
	AH – A	-13 (11)	12 (-8)	53 (15)	**-57 (-39)**	**200 (36)**
	UH – B	6 (-18)	-8 (-22)	**22 (3)**	**71 (-6)**	0 (-1)
	UH – A	**8800 (100)**	-60 (-57)	-36 (-1)	44 (15)	**800 (108)**
S3(L)	AH – B	0 (30)	-1 (10)	8 (-13)	**-48 (-22)**	**-87 (-18)**
	AH – A	2 (-32)	**34 (98)**	**-99 (-89)**	N/A	N/A
	UH – B	-19 (-9)	-35 (-30)	**63 (12)**	53 (1)	**205 (29)**
	UH – A	40 (42)	9 (12)	**-66 (-28)**	-2 (4)	**-56 (-12)**
S4(R)	AH – B	-4 (308)	-58 (-18)	**-80 (-44)**	**-62 (-31)**	N/A
	AH – A	3 (-27)	7 (-3)	**73 (37)**	**-10 (-25)**	N/A
	UH – B	0 (14)	29 (7)	**131 (35)**	-36 (-27)	**-57 (-23)**
	UH – A	-13 (49)	**-51 (-17)**	-17 (0)	17 (-3)	**51 (6)**
S5(R)	AH – B	46 (32)	-6 (7)	19 (25)	**89 (43)**	**-78 (-45)**
	AH – A	27 (50)	14 (-8)	**90 (14)**	-80 (-51)	**165 (37)**
	UH – B	-3 (9)	**9 (15)**	**-45 (-2)**	-5 (-5)	N/A
	UH – A	11 (9)	**70 (48)**	-48 (-18)	3 (-14)	**-53 (-27)**
S6(L)	AH – B	3 (0)	**61 (12)**	**-48 (-18)**	28 (4)	-2 (-11)
	AH – A	-10 (-32)	-7 (-7)	**159 (44)**	-39 (-11)	**110 (9)**
	UH – B	-33 (-39)	-12 (-17)	**94 (40)**	42 (15)	**124 (15)**
	UH – A	**73 (37)**	5 (9)	-23 (-2)	-25 (-14)	**-59 (-24)**

underlying mental processes.

Given the fact that selected topographies have been extracted and analyzed in the most discriminant time frame in terms of modulation of motor–related rhythms [119], they are very likely to be related to the short and transient mental processes associated with the motor imagery of the affected and unaffected hand. We believe that the results we present in this study strongly motivate further analysis in this direction, especially correlating functional recovery to BCI performance.

This time–constrained topographic analysis shows that changes in maps occurrence, rather than in their average duration, are more significant when comparing MI against rest. This suggests that the frequency of appearance of particular maps may be a good indicator of proper execution of the rehabilitation tasks. Consequently, it could be possible to use this measure to provide online feedback for therapists supporting the rehabilitation process. This will be particularly suited for the applications related to stroke treatments.

As previously proposed [132], the use of combined sessions of standard therapy and BCI-aided rehabilitation can serve as a way to facilitate recovery through mental rehearsal. In addition, proposed techniques represent an imaging modality to monitor long-term changes in produced patterns representing cortical reorganization.

Figure 2.11: **Stable EEG topographies associated to the motor task.** Stable EEG topographies associated with strongest changes in occurrences during motor imagery with respect to rest (see Table 2.3 for details) for Subjects S2 *(top)* and S6 *(bottom)*.

3 Enhancing Motor Function[1]

> There are two ways of being happy: we must either diminish our wants or augment our means - either may do - the result is the same and it is for each man to decide for himself and to do that which happens to be easier.
>
> Benjamin Franklin

Outlook. *Recent studies demonstrated that transcranial Direct Current Stimulation (tDCS) induces selective modulation of cortical excitability. This technique could be used to specifically enhance people's capacity to produce sensorimotor rhythms, normally used by Brain–Computer Interfaces (BCIs). Here we show evidence that tDCS modifies people's ability to generate discriminable patterns during a two-tasks motor imagery protocol, both in spinal cord injured (SCI) patients and able-bodied control subjects. Our results show that discriminant spectral activity is shifted towards the stimulated hemisphere after tDCS, with respect to sham stimulation. Also, we find an interesting carry-over effect of anodal tDCS lasting 60 to 90 minutes after stimulation, resulting in prolonged features discriminability in the stimulated hemisphere in both groups. These findings show that tDCS might be incorporated in BCI systems to achieve more reliable, efficient brain control, and could be used to have more usable BCI-aided assistive technology and neurorehabilitation.*

---

[1] This section was adapted from Chavarriaga, R., Biasiucci, A., Creatura, M., Carrasco C., León, V. S., Campolo, M., Oliviero, A., Millán, J.d.R. (2014), **"Selective Enhancement of Sensorimotor Rhythms for Brain Computer Interaction by Means of tDCS."**, In preparation [27]. **Contributions:** R.C., J.d.R.M., A.O. designed the study, A.B., C.C., V.S.L., M.C. recorded the data, A.B. provided support for the recordings and managed the data, A.B. developed the methods, A.B., R.C., M.C., J.d.R.M. analyzed the data. Preliminary results on a subset of patients are presented is reported in Chavarriaga et al. (2013), **"tDCS Modulates Motor Imagery-Related BCI Features."** In Converging Clinical and Engineering Research on Neurorehabilitation [26].

39

3.1 Methods

3.1.1 Experimental protocol

The study has a 2x2x2 factorial design, wherein factors are spinal cord lesion (presence or absence), stimulation type (anodal or sham tDCS), and time (we recorded data immediately after the stimulation and approximately 60 minutes after). Furthermore, the study was designed as a Consideration-of-Concept study (phase 1 or stage 1 according to the progressive staging of clinical trials proposed by Dobkin and colleagues in 2009 [41]) testing the effect of tDCS on the ability of people to produce discriminable EEG features while performing two different motor imagery tasks. One center in Spain (Hospital Nacional de Parapléjicos, Toledo) was involved in recruitment and therapy.

Twelve subjects with chronic spinal cord injuries (SCI group; 2 women; age 36.4 ± 5.4; lesions site ranged from C4 to C7) took part in the experiment. The lesion levels of these subjects is shown in **Table 3.1**. Thirteen able-bodied subjects also participated in the experiment as a control group (Control group; 7 women; age 33.2 ± 7.7). All patients have impaired or no residual hand functionality. None of them had any prior experience with BCI. The experiment consists of two recordings days separated by at least one week. At the beginning of each recording day, either sham or anodal tDCS was applied during 15 min. Then, subject performs one session of Motor Imagery (MI)-based BCI training (S1). After a pause, a second BCI session (S2) is performed at least one hour after the end of the stimulation (shown in **Fig. 3.2**). The type of stimulation (i.e. sham or anodal) is different on each day, and the order is randomly selected and counterbalanced within each group.

Subject	Age	Time since lesion (months)	Type of lesion
A	31	163.5	C5-C6
B	35	206.6	C7
C	36	209.9	C5-C6
D	41	198.8	C6-C7
E	28	105.3	C5
F	31	97.6	C5-C6-C7
G	42	108.1	C5-C7-D1
H	44	163.3	C3-C5
I	33	6.9	C4
J	40	95.6	C6-C7
AA	43	2.6	C4
AB	33	141.4	C3-C4-C5
Avg ± SD	36.4 ± 5.4	125.0 ± 69.9	

Table 3.1: **Patients information, time since lesion, and lesion level.**

During each BCI session the subject is asked to perform MI of both hands. Each session is
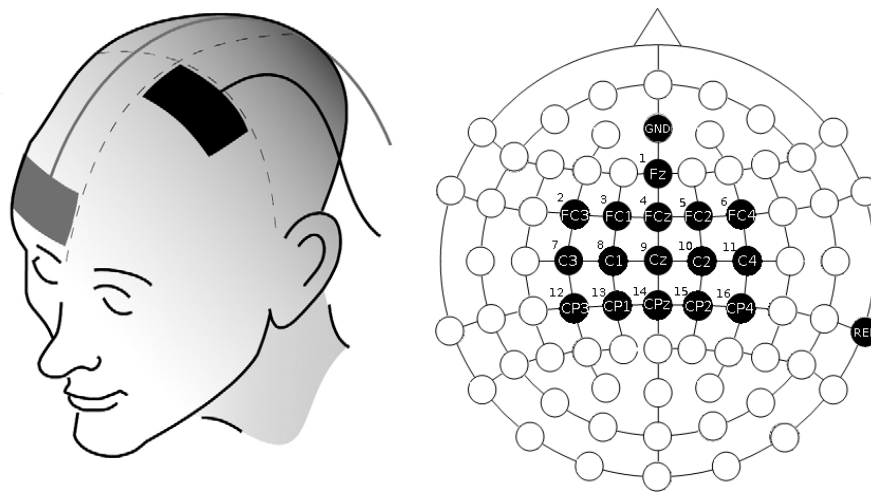
Figure 3.1: **tDCS and EEG montage.** *L*eft, tDCS setup covering the supraorbital region and the primary motor cortex, in order to have anodal stimulation of the primary motor cortex [145]. *R*ight, EEG montage covering premotor and motor areas of the underlying cortex.

composed of 4 runs, where each run contains 15 trials per motor task (i.e left, right MI); plus 5 trials of resting where the subject is asked not to perform any motor task. Each trial starts with a cue signaling the task to be performed and a cursor moving towards the target is presented on the screen (refresh rate 4 Hz), the trial order is randomly selected. The length of one trial is 8s and a time-varying pause is added in between two consecutive trials. The total duration of the session is about 30min.

3.1.2   tDCS stimulation

tDCS (HDCstim, Newronika, Milan) was applied through saline-soaked electrodes (size 50 x 70 mm^2) placed over the left motor cortex (anode, C3 position on 10/20 system) and the supraorbital area (cathode). The stimulation current was set to 1mA and the ramp time was 7s. For sham stimulation sessions, the current was applied for 30 seconds at the beginning of the stimulation and then turned off (20 seconds linear down-ramping until 0 mA was reached). Using this placebo stimulation technique subjects are not able to distinguish between real and sham stimulation [57].

3.1.3   EEG acquisition and processing

EEG (g·tec gUSBamp, Guger Technologies OG, Graz, Austria) was recorded at 512 Hz with 16 active surface electrodes: positions Fz, FC3, FC1, FCz, FC2, FC4, C3, C1, Cz, C2, C4, CP3, CP1, CPz, CP2 and CP4 of the 10/20 system (reference: right mastoid; ground: AFz). The signal was filtered in the [0.1 100] Hz range plus 50Hz notch filter, and spatially filtered with a Laplacian
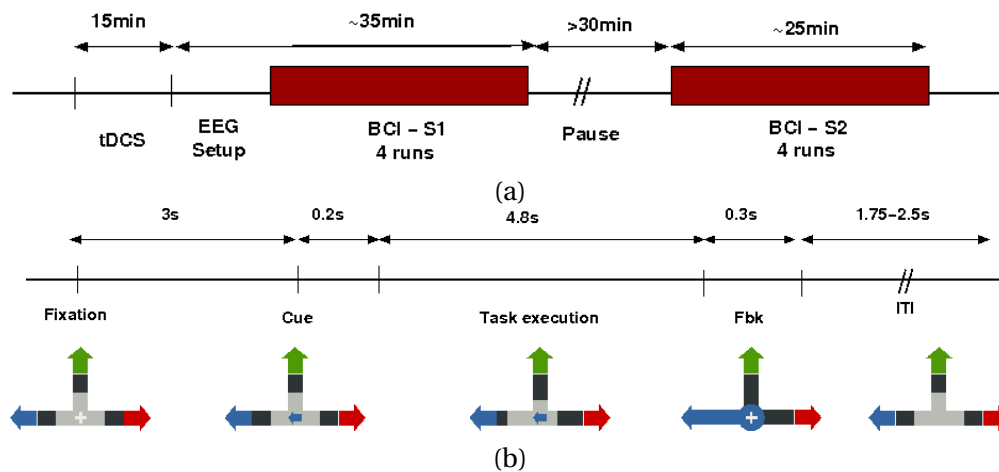
Figure 3.2: **Experimental protocol.** (a) Recording session. During each BCI session the subject is asked to perform motor imagery of both hands. Each session is composed of 4 runs, where each run contains 15 trials per motor task (i.e left, right hand motor imagery) and 5 trials of resting where the subject is asked not to perform any motor task. The total duration of the session is about 30min. (b) Training trial. Each trial starts with a cue signaling the task to be performed and a cursor moving towards the target is presented on the screen (refresh rate 4 Hz), the trial order is randomly selected. The length of one trial is 8s and a time-varying pause is added in between two consecutive trials.

derivation. For each channel we estimate its power spectral density (PSD) in the band 6-28 Hz with 2 Hz resolution over the last second. This process yields per each time sample a total of 192 features (i.e., 16 channels x 12 frequencies) .

The PSD was computed every 62.5ms using the Welch method with 5 overlapped (25%) Hanning windows of 500ms. These PSD features are often used in BCI applications, such as assistive technology [23] and rehabilitation [82]. Another application of BCI for rehabilitation, namely BCI-aided Neuromuscular Electrical Stimulation for Stroke rehabilitation, is presented in **Chapter 4** of this Thesis.

Discriminant analysis of EEG features

We assessed the ability of each feature (16 channels x 23 frequencies) to differentiate between left and right hand motor imagery by computing a score on their discriminant power (DP). This score computed using canonical variate analysis [55]. Changes in the DP are then used to quantify the effect of the stimulation on specific, localized brain activity.

To quantify the effects of the stimulation on specific features, we compared the cumulative DP per feature; i.e., the sum of DPs across subjects of the same group and session. Statistical differences were assessed using Wilcoxon rank-sum test ($p<0.05$).

We also analyzed the effects of group (SCI vs Control), stimulation type (tDCS vs Sham); and order (Day 1 vs day 2). The last condition aims at identifying any learning effect.

The most discriminant features (i.e., highest DP) were selected for further analysis. For the purpose of classification, the number of selected features has to be high enough to capture the process of interest, but it is in turn limited by the number of available trials. In the following analysis we used the 20-top ranked features based on previous experience and preliminary studies (See below).

In order to evaluate whether tDCS resulted in more stable discriminant patterns than sham stimulation, we compared the selected features for the two BCI sessions recorded on the same day (i.e., performed immediately after the stimulation and about one hour after, respectively). For this purpose we compute a stability index that reflects the consistency of the two feature sets [77]. This index, defined in equation 3.1, is equal to 1 if the discriminant features are exactly the same in both sessions, while a value of -1 corresponds to non-overlapping feature sets. Independently drawn feature sets will have values close to zero.

$$I = \frac{r\,n - k^2}{k(n-k)} \tag{3.1}$$

Classification analysis

We also evaluated whether tDCS produces observable changes in the brain activity patterns by performing single-trial classification on the different conditions. As mentioned above, the 20 most discriminant features were selected and used as input for a Gaussian. Classification of the reduced PSD feature vectors is achieved using a Gaussian mixture model (GMM) framework, commonly used in BCI studies [82]. Briefly, the classifier outputs a conditional probability distribution $\vec{p}_t = [p_t^1, p_t^2, ..., p_t^C]$ at time t over the C mental tasks given each feature vector $\vec{x}_t$ [96]. Whereby, $t = 0$ refers to the output timings of the feature extraction and classification which operates at 16 Hz. Therefore, $t = 0$ would be the arrival of the first sample in a trial and $t = 1$ (62.5 ms later in real time) the arrival of the second sample, and so one. t will increase within a trial until a decision is made (threshold reached). Each mental class is represented by a number of Gaussian units (usually $N = 4$). The class-conditional probability distribution function of class i is a superposition of N Gaussian prototypes. Equal priors for the classes and mixture coefficients are assumed, as well as shared, diagonal covariance matrices. The centroids of the Gaussian units are initialized by means of a self organizing map (SOM) clustering and their covariance matrices are subsequently computed as the pooled covariance matrices of the data closest to each prototype. Finally, the distribution parameters are iteratively re-estimated through gradient descent so as to reduce the mean square error (MSE). The training of the Gaussian classifier stops, if the MSE change after each iteration is

not improving, or after 20 iterations at maximum [96].

Two types of analysis were performed. The first one aims at assessing how separable the two conditions are within a specific session. To this end, we trained the classifier using 70% of the data, and tested it on the remaining 30%. The temporal order of the data was preserved, so as to test on the last part of the session.

Furthermore, the stability of elicited patterns was also evaluated by computing the classification accuracy across sessions. To this end, we used a classifier trained on the first session and tested on the second session.

In both cases the classification accuracy was assessed using the area under the receiver operating condition curve (AUC)[48]. This provides a measure of performance where 1 corresponds to perfect classification, and a value of 0.5 corresponds to chance level.

3.2 Results

Discriminant analysis of EEG features

With respect to the spectral features produced by both groups, we find that the able bodied control group shows higher capability, during both anodal and sham tDCS, to produce highly discriminant activity in the μ band (9-11 Hz), as shown in **Fig. 3.3a**. This observation does not apply to the β band, where groups exhibit similar features, shown in **Fig. 3.3b**.

Although small in absolute value, discriminant activity is consistently shifted under the stimulated hemisphere in SCI patients and healthy controls in the μ band **Fig. 3.4, top**. After sham stimulation, on the contrary, SCI patients show no discriminant activity under the stimulated side **Fig. 3.4, bottom**. In addition, we report a reduction in frontocentral-midline discriminant activity in the β (11-19Hz) for the SCI group, further documented through the statistical tests comparing tDCS and sham reported in **Fig. 3.6**.

An interesting carry-over effect seems to be present in both groups after actual tDCS, with no visible effect in the β band **Fig. 3.3**. In particular, the control group showed a significant effect in μ (5-13Hz) and low β (15-17Hz) bands over the stimulated hemisphere. This effect is pronounced during S2 – i.e. approximately 1 hour after stimulation – and might represent a facilitation in the production of stable EEG activity.

Fig 3.7 shows the stability index computed on the 20 most discriminant features for BCI sessions S1 and S2. Overall, control subjects exhibited more stable features after anodal tDCS stimulation, although no significant difference were found. The SCI group showed lower stability than controls in both conditions. Only two subjects in this group have a considerably higher K after sham than anodal stimulation. K-index have similar range values on sham

condition for both SCI and control. In contrast, higher range is shown for control subjects after tDCS.

Classification analysis

Fig. 3.8 shows the classification performance in terms of the area under the ROC curve (AUC), reporting large variability across subjects in both groups (i.e. SCI and control). Control subjects perform significantly better than than SCI subjects (p<0.001, Wilcoxon). Overall, we didn't find a direct effect of anodal tDCS on off-line classification accuracy with the metric we proposed.

3.3 Discussion

We report modulation of motor imagery BCI features by anodal tDCS on motor areas. Both SCI and control subjects showed localized discriminant activity under the stimulated areas that lasts for at least 90 minutes. Contrary to the sham condition, SCI subjects present discriminant activity over motor areas immediately after stimulation. These preliminary results suggest that tDCS may selectively enhance activity of targeted areas so as to produce patterns that can be better recognized by a BCI system, thus improving the potential role that BCI can play in supporting neurorehabilitation.

Remarkably, SCI subjects show bilateral discriminant activity on the first BCI session (S1, immediately after the stimulation), and features under the stimulated hemisphere remained discriminant during the second session. Although small in absolute value, discriminant activity is consistently shifted under the stimulated hemisphere in SCI patients and healthy controls in the μ band. After sham stimulation, on the contrary, SCI patients show no discriminant activity under the stimulated side. An interesting carry-over effect seems to be present in both groups after anodal tDCS. No effect is visible in β band. In contrast, after sham stimulation activity in motor areas was less discriminant on the first session. Similarly, in control subjects, tDCS resulted in strongly localized discriminant information on the stimulation site over the two sessions.

Concerning features stability, feature sets consistency between the two sessions (S1 and S2) show that anodal tDCS has a limited effect in modifying features stability in the SCI group with respect to sham tDCS. It also appears that anodal tDCS might have a stronger impact on the control group, probably representing a facilitation in the production of discriminable EEG features for prolonged periods.

Our results might reflect the modulation of event-related synchronization and desynchronization, as explained by a recent experiment comparing event-related desynchronization of sensorimotor rhythms before and after anodal, cathodal and sham tDCS, as well as the resting

and active motor thresholds of the right first dorsal interosseous muscle [93]. Stimulation lasted 10 min (10 s for sham) with electrodes (50 mm x 70 mm) located on the left M1 (found through transcranial magnetic stimulation (TMS)) and right supraorbital area. Event-related desynchronization increased after anodal stimulation and decreased after cathodal stimulation. No change was observed in the sham condition. Positive correlation was found between the desynchronization and the resting motor threshold of the right FDI muscle, but with no significant correlation with the active motor threshold. They recorded 6 healthy subjects and each subject performed 20 trials per session, 6 sessions per day (3 sessions before and 3 sessions after tDCS). The experiment was performed over 3 days separated by at least one week and the order of the stimulation types was balanced across subjects.

Overall, the effects of tDCS have modest size in SCI patients and they appear to be stronger in healthy controls (although not significant in terms of discriminability). This study extends current knowledge about the effect of tDCS on event-related synchronization and desynchronization on spinal cord injured individuals [81], and could be used as a basis to investigate the role of afferences in the generation of μ EEG rhythms. On this regard, it might well be that the effect on healthy controls is driven by the presence of actual subliminal muscle contractions during motor imagery. Unfortunately, this study does not allow us to draw conclusions on this point, and further research should address this question explicitly.

Concerning the absence of an effect of tDCS on off-line classification accuracy, another study on the effect of tDCS-aided stroke rehabilitation involving a BCI system found no effect on off-line accuracy but an effect on on-line performance [6], providing a hint that an increase in cortical excitability results in enhanced ability to generate EEG patterns. Under the same rationale, our results might provide a starting point for further investigation on the use of tDCS to improve on-line control of assistive technology devices in SCI individuals.

(a) f=10 Hz. Left: SCI. Right: Ctrl

(b) f=26 Hz. Left: SCI. Right: Ctrl
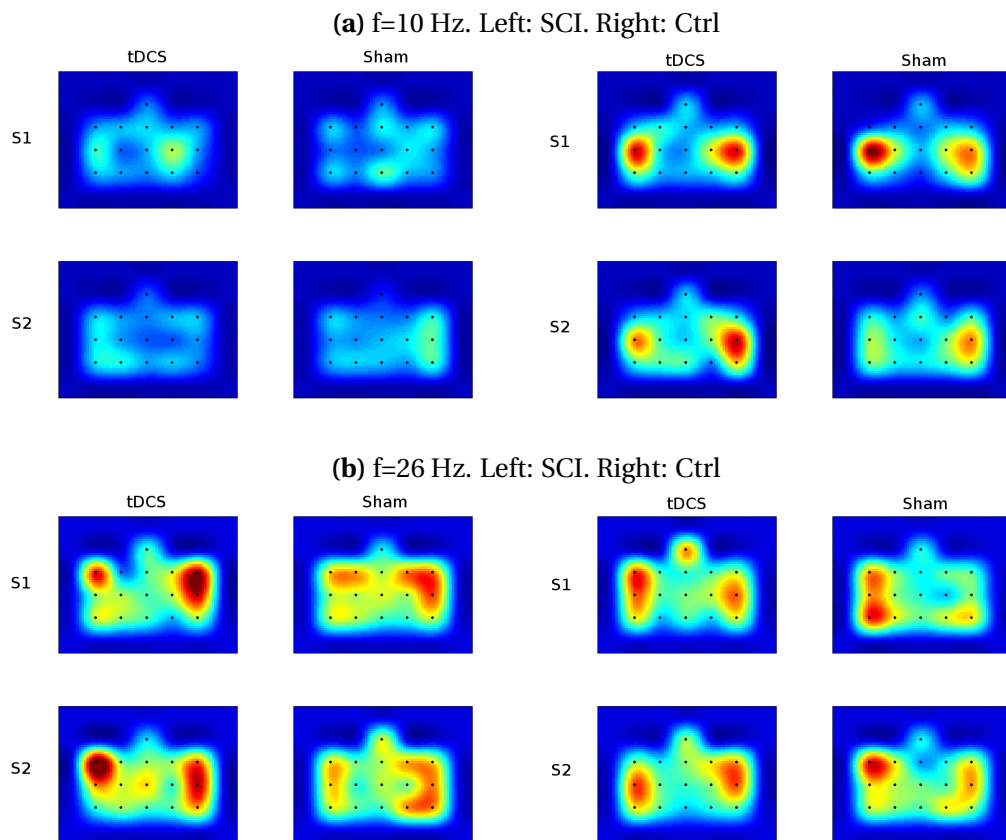
Figure 3.3: **Cumulative Discriminant Power (DP) in μ and β bands.** (a) Topographical localization of discriminant features in the μ band (9-11 Hz) (Top view, Nose up). Left, SCI subjects. Right, Control subjects. Top, first BCI session (right after tDCS). Bottom, Second BCI session (>1hr after stimulation). Left, SCI patients. Right, Control subjects. (b) Same as (a), but in the β band (25-27Hz). Although small in absolute value, discriminant activity is consistently shifted under the stimulated hemisphere in SCI patients and healthy controls in the μ band. After sham stimulation, on the contrary, SCI patients show no discriminant activity under the stimulated side. An interesting carry-over effect seems to be present in both groups after actual tDCS. No effect is visible in β band.
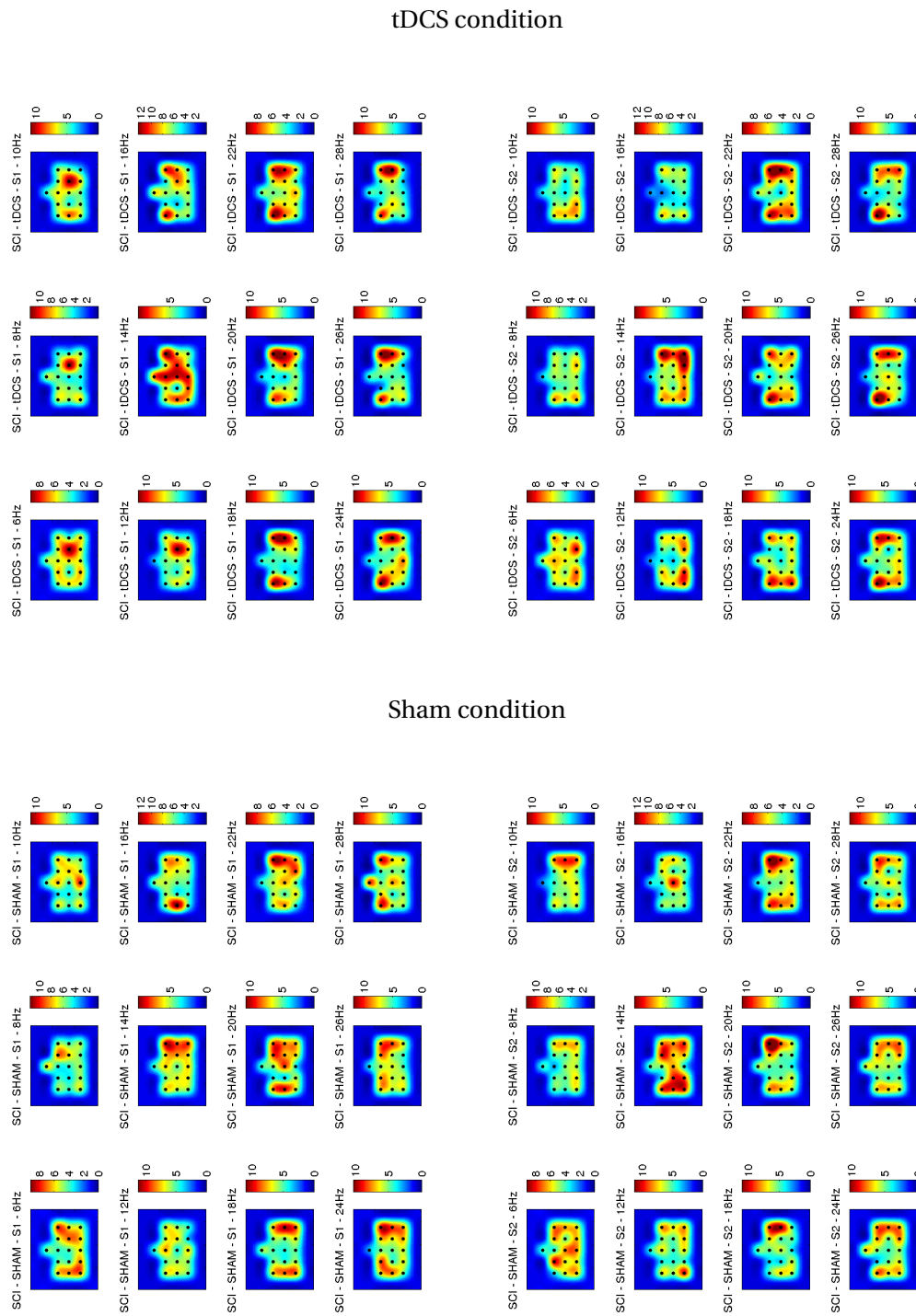
Figure 3.4: **Cumulative Discriminant Activity - SCI group** Topographical localization of discriminant features (nose left) in frequency bands between 5 and 29 Hz. We report a reduction in frontocentral-midline discriminant activity, further documented through the statistical tests comparing tDCS and sham reported in Fig. 3.6.

tDCS condition

Sham condition
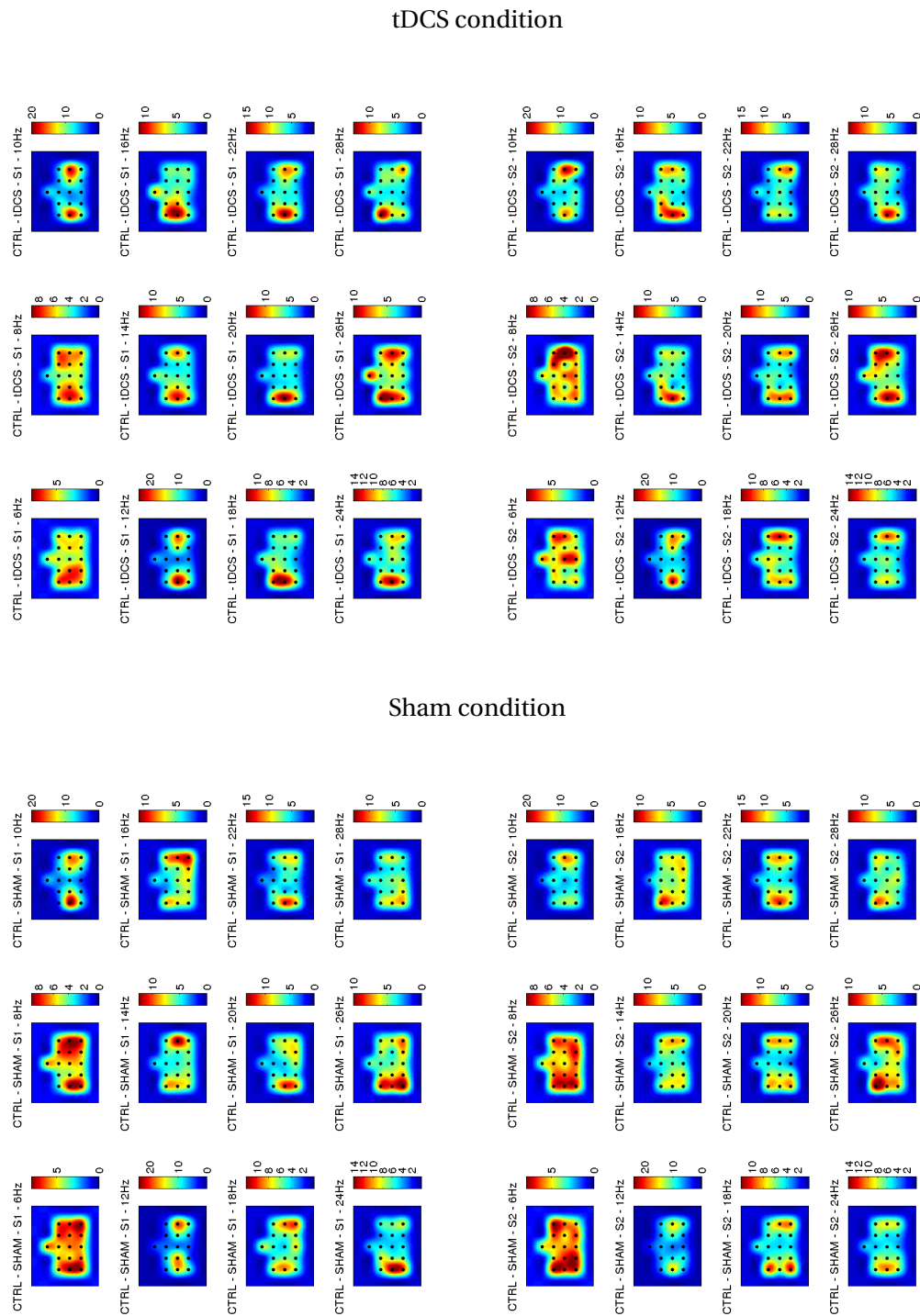
Figure 3.5: **Cumulative Discriminant Activity - Control group** Topographical localization of discriminant features (nose left) in frequency bands between 5 and 29 Hz. First, we report that discriminant EEG activity is distributed over the scalp in a more bilateral fashion and centered on electrodes C3 and C4 with respect to the SCI group data shown in **Fig. 3.6**, representing the activation of contralateral areas during right or left hand motor imagery. Overall,it seems that tDCS effects on healthy subjects allows them to produce stable discriminant patterns for longer time.

Control group

SCI group
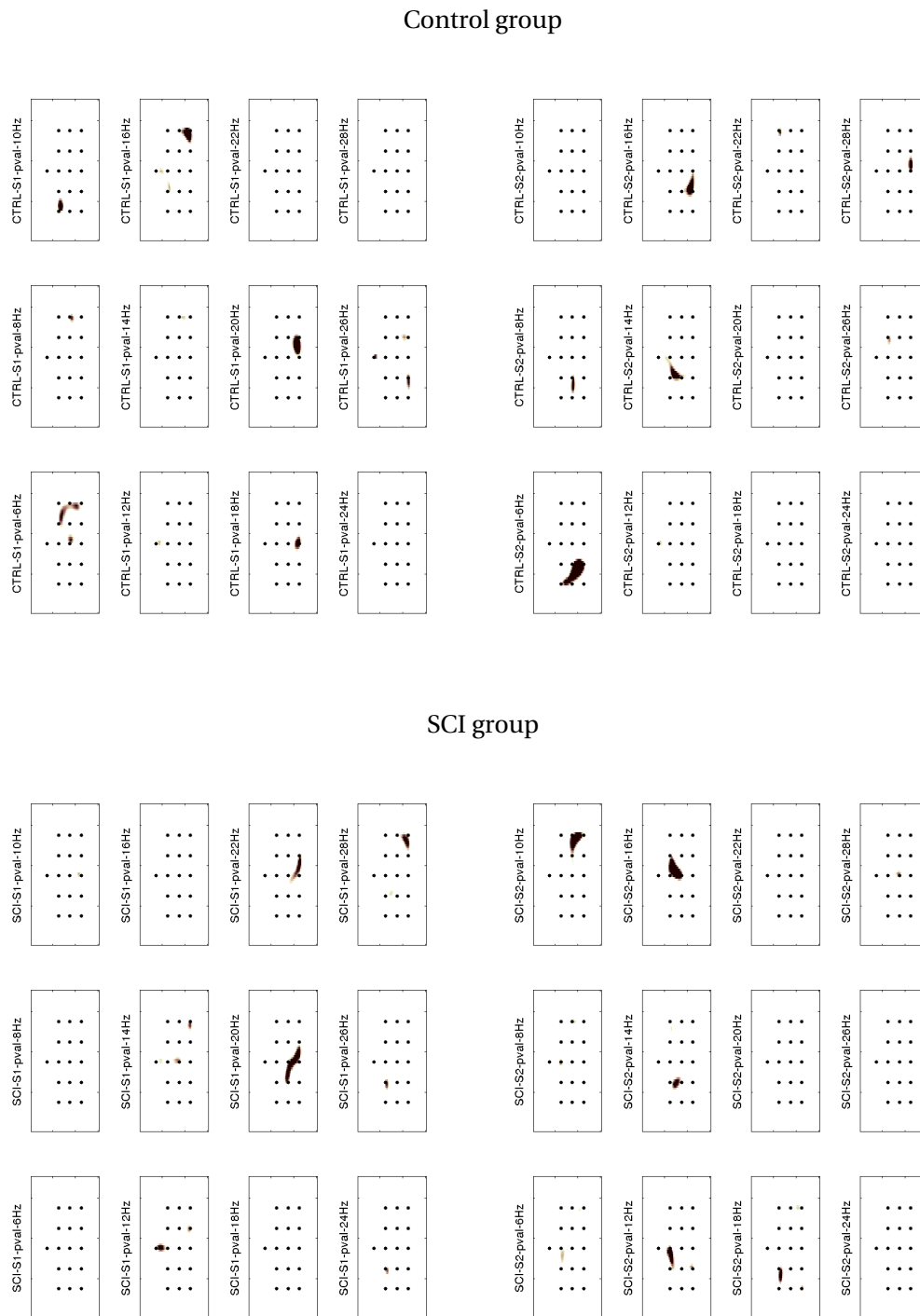
Figure 3.6: **Significant changes in Discriminant Activity due to tDCS** Discriminant activity characterizes left vs right hand motor imagery. Statistical differences were computed by uncorrected pairwise ranksum test (white>0.05) between tDCS and Sham conditions. Control group (top) shows a significant effect in μ (5-13Hz) and low β (15-17Hz) bands over the stimulated hemisphere. This effect is pronounced during S2 – i.e. approximately 1 hour after stimulation – and might represent a facilitation in the production of stable EEG activity. The SCI group (bottom) presents a reduction in frontocentral-midline discriminant activity, with some smaller effect on the stimulated areas in the β (11-19Hz) band.

(b)
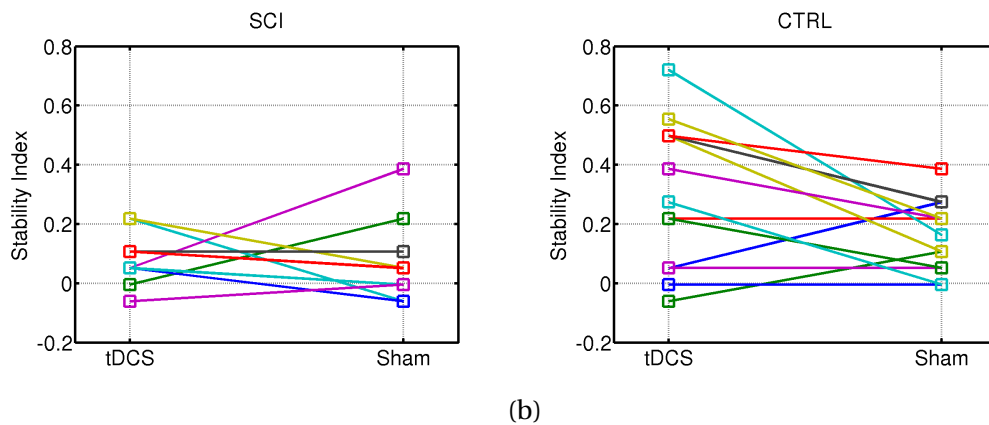
Figure 3.7: **Discriminant EEG features stability.** We tested whether tDCS resulted in more stable discriminant patterns than sham stimulation, by comparing features for the two BCI sessions (S1 and S2) recorded on the same day (i.e., performed immediately after the stimulation and about one hour after, respectively). The stability index reflects the consistency of the two feature sets: when its equal to 1 discriminant features are exactly the same in both sessions, while a value of -1 corresponds to non-overlapping feature sets. Independently drawn feature sets will have values close to zero. *Left* SCI group. *Right* Control group. While tDCS has a limited effect in modifying features stability in the SCI group, it appears to have a stronger impact on the Control group, which might represent a facilitation in the production of discriminable EEG features for prolonged periods.
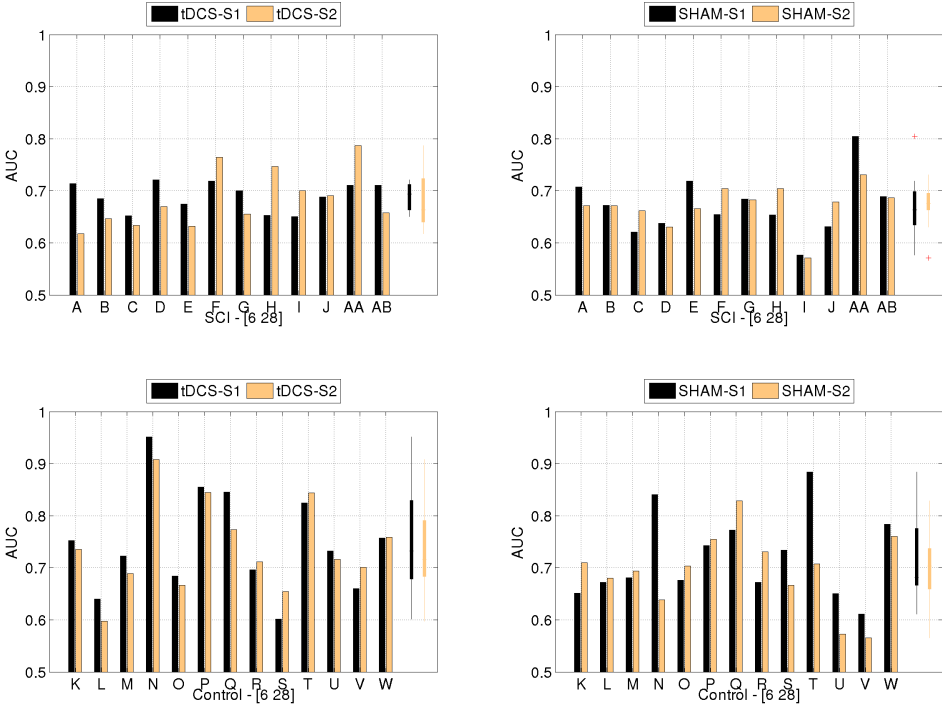
Figure 3.8: **Classification analysis.** Within-session Classification performance (AUC) for both tDCS and Sham conditions (left and right, respectively). *Top*, SCI subjects. *Bottom*, Control subjects. Bars represent the performance for each subject. Boxplots at the right end of each plot show the population distribution for each session.

4 Restoring Motor Function[1]

> You were sick, but now you're well again, and there's work to do.
>
> <div align="right">Kurt Vonnegut</div>

Outlook. *Brain Computer Interfaces (BCI) might be used in rehabilitation to decode motor attempts from brain signals and deliver Neuromuscular Electrical Stimulation (NMES) of the paralyzed limb, temporarily restoring motor function. Unfortunately, the added value of closed-loop neural control for motor recovery is still disputed. In this study, we aimed to assess the effect of NMES therapy triggered by a sensorimotor rhythm BCI over sham NMES therapy. We enrolled 15 chronic patients (>10 months from stroke) with moderate-to-severe arm paresis. Eight patients received BCI-NMES therapy, and seven matching patients received sham-NMES therapy consisting in identical instructions and random delivery of NMES at similar rates and timing as for the BCI-NMES group. Both interventions targeted fingers extension recovery, twice a week for five weeks. Surprisingly high and clinically relevant improvements of affected arm functions were found for subjects in the BCI-NMES group, and retained 36 weeks after therapy end. Only one patient receiving sham-NMES reported functional gains. Despite small group size, we show that feedback training of EEG sensorimotor rhythms, reinforced by the use of body natural pathways through NMES, modifies neural tissue properties both at a local and at a network scale, also in plegic patients and several years after stroke.*

---

[1]This section was adapted from Biasiucci, A., Leeb, R., Al-Khodairy, A., Zhang, H., Schnider, A., Schmidlin, T., Vuadens, P., Guggisberg, A., Millán, J.d.R. (2014) **Brain-Controlled Neuromuscular Electrical Stimulation Promotes Permanent Upper Limb Functional Recovery after Stroke**, In review [11]. **Contributions:** A.B., R.L., and J.d.R.M. designed and coordinated the study. A.A.K., A.S., T.S., P.V., and A.G. enrolled patients. A.B., R.L., A.A.K., T.S., and A.G. collected data. A.B., R.L., H.Z., and J.d.R.M. analyzed the data.

4.1 Methods

4.1.1 Study design and participants.

This sham-controlled, parallel group trial was designed as a Consideration-of-Concept study (phase 1 or stage 1 according to the progressive staging of clinical trials proposed by Dobkin and colleagues in 2009[41], **Fig. 4.10**) testing the added value for motor recovery of BCI-aided neuromuscular electrical stimulation (NMES) over sham NMES. Two centers in Switzerland (SUVACare - Clinique Romande de Réadaptation, Sion; University Hospital of Geneva, Geneva) were involved in recruitment and therapy. Inclusion criteria were first ever cerebrovascular accident resulting in chronic impairment (minimum 10 months from stroke), and moderate-to-severe disability. We used chronic patients because we wanted to isolate effects that are only induced by the rehabilitation therapy, excluding any effect due to spontaneous recovery[41]. All patients were in their plateau phase of recovery, and they all received conventional physical therapy in addition to BCI-NMES or sham-NMES in order to filter out potential effects due to non-use and atrophy. Patients were ineligible if they presented any concomitant neurological pathology.

The institutional ethical committees approved the study protocol and each participant gave written informed consent prior to their eligibility assessment. The trial was performed in accordance with the Declaration of Helsinki. Sensitive data was collected and protected on the servers of the École Polytechnique Fédérale de Lausanne, Switzerland.

4.1.2 Lesion Analysis

Information concerning stroke type (ischemic or hemorrhagic) and location (cortical or sub-cortical) are reported in **Table 4.1**.

4.1.3 Randomization and masking.

Participants were enrolled sequentially and randomly assigned to either receive conventional therapy + BCI-NMES or conventional therapy + sham-NMES. If eligible for the study (provided informed consent and met all inclusion criteria), participants were sequentially given unique patient identification numbers and assigned to a group. Patients were initially enrolled at SUVACare Sion, Switzerland, to the BCI-NMES group. Relevant metrics concerning brain control were extracted from these first four subjects and used to simulate brain control in the sham group (i.e. average time to deliver a brain command, average number of detected commands, average number of repetitions per session). Then, three additional patient received sham-NMES and three more BCI-NMES at SUVACare Sion. The same procedure was replicated at the University Hospital of Geneva, Switzerland, where four patients received

Table 4.1: **Patients information, stroke type, and etiology.**

patient	sex	age (y)	diagnosis	lesion site	lesion side	time since stroke (m)
				BCI-NMES group		
E1	M	64	ischemic	subcortical	right	10
E2	M	71	ischemic	cortical	right	14
E3	M	49	ischemic	subcortical	right	10
E4	F	50	ischemic	cortical	right	19
E5	F	49	ischemic	cortical & subcortical	left	13
E6	F	67	ischemic	subcortical	left	176
E7	F	41	ischemic	subcortical	left	39
E8	M	48	ischemic	cortical & subcortical	right	14
				Sham-NMES group		
C1	M	40	hemorrhagic	cortical & subcortical	right	18
C2	M	58	ischemic	cortical & subcortical	right	23
C3	M	75	hemorrhagic	subcortical	left	15
C4	M	53	ischemic	subcortical	left	21
C5	M	65	hemorrhagic	subcortical	left	38
C6	M	57	ischemic	cortical & subcortical	left	62
C7	F	62	— missing —	— missing —	left	121

sham-NMES and one additional patient received BCI-NMES. This procedure is frequently used in animal studies concerning brain controlled interfaces[60] and was essential to build a conservative sham intervention where the only key therapeutic factor missing is direct brain control (by providing comparable sham therapy). Hardware equipment used during the therapy by both groups was identical, and software tools were developed as to hide whether they would implement actual or sham brain control. Patients and caregivers were masked to treatment allocation throughout the study. Treatment assignment was known only by investigators and data analysts at the École Polytechnique Fédérale de Lausanne, Switzerland.

4.1.4 BCI-aided and sham therapy procedures.

Both groups received therapy two times per week for a period of 5 weeks, directly in the centers (10 sessions in total). We rescheduled missed session and for none of the patients training duration exceeded 6 weeks. Each session lasted approximately 60 min, including preparation and device setup time. We used a commercial EEG amplifier (g·tec gUSBamp, Guger Technologies OG, Graz, Austria), recording at a sampling frequency of 512 Hz with 16 active surface electrodes placed on Fz, FC3, FC1, FCz, FC2, FC4, C3, C1, Cz, C2, C4, CP3, CP1, CPz, CP2 and CP4 of the 10/20 system (reference: right mastoid; ground: AFz). We also recorded 4 bipolar EMG of the biceps, triceps, extensor digitorum communis (target muscle),
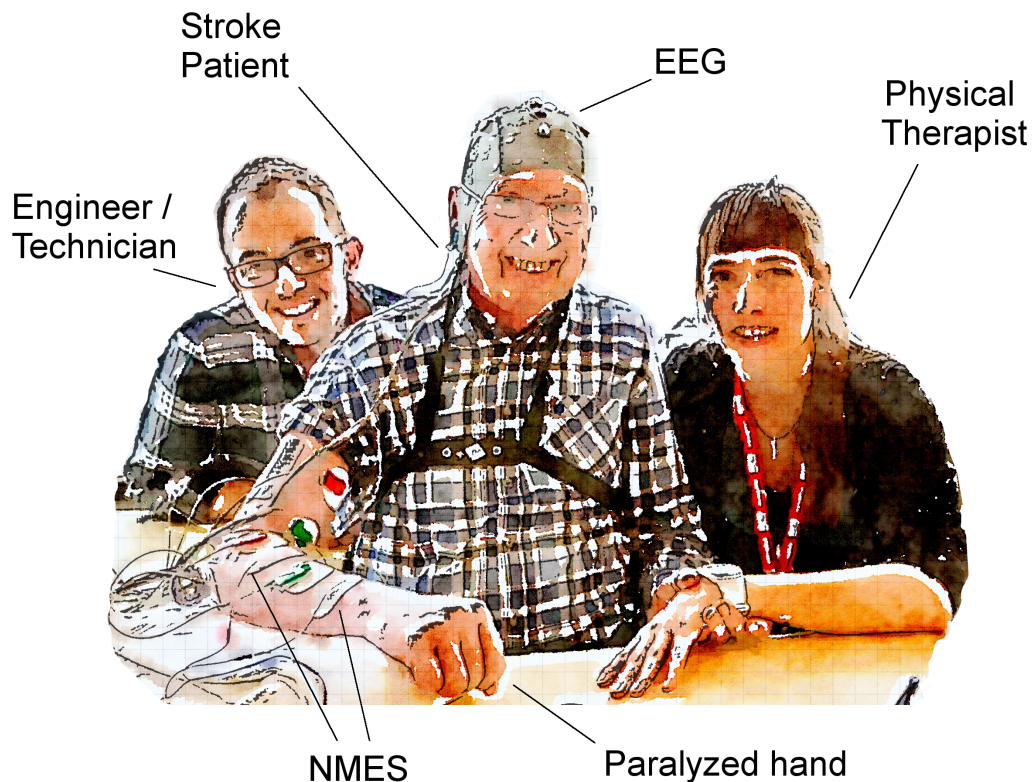
Figure 4.1: **BCI-NMES montage and actors.** During the experiment, the stroke patient wears a 16-channels EEG system and NMES electrodes are placed on his/her forearm as to stimulate the paralyzed extensor digitorum communis muscle. During the whole session, a physical therapist monitors the performance and motivates the patient, avoiding abnormal and compensatory movements. In addition, an engineer expert in BCI provides technical support to calibrate the system and fix problems that might arise at run-time, either on site or remotely.

and flexor digitorum communis muscles.

During each therapy session, patients were asked to perform 3 to 7 series of 15 movement attempts, and they were encouraged to do as many series as they could. Timing of each trial (i.e. movement attempt) was determined by a cursor moving on a screen (**Fig.4.2g**). A physical therapist monitored the cursor and gave verbal instructions to patients and avoided abnormal compensatory strategies; an engineer would provide technical support to calibrate the device and fix malfunctioning on site, or remotely (**Fig.3.1**).

Whenever the cursor reached a pre-defined threshold on the screen, a BCI command was detected and NMES was activated, accordingly. Possible visual cues and timing were: preparation

(for 3.5s), attempt movement (1s). If no mental command was detected in the 7s after "Start" cue, trial was terminated. Two patients in the BCI-NMES group required longer time-outs to be able to deliver a BCI commands, so maximum trial length was set to 15s. Each trial was started by the therapist through a key press. For the Sham-NMES therapy, patients received identical instructions and wore identical equipment to that worn by subjects in the BCI-NMES group. The data of first 4 patients in the BCI-NMES group was used to provide an estimate of the real time behavior of the neural interface. This resulted in pre-setting an average time to deliver an NMES of 3.5 to 4.5s, and a command delivery rate of 60 to 70% of single trials. NMES was performed through a commercially available neuromuscular electrical stimulator (Krauth & Timmermann MotionStim8), with a single bipolar channel applied on the affected limb in order to inject a current (having a pulsed, square waveform) into the extensor digitorum communis muscle. Electrical stimulation parameters such as current amplitude (ranging between 10 and 25mA), pulse-width (500μs), and stimulation frequency (ranging from 16 to 30Hz), as well as electrodes placements were setup at each session by an expert therapist. Therapists were asked to give regular therapy at the end of each session for additional 45 min, usually including mobilization, and activities of daily living. The same occupational and physical therapists within each clinical site, having at least 4 years of experience, provided training to patients in both groups.

4.1.5 Electromyography data analysis.

An objective quantification of voluntary muscle contraction was performed by means of EMG analysis. Raw EMG signal recorded through bipolar montages around the extensor digitorum communis and flexor digitorum muscles were band-pass filtered between 50 and 200 Hz, and the EMG envelope was extracted by squaring the bandpass-filtered EMG signal and by applying a moving-window smoothing filter having a window length of 125ms.

In addition, we tested whether changes induced by the therapies resulted in objective changes in the distributions of EMG potentials generated during an attempted movement. To do so, we extracted and compared the probability density functions of EMG potentials recorded from the extensor digitorum communis muscle (target muscle of the therapy) in the 2s following the "Start" cue.

4.1.6 Clinical indexes of recovery.

Before starting the therapy, patients underwent a neurological baseline assessment of their upper limb functionality (**Fig. 4.10**). The primary outcome was change in the Fugl-Meyer assessment for the upper extremity (FMA-UE) score [54]. This motor impairment test involves 33 items that assess voluntary movement, reflex activity, grasp, and coordination by ranking
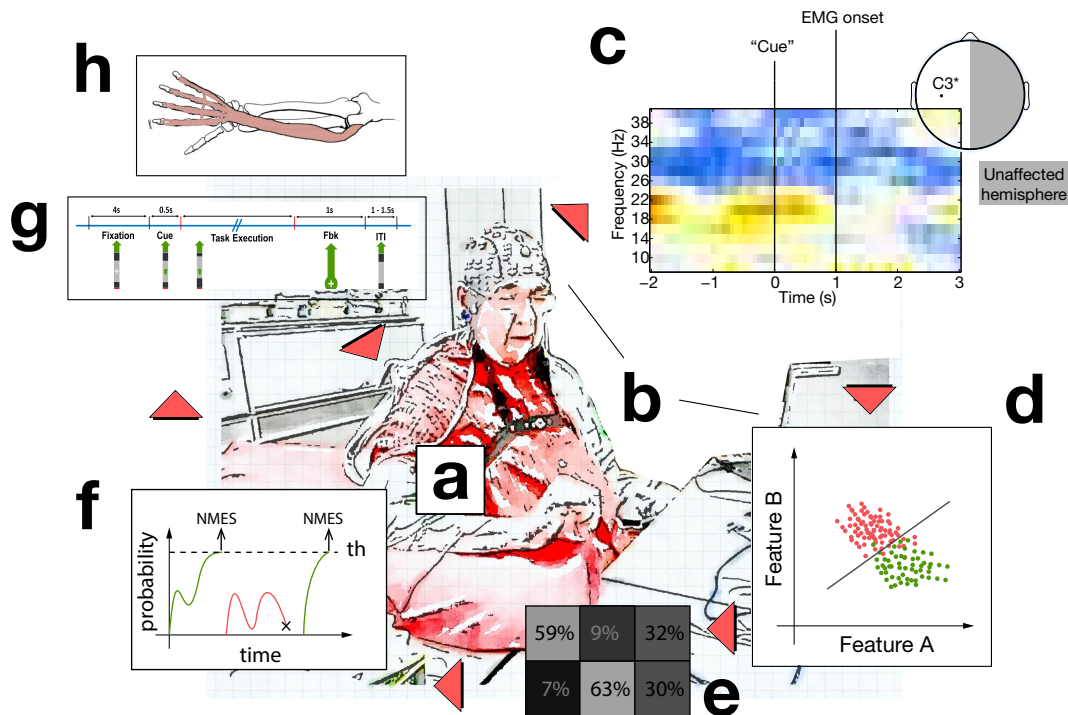
Figure 4.2: **Brain-controlled neuromuscular electrical stimulation.** During the therapy, participants were comfortably sit and they were asked to concentrate on their affected limb for the whole time of the experiment (a). For the BCI-aided neuromuscular electrical stimulation group (BCI-NMES), a brain-computer interface (BCI) system (b) was calibrated to distinguish motor attempts from resting during an initial dedicated session by identifying subject-specific EEG features representing spared motor networks activated during motor attempts (c) and building a statistical classifier (d) for each of the possible tasks – i.e. attempt to move and resting. Closed-loop control of NMES was performed through the BCI by accurately decoding user's attempts to open the affected hand or resting, resulting in low false positive classification rates (e). The BCI computed probabilities from EEG features 16 times per second, and accumulated this evidence until a confidence threshold was reached (f); probabilities and the threshold were visualized to the patient and the therapist by a cursor moving on the screen and updated according to current probabilities (g). If the threshold was reached, the system delivered NMES of the affected extensor digitorum communis muscle (h), causing muscular contraction, fist lifting, and fingers extension, providing a reward signal for patients. Patients in the sham-NMES group wore exactly the same hardware as patients in the BCI-NMES group, but no BCI system detected motor attempts. NMES, instead, was delivered in 60 to 70% of each run's trials following the same timing of the BCI-NMES group. Both therapies lasted 10 sessions.

actual performance from 0 (no function) to 66 points (normal function). The threshold for the minimum clinically important difference in patients with minimum to moderate chronic impairment after stroke is about 5 points [138]. Our secondary outcome measures targeted spasticity (Modified Ashworth Scale), strength (Medical Research Council strength test), and overall status (European Stroke Scale). The same tests were repeated immediately after the end of the therapy to quantify the outcomes.

4.1.7   EEG markers of neuroplasticity and related signal processing.

In addition to the clinical functional indexes, patients participated to a pre- and post-treatment high-density EEG imaging session, where they were asked to perform 45 attempts of affected hand opening or resting, in random order. 64 EEG channels covering the whole scalp were recorded with a Biosemi ActiveTwo system with a sampling frequency of 2048 Hz. In order to uniform data among patients and have comparable results, EEG data of patients with a lesion in the right hemisphere were flipped in order to have the lesion over the left hemisphere for all subjects – i.e. electrode C3 covers the lesioned hemisphere, electrode C4 the intact hemisphere. For this reason, electrode notation in the text is presented as C3*/C4*.

4.1.8   Effective EEG connectivity.

Data were bandpass filtered using a 4th order causal Butterworth filter between 1 and 40 Hz and used to compute brain connectivity through the short time direct directed transfer function (SdDTF) [76]. This method is a modification of the directed transfer function (DTF) using multi-trials to increase the temporal resolution and adopting partial coherence to avoid indirect cascade influences [70]. The brain connectivity was transferred to frequency domain by FFT to reflect the causal influences in different bands. The SdDTF was computed with a sliding window of 500ms for 41 EEG channels (excluding peripheral channels) with overlapping 450ms in order to obtain smooth modulation. Epochs of 10s data were used: 5s before and 5s after the onset of the "Start" cue. For each dataset (i.e. a recording session), all motor attempt and rest trials were used to compute the SdDTF. Then, for each of the electrodes SdDTF results computed between all pairs of electrodes were referenced to the baseline level, computed from 4s to 1s before "Start" cue onset. SdDTF results were averaged for movement attempt and resting trials, then a relative measure of connectivity was extracted as

$$\eta_{Rel} = \eta_{Motor} - \eta_{Rest}$$

where η_{Motor} is the average SdDTF during motor attempts, and η_{Rest} is the average SdDTF during resting trials. Negative values of η_{Rel} show that the SdDTF is higher during resting trials, positive values of η_{Rel} is higher during motor attempts, and close to 0 values show that

the average SdDTF is similar during both conditions. Time-frequency blocks of the SdDTF were further averages in the [0 2.5]s time window after the visual cue and in the [25 40]Hz frequency band (shown in **Fig. 4.7a-b**).

After swapping electrodes to have the lesion on the left hemisphere for all patients, two hemispheres were defined by clustering together the information coming from electrodes FC5, FC3, FC1, C1, C3, C5, CP5, CP3, CP1 (left hemisphere) and FC6, FC4, FC2, C2, C4, C6, CP6, CP4, CP2 (right hemisphere), we computed the average relative measure of connectivity between/within the two hemispheres (shown in **Fig. 4.7c-d**).

4.1.9 Slow motor-related potentials

Slow components of the EEG were isolated by applying a 5th order causal Butterworth filter in the [0.3 1] Hz frequency band in order to identify movement-related potentials reflecting cortical reorganization after stroke [63] and changes in cortical excitability [44]. The filter settings were chosen in order to maximize single trial information [58]. Trials with potentials exceeding ± 100 μV were discarded before averaging. Single trials recorded from electrode C3* (lesional hemisphere) were averaged by group before and after therapy.

All trials were aligned on EMG onset before averaging. To extract the EMG onset, raw bipolar derivations recorded from the extensor digitorum communis muscle were band-pass filtered between 50 and 200 Hz, squared, and smoothed with a moving average filter having a window length of 125 ms. Onset of a trial is defined as the time when the processed EMG values exceeded the mean EMG value computed between 1 and 0.5 s before the "Start" cue by twice its standard deviation.

In order to validate the presence of modulations in slow movement-related activity, multivariate topographic analysis was performed by computing the global dissimilarity (DISS) of the entire EEG topography between pre- and post-intervention group-averaged slow potentials, for the two groups separately [106]. Topographic ANOVA (TANOVA) consists in a permutation test that preserves the temporal structure of the signal and shuffles the topographies belonging to each of the conditions. Statistical significance was assessed by considering a 95% confidence interval. Stable template maps were further extracted from concatenated group-averaged slow EEG potentials, and the number of templates was chosen through a cross-validation criterion [113]. Finally, single-subject fitting of extracted topographies was performed on the time windows identified by TANOVA [106], ensuring that windows had a minimum length of 100 ms in order to remove isolated statistically significant time points arising from the permutation procedure.

Qualitatively, a slow motor-related potential (SMRP) would appear as a slow negative deflection of the EEG preceding the muscular onset (time 0), and none of the groups presented

normal SMRPs before the therapy (**Fig. 4.3a,b**). A consistent negative deflection preceding the muscular onset appears in the BCI-NMES group after therapy (**Fig. 4.3a**), but not in the sham-NMES group (**Fig. 4.3b**). TANOVA shows that statistical significance was reached in the BCI-NMES condition in the time window [-830 -460] ms (**Fig. 4.3c**), but not in the sham-NMES (**Fig. 4.3d**). The number of stable template maps for the BCI-NMES group was 4, yielding a R^2 value with original signal of 0.87 (**Fig. 4.3e**). Within the statistically significant window, two stable topographic voltage templates appeared consistently modulated, after single subject fitting after the therapy in the BCI-NMES group: a frontal pattern became more frequent, and a posterior pattern occurred less frequently (**Fig. 4.3f**). Both patterns appear to be located over the lesioned hemisphere.

4.1.10   Brain Computer Interface calibration and real time control.

For the BCI-NMES therapy, the BCI classifier was calibrated to classify brain activity into "motor attempts" and "resting" for each patient during a low-density EEG session not included in the therapy time. During the calibration session patients were asked to attempt opening the affected hand or to rest; patients were comfortably sit in front of a screen providing information concerning current task and timing by means of moving visual cues. These data were analysed offline and most discriminant EEG features between resting and motor attempts were extracted through state of the art machine learning techniques [82] and manually selected by BCI experts. As a general principle, BCI experts selected discriminant EEG features in the ipsi- and contra-lesioned hemispheres in frequency bands normally associated to voluntary movements, i.e. in the mu and beta bands.

EEG Features used for the procedure described above were the power spectral densities (PSDs) of the signal, computed through a sliding window every 62.5ms over last 1s of data. These features were used to train a Gaussian Mixture Model composed of two prototypes per task, assuming equal variances of each Gaussian [96].
Finally, the BCI system decoded motor attempt by computing the probability of each PSD value to belong to either class "Motor Attempt" or "Resting", and integrating probabilities through exponential smoothing. Whenever integrated probabilities reached a pre-set confidence level, a BCI command was detected, and NMES of extensor digitorum communis muscle was delivered, accordingly. This threshold was adjusted at each therapy session as to allow stroke patients to deliver BCI commands, i.e. shaping of task complexity was performed in order to have a hard but feasible task [141].

On-line accuracy was computed by dividing the average number of BCI commands over the total number of attempts in a run.
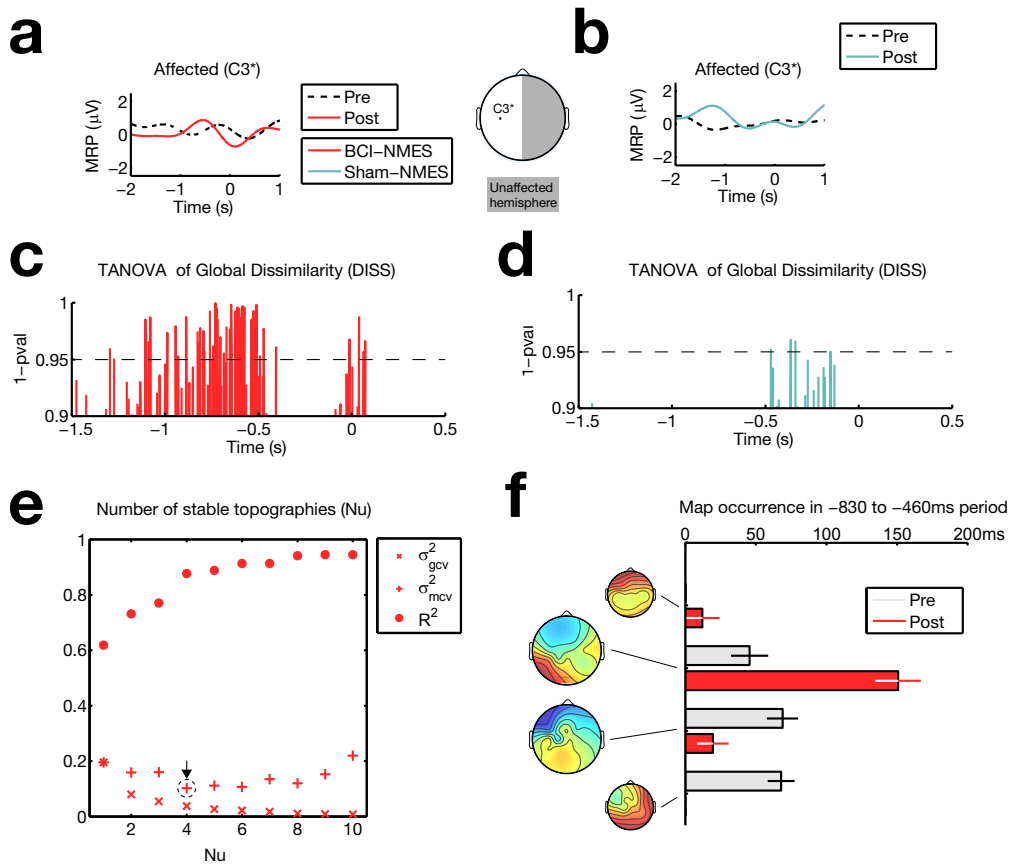
Figure 4.3: **Modulations of slow cortical movement-related potentials.** Group-averaged EEG waveforms at electrode C3* (all data were flipped in order to always have the affected hemisphere on the left side of the head), representing movement-related potentials (MRP) before and after the therapy (a and b). All trials were aligned on EMG onset before averaging, and slow components were extracted in the [0.3 1]Hz frequency band. A consistent negative deflection preceding the muscular onset appears in the BCI-NMES group after therapy (a), but not in the sham-NMES group (b). In order to validate this observation, multivariate topographic analysis was performed by computing the global dissimilarity (DISS) of the entire EEG topography between pre- and post-intervention group-averaged event related potentials, for the two groups separately (c and d). Topographic ANOVA (TANOVA) consists in a permutation test that preserves the temporal structure of the signal and shuffles the topographies belonging to each of the conditions. After applying a smoothing filter of 10ms to remove glitches, statistical significance was reached only in the BCI-NMES condition in the time window [-830 -460]ms (c). Stable template maps were extracted from concatenated group-averaged ERPs, and the number of templates was chosen through a cross-validation criterion, resulting in 4 template maps for the BCI-NMES group (yielding a R^2 value with original signal of 0.87) (e). Within the statistically significant window, two stable topographic voltage templates appeared consistently modulated, after single subject fitting, after the therapy in the BCI-NMES group (f). Both patterns appear to be located over the affected hemisphere.
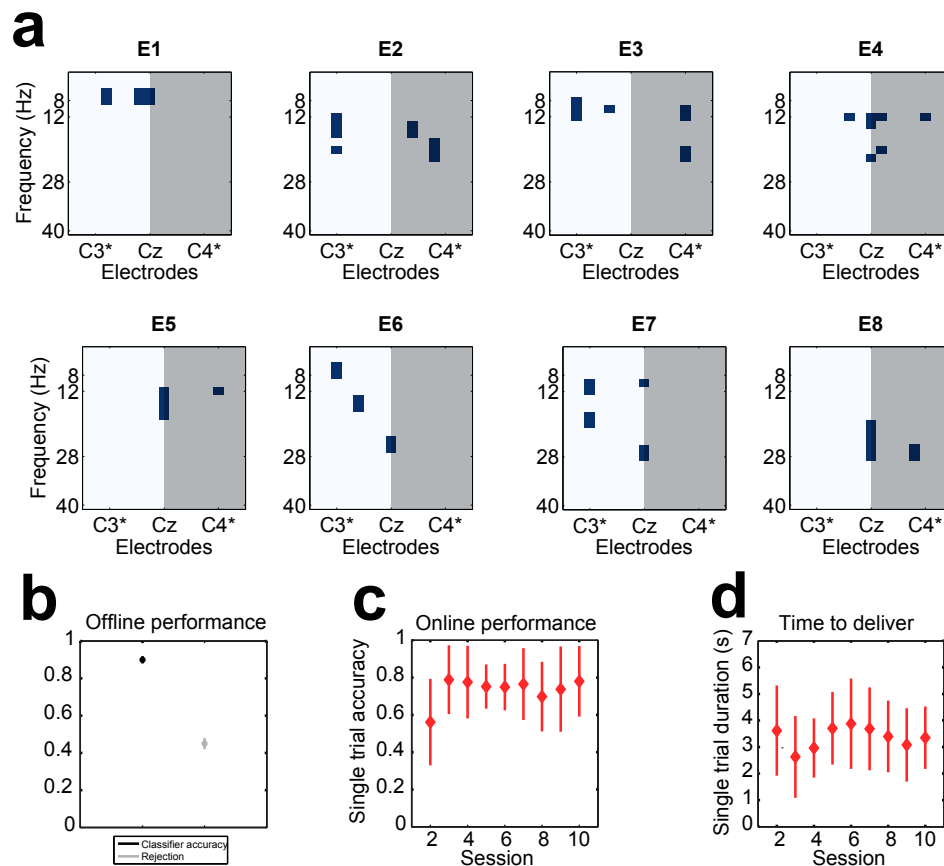
Figure 4.4: **BCI features and performance.** EEG features used for closed-loop control, presented for all subjects of the BCI-NMES group by their frequency and electrode location (a). For each patient, the white area of the plot represents all electrodes located on the lesioned hemisphere (surrounding C3*), while the dark gray area represents all electrodes located on the intact hemisphere (surrounding C4*). Average offline single-sample accuracy and rejection extracted from calibration data – i.e. first recording session (b), average online single-trial classification performance across all subjects (c), and average time required by the BCI to detect a motor attempt from the EEG across all subjects (d).

4.1.11 Statistical analyses.

All tests for clinical scores were done with SPSS. We used a significance level 0.05 for all analyses. Effects of the treatment over the entire course of the study were assessed by means of mixed-design repeated measures ANOVA having session (pre- and post-therapy; i.e., 2 levels) as within-subject factors and the allocation group as the between-subject factor.

For missing data, we used the last recorded value (last observation carried forward). For missing EEG data, if no former session data was available, we used data recorded in the next session (next observation carried backward).

4.2 Results

In this study, we aimed at assessing whether five weeks of therapy involving BCI-aided NMES (later called BCI-NMES, whose functioning is described in **Fig. 4.2**) could elicit stronger functional recovery than sham-NMES therapy, and whether signatures of neuroplastic changes would be detectable from the EEG.

NMES is a rather common therapeutic approach in rehabilitation[37], it is safe and affordable by the healthcare system[114], its application to post-stroke hemiplegia has shown benefits for patients [123], and its use has the general advantage of directly engaging body's natural pathways - the muscles and nerves[25].

Between September 18, 2012, and January 31, 2014, 18 individuals were clinically tested for eligibility, of whom 15 were eligible and agreed to participate. One patient withdrew and did not participate to the follow-up assessment. Ten participants from SUVACare - Clinique Romande de Réadaptation, Sion (seven assigned to BCI-NMES, three assigned to sham-NMES) and five from University Hospital of Geneva (four assigned to sham-NMES, one to BCI-NMES) participated to the study. One patient in the sham-NMES group had fewer than 10 therapy sessions.

The BCI was calibrated for each subject in order to monitor time-frequency EEG features, i.e. sensorimotor μ and β EEG rhythms, (**Fig. 4.2c**) representing the activity of spared motor networks. Whenever a movement attempt was decoded from the EEG (**Fig. 4.2d-f**), the BCI activated NMES of the extensor digitorum communis muscle (**Fig. 4.2g-h**). Patients that received sham-NMES therapy wore identical hardware and received identical instructions as patients who received BCI-NMES, but NMES was not connected to specific neural activity and it was instead delivered randomly with similar timings and amount of stimulation.

Off-line accuracy (on calibration data) is >90% for each of the patients who received BCI-NMES, with an average single sample rejection of 58% (**Fig. 4.4a**). On-line (i.e. single trial) accuracy is approximately 75% across sessions (see **Fig. 4.4b**), with an average time to deliver

an online command shown in **Fig. 4.4d**.

The primary clinical outcome metric of the study was the Fugl-Meyer assessment for the upper extremity (FMA-UE) [54]. Secondary outcomes included modified Ashworth scale (MAS) for the evaluation of spasticity, Medical Research Council (MRC) score for muscle strength and European stroke scale (ESS) score for general disability. Clinical evaluation was performed before the beginning and after the end of the intervention. An additional evaluation of primary outcome metric was carried on 6 to 12 months after the end of the intervention (later indicated as 36 weeks). Clinical scores are reported in **Fig. 4.5a-b**.**Fig. 4.5c** shows baseline characteristics of the two groups, including age, time since stroke, baseline FMA-UE score, number of patients per group, gender and affected hemisphere. No statistical significant difference between groups could be found at baseline.

We assessed whether two groups received a comparable amount of therapy by computing the mean number of detected commands (i.e. NMES of the extensor digitorum communis muscle) per run, the number of runs per session and the average time to deliver a command per run. No statistical difference was found. Despite small group size, changes in FMA-UE scores (**Fig. 4.5a**) exhibited a significant $session \times group$ interaction ($F_{(1,13)}=17.71$, $p<0.01$). BCI-NMES patients improved by 9.0 ± 3.4 points, whereas sham-NMES did by 1.7 ± 3.3 points. Mean difference between groups is 7.3 points, above the threshold of 5 points considered to be clinically important [112]. Remarkably, all BCI-NMES patients improved, what was not the case for the sham-NMES group. Furthermore, seven BCI-NMES patients (87.5%), but only one sham-NMES patient (14.2%), gained at least 5 points after 5-week therapy. Subjects who already completed the follow-up clinical evaluation (4 BCI-NMES, 4 sham-NMES, average 36 weeks after end of therapy) retained functional improvements. **Fig. 4.9** documents two case reports of BCI-NMES patients who were completely paralyzed and regained voluntary muscle contraction after intervention. One of the patients was plegic for 15 years. Despite small group size (N=15), between-group differences in the primary outcome metrics were unexpectedly high and statistically relevant (average increase of 9 FMA-UE points, with seven patients showing more than 5 points increase in the BCI-NMES group against an average increase of 1.4 points, with only one patient improving more than 5 points in the sham-NMES group).

Figure 4.5b shows changes in secondary clinical outcomes. For the MRC score (strength of the target muscle extensor digitorum communis), we also found a significant $session \times group$ interaction favoring the BCI-NMES group ($F_{(1,13)}=6.26$, $p<0.03$). Sham-NMES patients improved their spasticity of wrist extensor and flexor muscles (MAS score), while BCI-NMES did not. The $session \times group$ interaction was significant ($F_{(1,13)}=9.04$, $p<0.02$). ESS score increased for six of the eight BCI-NMES patients (75%), with one patient recovering 21 points. Three sham-NMES patients (43%) also improved. Nevertheless, changes were not significant.
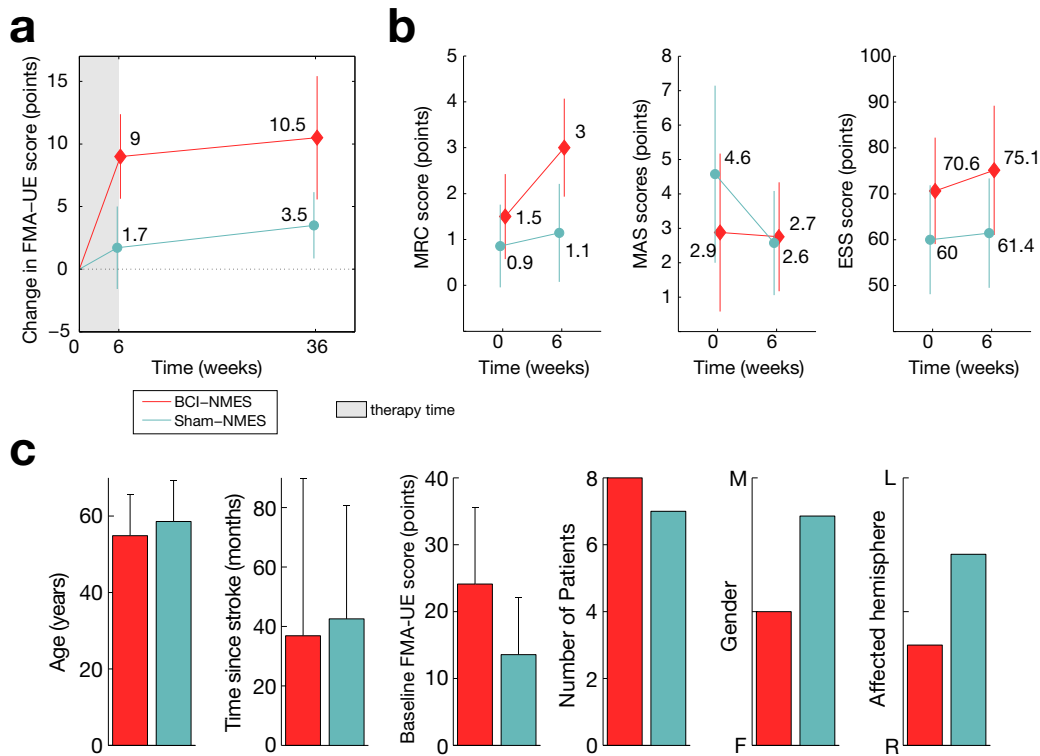
Figure 4.5: **Clinical indexes of functional recovery.** Fugl-Meyer assessment for the upper extremity (FMA-UE), measuring motor function (a); Secondary outcome scores: Modified Ashworth Scale (MAS), measuring spasticity, Medical Research Council Scale (MRC), measuring muscle strength, and European Stroke Scale (ESS), measuring the overall motor and cognitive state (b). Changes in the primary outcome metric (FMA-UE, a) are presented with respect to baseline value recorded immediately before patients received the intervention, immediately after it ended (6 weeks after) and at a 6 - 12 months follow-up session (on average 36 weeks after). Seven of the eight patients in the BCI-NMES group recovered more than 7 FMA-UE points, showing clear signs of a clinically significant recovery driven by the restoration of voluntary contraction of the extensor digitorum communis muscle; only one patient in the sham-NMES recovered more than 7 FMA-UE points and nearly no change was observed on the other patients, despite they received NMES. Secondary outcomes are presented in absolute values at baseline and at the end of the therapy (b). Both groups show a similar decrease in spasticity that one would expect as one of the effects of NMES. Muscle strength recovery, though, appears moderately stronger in the BCI-NMES group than in the sham-NMES group, but this difference is not statistically significant. The recovery of motor function is also reflected in the increase of the general patient status having a stronger, but not statistically significant, magnitude in the BCI-NMES than in sham-NMES.

Due to logistic needs, we were not able to balance the number of patients recorded at each clinical site. For this reason, we ensured that patients received the same treatment across site by providing standard conventional therapy to all patients included in the study. Another problem that might affect our results concerns inter-rater variability in clinical tests[149]. Still, the magnitude of the effect on the primary outcome metrics can rule out this possibility[112]. In addition to clinical indexes, a quantitative measure of muscle contraction was extracted through the analysis of EMG patterns of extensor digitorum communis (target muscle) (**Fig.4.8a-b**) and flexor digitorum communis muscles (**Fig.4.8c-d**). Extensor digitorum communis muscle activity appears highly increased in the BCI-NMES group, but not in the sham-NMES group (as shown in **Fig.4.8a and c** from 0 to 3s). This increase results in a shift of the distribution of EMG envelope time points during the contraction towards higher values for the BCI-NMES group, but not for the sham-NMES group **Fig. 4.8e-f**.

High-density EEG sessions were held before the beginning and after the end of the intervention in order to quantify group-specific neuroplastic effects affecting cortical excitability, reflected by changes in slow movement-related potentials[44], and interhemispheric connectivity, reflected by changes in directed EEG functional connectivity[70].

Group-averaged slow EEG potentials, aligned on the EMG onset, recorded from electrode C3* show no sign of motor-related potentials (MRP) in any of the groups before the therapy (**Fig.4.6a**). A MRP, consisting in a negative deflection starting around 1s before the movement and having its maximum negativity at the muscular onset (0s), is restored in the BCI-NMES after therapy. Multivariate topographic analysis of variance (TANOVA)[106] reveals that pre- and post- group-averaged EEG topographies yield statistically significant differences in global dissimilarity (DISS) from 830 to 460ms before EMG onset and only for the BCI-NMES group (**Fig.4.6b**). Stable topographies that were modulated in this time window showed a more frontal pattern and a more posterior pattern, and single subject fitting reveals significant modulations that increase the occurrence of frontal pattern and decrease the occurrence of posterior pattern, after the intervention (**Fig. 4.6c**). Further details on the topographic analysis can be found in **Fig. 4.3**.

Effective EEG connectivity provides a measure of the information flowing from one hemisphere to the other during a specific task[76]. We quantified motor-related information flowing from and to the affected and unaffected hemispheres before and after the therapy, for the two groups. Results show that a significant reduction of directed interhemispheric connectivity occurs when considering the direction factor ($F(1,8) = 5.463$, $p = 0.048$) with an effect on the session x allocation group interaction ($F(1,8) = 7.308$, $p = 0.027$), shown in **Fig.4.6d-e**. Even though pre- and post-intervention data of patients who received BCI-NMES shows a consistent decrease of connectivity in any direction, the effect appears to be driven by the directional change from the unaffected to the affected hemisphere. Further information on EEG connectivity analysis can be found in **Fig. 4.7**.

4.3   Discussion

In this study, we provide evidence that closed-loop BCI-aided NMES therapy induces consistent and clinically important recovery of upper limb function, and we show that direct BCI control is the key therapeutic factor underlying motor recovery. The parallel group experimental design also allowed us to identify a possible mechanism underlying these changes, consisting in a reduction of abnormal inter-hemispheric connections [104], reflected by the strong decrease in directed inter-hemispheric EEG connectivity, and in an increase of cortical excitability over the affected hemisphere [136], reflected by the significant change in pre-post stable topographies and associated to slow movement-related potentials.

Beneficial neuroplasticity underlying the restoration of motor function after stroke should meet three critical assumptions: that the mechanism of neural repair inherently involve cellular and circuit plasticity; that brain plasticity is fundamentally a synaptic phenomenon that is largely stimulus-dependent; and that brain repair must incorporate biological interventions replacing or augmenting some lost brain tissue through carefully tailored interventions involving specific brain circuits[138]. The use of spared EEG sensorimotor rhythms to control the electrical stimulation of nerves and muscles meets these three assumptions, thus explaining the strong recovery we observed in the BCI-NMES group.

It is important to highlight the fact that NMES, per se, can provide motor gains and limited functional gains[38] by lessening the excitability of spinal reflex pathways, strengthening muscles, augmenting sensorimotor integration for the task at spinal and supraspinal levels, and augmenting the cortical sensory drive for activity-dependent plasticity[37]. Despite the fact that recent meta-analyses have shown a potentially beneficial effect of electrostimulation on upper limb functional recovery [79], national guidelines for clinical practice indicate that this type of therapy should not be performed on a routine basis [128].

Interestingly, motor recovery was present in the BCI-NMES group disregarding paralysis severity: all patients presenting hand plegia regained voluntary muscular contraction resulting in fist lifting and signs of fingers extension (see **Fig. 4.9** for two anecdotal case reports on the topic). None of the plegic patients that received sham-NMES showed any sign of recovery. One of the limitations of the study is that patients were evaluated in different clinical sites by different therapists, and that patients in each group were not balanced across sites. Two arguments speak in favor of the validity of our conlusions: the first is that the primary outcome metric, namely the Fugl-Meyer Assessment for the Upper Extremity, has shown inter-tester reliability in quantitative studies [134]; the second is that the large effect size in the BCI-NMES group and large difference across groups provide hints of a phenomenon that occurred at both clinical sites.
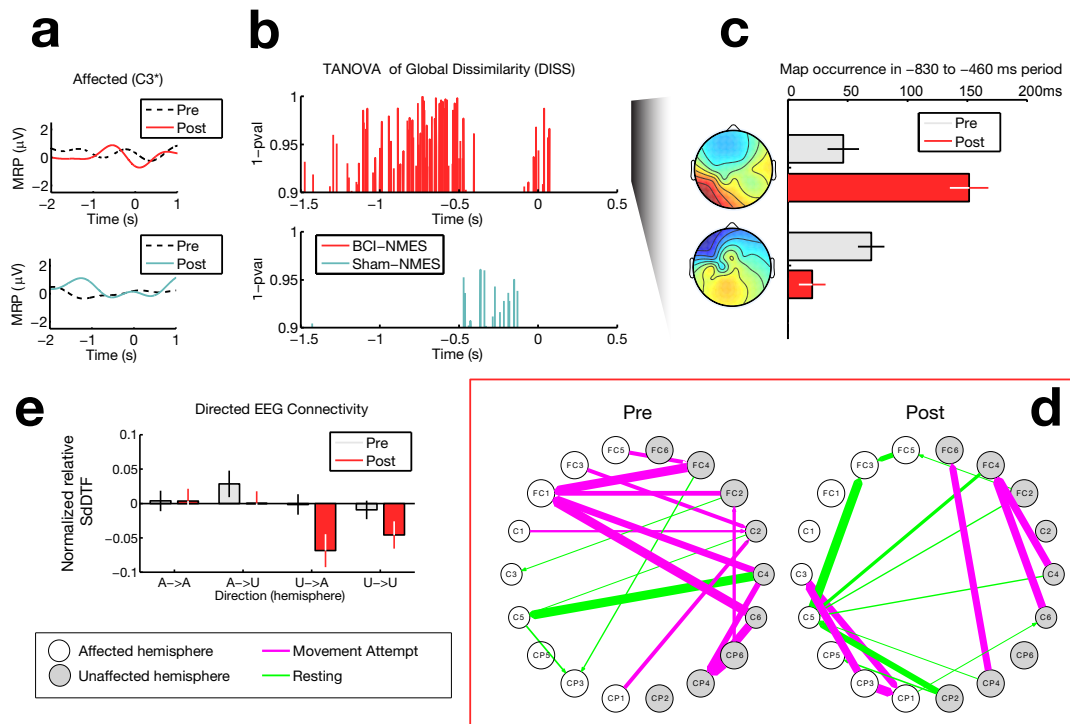
Figure 4.6: **EEG markers of cortical plasticity.** Group-averaged slow EEG potentials recorded from electrode C3* showing no sign of movement-related potentials in both groups before the therapy (a top and bottom, dashed lines) and showing a strong negative deflection aligned to the muscular onset (a top, red line, time 0) in the BCI-NMES group, but not in the sham-NMES (a bottom, blue line). TANOVA of global dissimilarity between pre- and post-intervention ERP topographies reveals stable statistically significant difference only for the BCI-NMES group in the [-830 -460]ms time window (b). Stable topographies that were modulated in this time window, in the BCI-NMES group, showed a more frontal pattern and a more posterior pattern, and single subject fitting reveals significant modulations that increase the occurrence of frontal pattern and decrease the occurrence of posterior pattern, after the intervention (c). Effective EEG connectivity shows that before therapy very strong connections could be found between electrodes belonging to different hemispheres whenever patients were engaged in a motor task, and these connections vanish after therapy; interhemispheric connections appear rather stable during resting trials (d). Average directed interhemispheric connectivity reveals that after therapy normalized relative SdDTF has a very strong increase in negativity, showing that the overall connectivity is stronger during resting than during the motor attempt (e).

In conclusion, we propose a 5-weeks therapy based on a BCI system that decodes spared neural motor networks activity to trigger NMES of the paralyzed limb. The system is non-invasive and is personalized depending on patient's representation of hand movements. We believe that the use of EEG feedback training in conjunction with sensorimotor stimulation through body's natural pathways might represent a new frontier for neuroprosthetics and rehabilitation medicine, opening the way for novel systems providing purposeful modulation of excitability in motor regions of intact and affected hemisphere overall contributing to improvements in motor function[72].

Future research on BCI-NMES should therefore focus on two directions: first, increasing the population size while keeping the active sham intervention, and possibly stratifying the population by age and level of disability, also quantifying potential synergistic effects on cognitive disability; second, investigating the mechanisms underlying the strong motor recovery, in particular the relation between closed loop control of NMES via spared neural motor networks, reduction of interhemispheric inhibition and increase of cortical excitability over the ipsi lesioned hemisphere.

Figure 4.7: **Topological changes in directed EEG connectivity.** Topological changes in directed connectivity between electrodes in the BCI-NMES group (a) and in the sham-NMES group (b). Normalized SdDTF was obtained by grouping all electrodes on each hemisphere and calculating the average connectivity for each direction. Then, SdDTF extracted during resting trials was subtracted from that obtained during movement attempts, providing a measure of normalized relative SdDTF. Changes are statistically significant in the BCI-NMES group, and appear to be driven by a strong decrease in unaffected to affected hemisphere connectivity during movement attempts (c). A similar trend having less statistical power is present in the sham-NMES group (d), and might represent benefits for patients deriving from the therapy but not sufficient to translate in functional improvements.
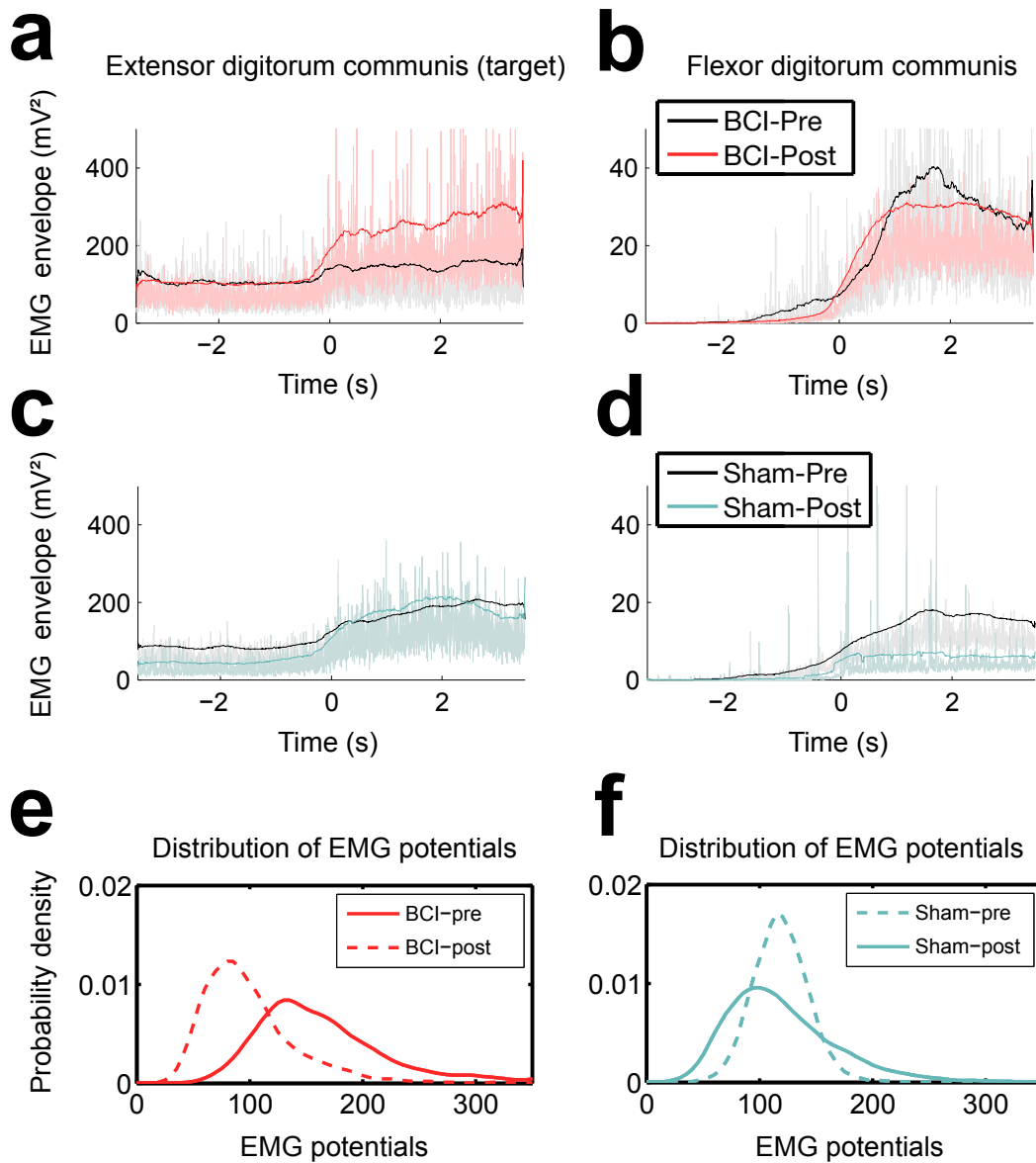
Figure 4.8: **Objective evaluation of voluntary contraction recovery.** Squared EMG envelope of extensor digitorum communis muscle appears highly increased after therapy in the BCI-NMES group (a) but not in the sham-NMES (b) groups. Squared EMG envelope of flexor digitorum communis for the BCI-NMES group has comparable values before and after therapy (c), while its activity shows a reduction for the sham-NMES (d) group. This increase in the muscle targeted by the therapy results in a shift of the distribution of EMG envelope time points during the contraction towards higher values for the BCI-NMES group (e), but not for the sham-NMES group (f).
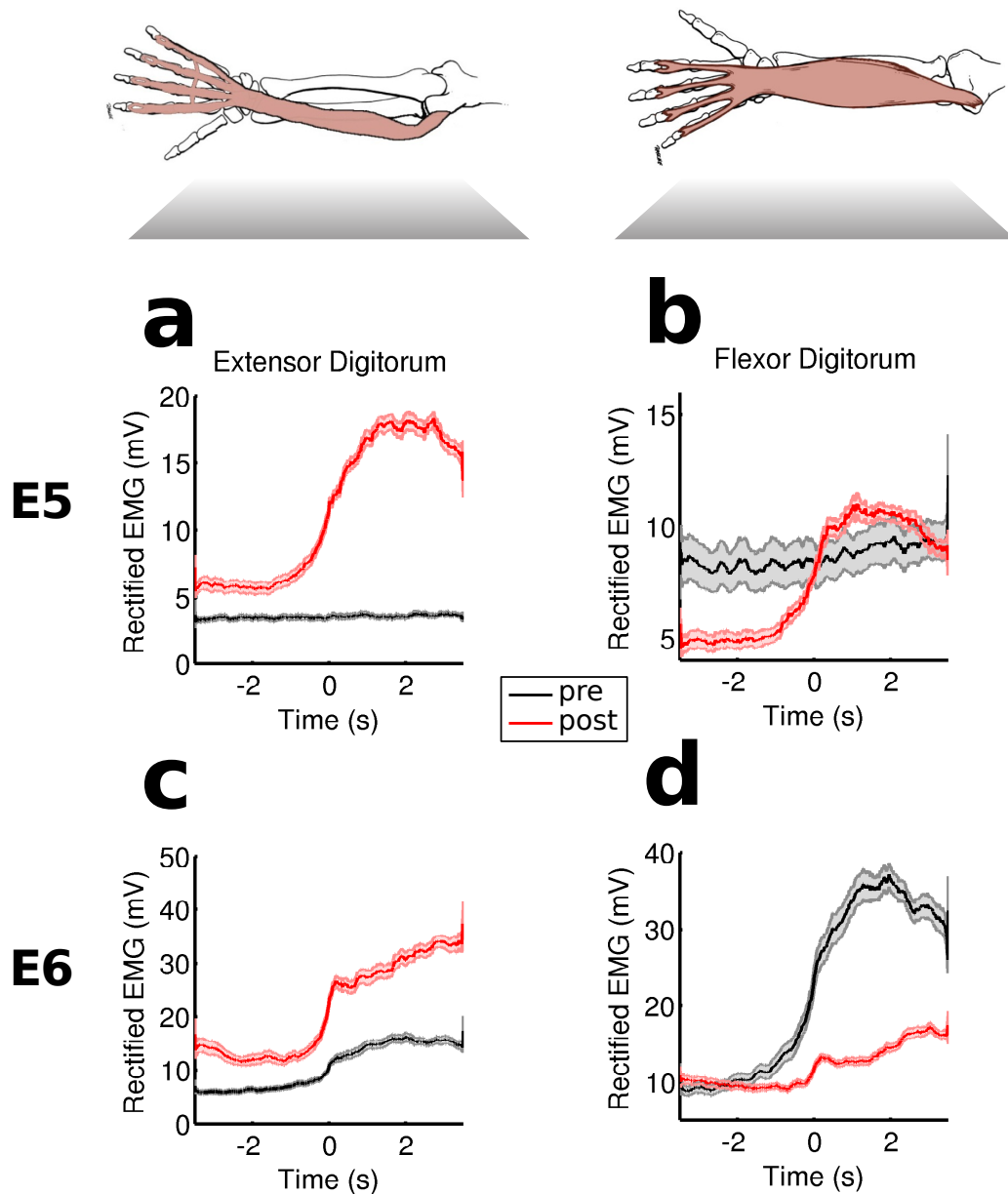
Figure 4.9: **Anecdotal case reports.** Patient E5 (woman, 48 years old) presented an ischemic stroke of cryptogenic origin in the territory of the right middle cerebral artery. Despite intensive inpatient and outpatient rehabilitation, her left upper extremity remained completely paralyzed. After the therapy, she presented voluntary muscle contractions of the extensor digitorum (left) and spasticity reduction in the flexor digitorum (right). Red traces indicate EMG activity after BCI-NMES therapy, while orange traces correspond to EMG activity before. Patient E6 (woman, 51 years old) suffered from a right lenticular ischemic stroke with hemorrhagic transformation, leading to persistent left sided hemiparesis in 1999. After BCI-NMES therapy she recovered voluntary muscle contractions of the extensor digitorum muscle (left) and presented a strong reduction of flexor digitorum spaticity (right). Color traces: black refers to pre-treatment EMG, red refers to post-treatment EMG.
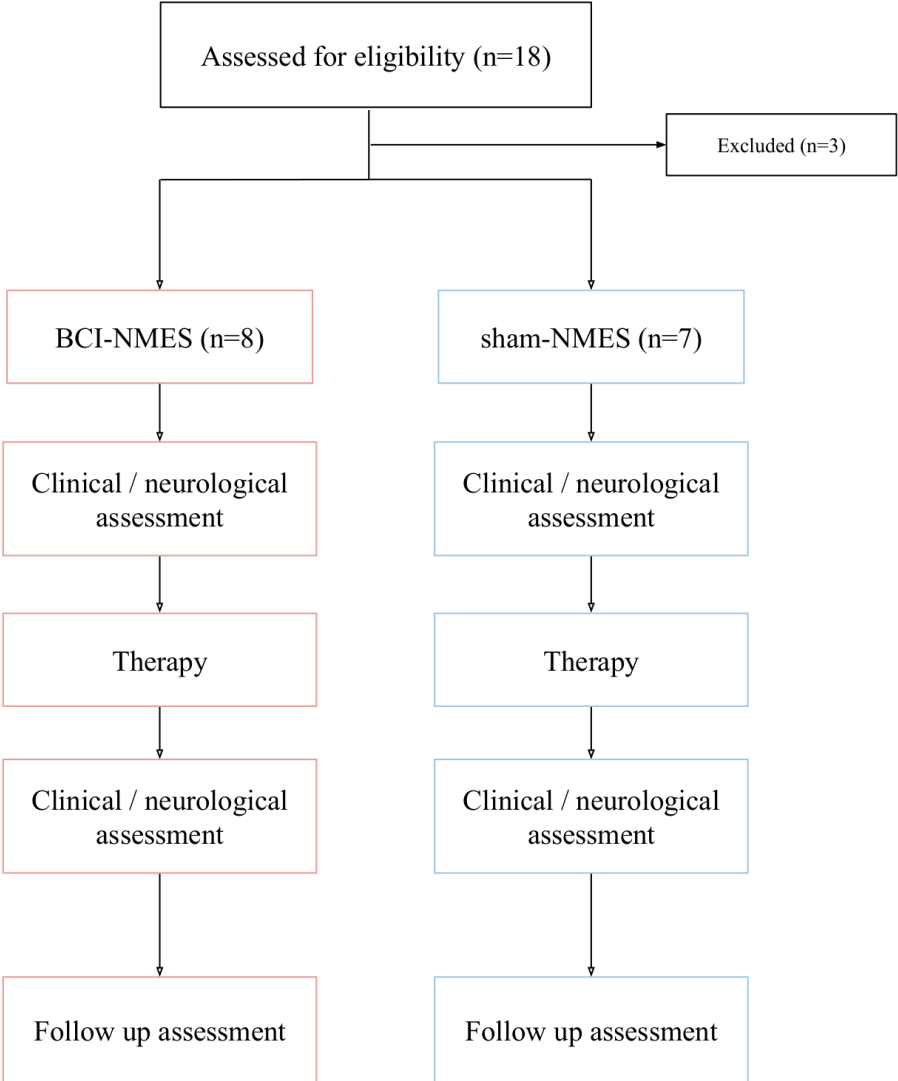
Figure 4.10: **Trial Profile.** Structure of the parallel-group clinical trial. BCI=Brain-computer interface; NMES=Neuromuscular electrical stimulation.

5 | Discussion & Conclusion

> Simplicity is the ultimate sophistication
>
> ───────────────────────────
>
> Leonardo da Vinci

The goal of this Thesis is to provide the conceptual framework, scientific rationale, technical details and clinical evidence supporting translational Neurotechnology that improves, optimizes and disrupts current medical practice in the treatment of upper limb motor disability.

The studies presented in previous Chapters capitalize on state-of-the-art in EEG imaging (**Chapter 2**, "Imaging Motor Function"), transcranial direct-current stimulation (**Chapter 3**, "Enhancing Motor Function"), and brain-computer interfaces (**Chapter 4**, "Restoring Motor Function") to demonstrate how Neurotechnology might play a key role in the future of restorative medicine.

This Chapter summarizes the main findings of the Thesis and discusses their significance with respect to the state-of-the-art, also proposing a road-map for the prosecution of the investigation on *Imaging, Enhancing, Restoring* motor function. A brief summary of the state-of-the-art, of the main findings, and of the contribution of this Thesis to the cause of Neurotechnology for brain repair is presented in **Fig. 5.1**.

Guiding diagnostics and rehabilitation through functional EEG imaging

Even though EEG has a nearly 100 years old history [8], its potential as a low-cost, precise and reliable diagnosis system has been addressed only in recent years [95]. Due to its inherent properties such as low signal-to-noise ratio and non-stationarity, voltage potentials recorded at the scalp were know as a "tough signal" to interact with. Recent advances in computational
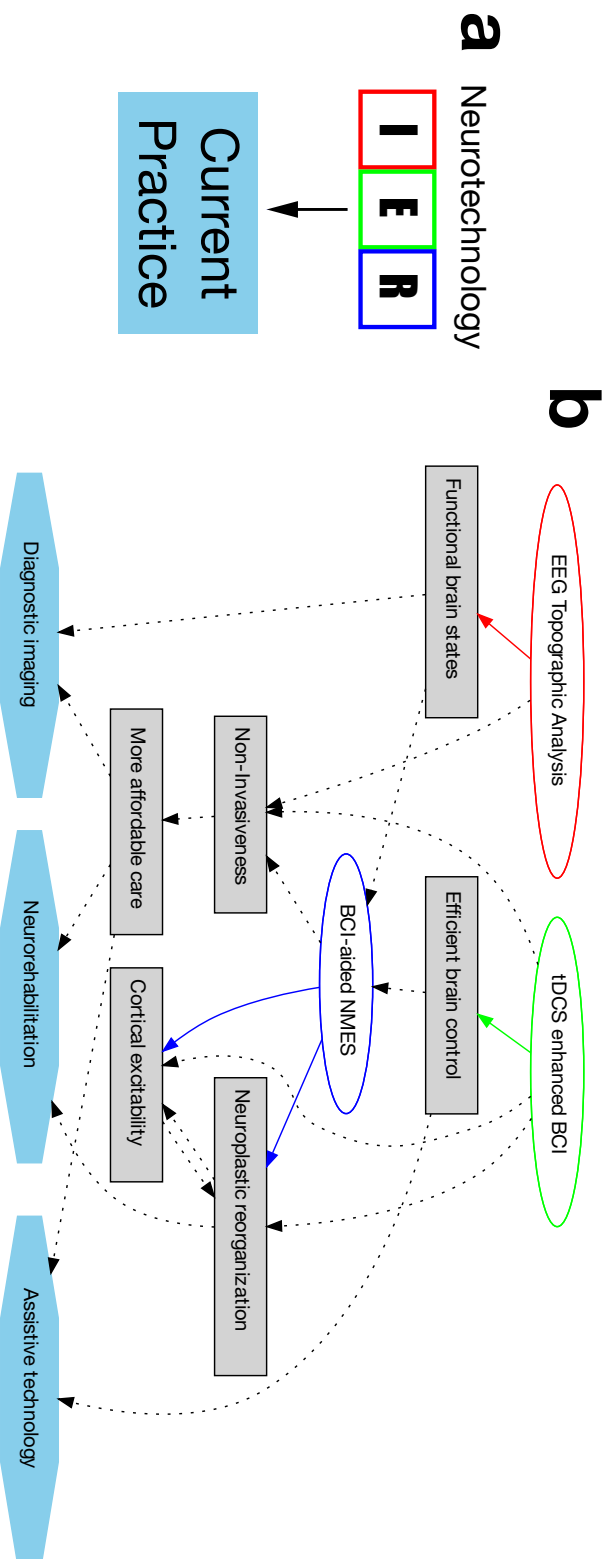
Figure 5.1: **Neurotechnology for brain repair.** Graphic summary of the contribution of this Thesis to the cause of Neurotechnology for brain repair and on how these novel tools for human motor function imaging (I), enhancement (E), and restoration (R) could affect current medical practice (a). Panel (b) introduces few interconnected concepts: dashed lines represent the state-of-the-art, solid lines represent the advancements introduced by this Thesis. Briefly, **Chapter 2** demonstrates that single-trial analysis of stable EEG topographies is suitable to represent brain motor function at the single-subject level (red). Decoding functional brain states from EEG has important implications in Diagnostic Imaging and in future Brain-Computer Interaction applications. **Chapter 3** we exploit changes in cortical excitability induced by tDCS to modify EEG sensorimotor rhythms with the goal of having a more efficient brain-control channel (green). Improving the way people interact with devices through neural activity could have a strong impact on BCI applications in rehabilitation and assistive technology. Finally and most importantly, **Chapter 4** demonstrates that BCI-aided NMES produces beneficial neuroplasticity after stroke (blue), resulting in strong functional gains also in plegic patients and several years after stroke. **Chapter 4** also suggests a possible direct influence of BCI-aided NMES on cortical excitability, based on the analysis of EEG neuromarkers. In conclusion, this Thesis demonstrates that these non-invasive systems provide a new tool that might improve the way we currently treat disorders of human motor function.

power, basic neurophysiological understanding, and the rise of data analysis techniques might suggest that the next big thing in medical practice might be the adoption of closed-loop systems for diagnosis, monitoring and rehabilitation based on EEG. **Chapter 2** of this Thesis covers and extends current knowledge about single-trial EEG signatures of motor actions, i.e. actual, imagined or attempted movements.

In **Section 2.1**, we demonstrate that GFP can be used to discriminate a motor task from rest on single-subject and single trial data and that a subject-independent topographic structure emerges from the EEG through single trial analysis of stable topographies generated during the execution of a movement or resting.

These results might provide the basis for building a novel family of BCI systems requiring minimal a-priori information (we only used a broad band-pass filter and common average referencing). With an analogy, we might think the property we demonstrated as a common sequence of "brain letters", shared among subjects. During rest, these letters appear in a pseudo-random fashion, while an order in the generation of certain topographies emerges during a motor task, composing ordered "brain words". Detecting these words of the brain should be the focus of future research in this topic. Also, future studies applying this methodology should focus on overcoming current limitations – i.e. the effects of artifacts on decoding accuracy – and characterize single trial topographic information on a clinically relevant homogeneous group of patients.

One of such groups was tested in **Section 2.2**, where we combined standard BCI discriminant analysis with stable topographies extraction in order to identify potential EEG topographies related to motor imagery in chronic stroke patients. The use of a discriminant framework allowed us to constrain the analysis on a relevant time window related to motor imagery only. The use of stable EEG topographies captured short, transient voltage configurations on the scalp, thus providing insights on underlying mental processes.

Given the fact that selected topographies have been extracted and analyzed in the most discriminant time frame in terms of modulation of motor–related rhythms [119], they are very likely to be related to the short and transient mental processes associated with the motor imagery of the affected and unaffected hand. These results strongly motivate further analysis in this direction, especially correlating functional recovery to BCI performance.

This time–constrained topographic analysis shows that changes in maps occurrence, rather than in their average duration, are more significant when comparing MI against rest. This suggests that the frequency of appearance of particular maps may be a good indicator of proper execution of the rehabilitation tasks. Consequently, it could be possible to use this measure to provide online feedback for therapists supporting the rehabilitation process. This will be particularly suited for the applications related to stroke treatments.

As previously proposed [132], the use of combined sessions of standard therapy and BCI-aided rehabilitation can serve as a way to facilitate recovery through mental rehearsal. In addition, proposed techniques represent an imaging modality to monitor long-term changes in produced patterns representing cortical reorganization.

In conclusion, we show a possible methodology to decode single-trial information about functional states of the brain while performing a motor task or resting. Further studies are required to evaluate the diagnostic value of single-trial topographic information and its impact on motor rehabilitation. For example, one might characterize the stable topographies generated by groups of stroke patients at different stages of their recovery, then clustering results depending on the outcome: subjects could then be trained through a BCI system as to generate specific topographies associated to better outcomes.

Improving brain-computer interaction by means of tDCS

Transcranial direct current stimulation (tDCS) induces selective modulation of cortical excitability [110]. Several studies suggested that this technique could be used to specifically enhance people's capacity to produce sensorimotor rhythms. In **Chapter 3**, we show that modulation of MI-related BCI features by anodal tDCS on motor areas can be induced by means of tDCS in spinal cord injured individuals (SCI) and healthy control subjects. Both groups show localized discriminant activity under the stimulated areas that lasts for at least 90 minutes. Contrary to the sham condition, SCI subjects present discriminant activity over motor areas immediately after stimulation.

Our results reproduce part of the tDCS effects in modulating motor imagery that were previously reported in healthy volunteers, namely polarity-dependent modulation effects of tDCS on the μ-rhythm, i.e. - anodal tDCS led to μ synchronization [81]. A recent study on the facilitating effect of tDCS on BCI control for stroke patients showed that there were no significant difference in the accuracies of the calibration session when comparing it to sham tDCS, but the online accuracies of the evaluation part of 10 rehabilitation sessions of the tDCS group were significantly higher than the sham-tDCS group [6]. Our data show similar accuracies between groups and conditions, and an interesting research venue would try to replicate findings regarding online performance.

Further, our results on SCI individuals show no behavioral gain in residual function (*subjective reports from subjects, data not shown here*). On the other hand, stroke appears to be a more suited pathology, as our knowledge in basic neurobiology of tDCS expands [111] from initial models of interhemispheric competition [52].

The preliminary results reported in this Thesis suggest that tDCS may selectively enhance activity of targeted areas so as to produce patterns that can be better recognized by the BCI in

SCI individuals, with a very interesting carry-over effect that appears to facilitate the motor imagery task – or at least its recognition by a machine. Thus, tDCS can have beneficial effects for BCI control, and could be applied to have more reliable BCI-aided assistive technology, such as a brain-controlled wheelchair [23] or telepresence robot [96] by the severely disabled, and neurorehabilitation.

Restoring upper limb function through BCI-aided NMES

In **Chapter 4**, we provide evidence that closed-loop BCI-aided NMES therapy induces consistent and clinically important recovery of upper limb function in chronic stroke patients, and we show that direct BCI control is the key therapeutic factor underlying motor recovery. A very important aspect of these results is that the parallel group experimental design also allowed us to identify a possible mechanism underlying these changes, consisting in a reduction of abnormal inter-hemispheric connections [104], reflected by the strong decrease in directed inter-hemispheric EEG connectivity, and in an increase of cortical excitability over the affected hemisphere [136], reflected by the significant change in pre-post stable topographies and associated to slow movement-related potentials.

Beneficial neuroplasticity underlying the restoration of motor function after stroke should meet three critical assumptions: that the mechanism of neural repair inherently involve cellular and circuit plasticity; that brain plasticity is fundamentally a synaptic phenomenon that is largely stimulus-dependent; and that brain repair must incorporate biological interventions replacing or augmenting some lost brain tissue through carefully tailored interventions involving specific brain circuits[138]. The use of spared EEG sensorimotor rhythms to control the electrical stimulation of nerves and muscles meets these three assumptions, thus explaining the strong recovery we observed in the BCI-NMES group.

It is important to highlight the fact that NMES, per se, can provide motor gains and limited functional gains[38] by lessening the excitability of spinal reflex pathways, strengthening muscles, augmenting sensorimotor integration for the task at spinal and supraspinal levels, and augmenting the cortical sensory drive for activity-dependent plasticity[37]. Despite the fact that recent meta-analyses have shown a potentially beneficial effect of electrostimulation on upper limb functional recovery [79], national guidelines for clinical practice indicate that this type of therapy should not be performed on a routine basis [128].

Interestingly, motor recovery was present in the BCI-NMES group disregarding paralysis severity: all patients presenting hand plegia regained voluntary muscular contraction resulting in fist lifting and signs of fingers extension (see **Fig. 4.9** for two anecdotal case reports on the topic). None of the plegic patients that received sham-NMES showed any sign of recovery.

In conclusion, we propose a 5-weeks therapy based on a BCI system that decodes spared neural motor networks activity to trigger NMES of the paralyzed limb. The system is non-invasive and is personalized depending on patient's representation of hand movements. We believe that the use of EEG feedback training in conjunction with sensorimotor stimulation through

body's natural pathways might represent a new frontier for neuroprosthetics and rehabilitation medicine, opening the way for novel systems providing purposeful modulation of excitability in motor regions of intact and affected hemisphere overall contributing to improvements in motor function[72].

Future research on BCI-NMES should therefore focus on two directions: first, increasing the population size while keeping the active sham intervention, and possibly stratifying the population by age and level of disability, also quantifying potential synergistic effects on cognitive disability; second, investigating the mechanisms underlying the strong motor recovery, in particular the relation between closed loop control of NMES via spared neural motor networks, reduction of interhemispheric inhibition and increase of cortical excitability over the ipsi lesioned hemisphere.

Neurotechnology for future restorative medicine

The translational nature of the studies presented in this document provides a seminal demonstration of "bench-to-bedside" Neurotechnology. The modularity of the techniques shown in this Thesis give a measure of the extraordinary potential of this field for the future of restorative medicine. It is with great excitement that we envision non-invasive or minimally invasive systems able to provide affordable and effective restoration of lost function: a further step towards the eradication of physical disability.

Some of the principles and techniques presented in this Thesis went beyond pure scientific investigation, and were adopted with great success in clinical practice. The most striking example is the Stroke rehabilitation framework introduced in the **Introduction** and presented in **Chapter 4**, that allowed us to restore voluntary contraction of the extensor digitorum communis muscle in the participants that received our BCI-aided NMES therapy. To our surprise, this was also the case for plegic patients and several years after stroke.

Beyond the clinical value of our findings, we were able to provide an early quantification of the acceptance of Neurotechnology in the clinical setting by patients, therapists, clinicians. The **Appendix** of this Thesis contains two integral interviews we were able to provide to the first two patients involved in the BCI-aided neurorehabilitation framework. Even though their words reflect an extreme optimism towards the future developments of this technology, probably driven by their relatively good outcome, a lot has still to be done before we can consider current systems ready to become commercially available solutions [82]. Overcoming these technological limitations in usability, understanding the basic mechanisms underlying beneficial outcome driven by neural interfaces as well as establishing their efficacy for motor recovery in large clinical studies should be a research priority in the coming years.

A | An appendix

This chapter collects additional material concerning my doctoral research at the Defitech Chair in Non-Invasive Brain-Machine Interface (CNBI) of the École Politechnique Fédérale de Lausanne (EPFL), during the period between 2009 and 2014.

A.1 Two end-users interviews on BCI-aided NMES (French)

Date of interview : 27.11.2012

DOB : 27.03.1948

TOBI ID : DE27LE

Sex : masculin

☒ BCI training   ☒ Prototype(s) : WP4 hybrid

Diagnosis : Stroke July 2011, right sided-spastic hemiplegia

1. Comment vous êtes-vous retrouvé(e) impliqué(e) dans l'étude BCI ?

C'est Vanessa qui a contacté Valérie et m'a demandé si j'étais intéressé et j'étais intéressé, forcément.

2. Quel type de technologie d'assistance utilisez-vous actuellement

Uniquement l'étude des deux mains contre un miroir, se refléter dans un miroir (thérapie). Moyens auxiliaires : la canne. Autre chose ? pas de service spécial pour manger

3. Est-ce que cette canne vous est utile ? Elle m'est utile en aide à l'extérieur et dans la maison.

4. Aviez-vous déjà eu recours à la technologie BCI ?

Jamais

5. Que saviez-vous à propos de la technologie BCI ?

Moi je ne savais rien du tout, j'ai juste vu un extrait à la télévision où on utilisait ces outils pour aider des paraplégiques complets. Mais, pour moi, je n'avais jamais vu.

6. Vous êtes-vous senti(e) bien informé(e) quand vous avez commencé à participer aux essais BCI ?

Oui, oui je crois.

7. Qu'attendiez-vous de cette technologie ?

Beaucoup de curiosité, j'étais très très surpris du résultat.

8. Une fois sollicité(e) pour participer, quelles ont été vos motivations pour répondre favorablement à cette demande ? Pour quelles raisons êtes-vous devenu(e) un(e) participant(e) à l'étude BCI ?

Au début, j'ai eu des tests électriques pour voir la réponse électrique, et voilà puis cela jouait et puis je me suis dis pour autant que ça joue, ça joue.

Après les tests électriques, vous vous êtes dit puisque cela marche, alors j'y participe : oui.

9. Comment avez-vous vécu toute la procédure d'utilisation d'un dispositif BCI impliquant toute cette préparation obligatoire et tous ces efforts ?

C'était un peu long, il fallait compter ¼ h de préparation, mais en fait cela allait bien, on discutait, cela était en ordre.

10. Selon vous, la technologie est-elle utile et apporte-t-elle une aide ? Si oui : quel bénéfice vous a apporté l'utilisation de la BCI ? Si non : quels sont les types de problèmes auxquels vous avez dû faire face ?

Je ne sais pas si cela peut-être cela peut rendre utile à certaines personnes, mais à moi cela n'a pas été très utile. Je ne sais pas si à d'autres peut-être ça rend service.

Pourquoi pas utile ? Parce que je ne peux pas manœuvrer la manette comme j'aurai pu.

Quels types de problèmes ? Le problème des doigts et puis le problème du poignet, les doigts étaient ensemble, ils ne se développaient pas comme ils devraient se développer.

11. Êtes-vous plutôt satisfait(e) de vos expériences ou êtes-vous déçu(e) ? Veuillez préciser dans quelle mesure vos attentes ont été satisfaites ou insatisfaites ?

85

Non, je suis satisfait parce qu'ils ont vu que ce projet peut être obtenu avec d'autres patients, cela pourrait rendre service pour plus tard.

12. S'agit-il d'une performance spéciale que vous avez été capable d'entreprendre et qui vous a surpris ou étonné ?

Non, cela n'a pas surpris. Ce qui m'a étonné un peu quand même ça a été de pouvoir lever mon poignet chaque fois le bip retentissait

13. Avez-vous ressenti une différence entre l'utilisation du dispositif BCI et l'utilisation d'outils ou de dispositifs plus traditionnels ? Si oui, comment avez-vous vécu la différence ?

Pas forcément, non.

14. Pouvez-vous décrire à quoi ressemble l'utilisation d'un dispositif BCI ?

On a des électrodes qui viennent jusqu'aux bras et puis on suit sur l'écran de télévision une sorte de flèche et on doit réagir quand la flèche atteint le total au moment où elle monte et si ça monte ça fait le mouvement.

15. Comment avez-vous vécu le rôle de votre cerveau lors de l'utilisation d'un dispositif s'appuyant sur la BCI ?

Je me concentrais sur le fait que mon poignet devait faire des mouvements que je lui commandais.

16. Avez-vous eu l'impression que le dispositif BCI et vous-même formiez ensemble une sorte d'unité fonctionnelle ? Tout à fait oui.

En d'autres termes, avez-vous appréhendé le dispositif BCI, au moment de son utilisation, comme une partie de vous-même, dans tous les sens du terme ?

Absolument.

17. Lors de l'utilisation de la BCI, étiez-vous capable de vous concentrer directement sur le travail que vous tentiez d'accomplir ? Je veux dire par là : avez-vous pu faire

abstraction de la technologie et des stratégies d'utilisation apprises pour l'utiliser, et faire uniquement ce que vous souhaitiez faire ?

Oui, on a eu l'occasion de nous concentrer sur le projet ¼ h avant et puis quand ça marchait on était 100% content comme on le souhaitait.

18. Imaginez que le dispositif que vous avez testé devienne une solution standard largement employée dans la vie de tous les jours. Pouvez-vous en envisager certains problèmes spécifiques provenant d'une telle utilisation ?

Non, je ne vois pas.

19. Selon vous, faudrait-il mettre en place des dispositions formelles spécifiques réglementant l'utilisation de la technologie BCI en général ou du dispositif que vous utilisez en particulier

Non, c'est uniquement pour nous, ce n'est pas nécessaire faire une réglementation spéciale.

20. Si vous revenez sur votre participation, de quelle manière évalueriez-vous votre contribution à ce projet ? Avez-vous le sentiment que votre participation a été utile ?

Oui, je pense.

21. Si une personne vous demandait si elle devait participer à une étude similaire, quelle serait votre réponse ?

Oui tout le monde devrait entreprendre cette chance- là.

22. Aujourd'hui que les études sont terminées, vous sentez-vous soulagé(e) ? Ou regrettez-vous qu'elles le soient ? (ou : vous sentirez-vous mieux une fois les études terminées? ou regretterez-vous qu'elles le soient ?

Non pas forcément parce que j'aurai aimé aller plus longtemps. Oui, je regrette qu'elle soit terminée, forcément c'était un truc intéressant cela m'aurait plus de le prolonger longtemps.

23. Si vous revenez sur votre participation, quels sont vos conclusions et commentaires personnels ?

Je suis un peu..., je ne sais pas exactement quand concevoir... cela a été utile que j'ai fait cela. Pas de commentaire.

(Commentaire de l'épouse) : je pense que les réponses sont peut-être un peu sur la réserve parce que peut-être que ses attentes étaient plus grandes que le résultat donné. Vous nous avez bien expliqué au départ que c'était du 50-50 et je pense que malgré tout quand on participe à un projet comme ça, l'espérance est peut-être plus grande. Je pense que c'est un petit peu ça qui fait ses réactions, ses réponses sont un petit peu mitigées. Mais en tout cas moi ce que je peux dire c'est qu'il y est toujours allé de bon cœur, qu'il avait du plaisir. J'ai même pu assister une fois à une séance que j'ai trouvée très intéressante. C'est vrai que la mise en place prend du temps, mais après le travail cela se passait bien, soit en regardant l'écran soit sans regarder l'écran. C'était impressionnant. Il a été prévu ou discuté en tout cas avec Vanessa qu'il y aurait encore une séance possible au mois de janvier, une fois que l'injection de Botox aura eu lieu pour voir un petit peu les changements, peut-être que là il y aura plus de réaction, je ne sais pas. En tout cas, le Botox on ne savait pas tellement à quoi cela servait, mais maintenant on a réalisé la peine qu'il a à marcher, qu'il y a 2 mois qu'il attend son Botox et on se rend bien à quoi ça sert. Alors que tout au début, on n'a jamais réalisé du fait qu'il avait eu les premières injections quand il était encore en chaise roulante, donc on n'a pas vraiment vu le bénéfice apporté par ces injections.

Le Botox il l'a pour la jambe et le bras, ou seulement la jambe ? Les deux, jambe et bras.

Merci beaucoup de votre participation !

Botox le 25.06.2012

Membre supérieur droit

Muscle fléchisseur superficiel des doigts II à V	:	80 UI
Muscle fléchisseur profond des doigts	:	40 UI
Muscle long fléchisseur du pouce	:	20 UI
Muscle court fléchisseur du pouce	:	10 UI
Muscle fléchisseur radial du carpe	:	40 UI
Muscle fléchisseur ulnaire du carpe	:	30 UI

88

Membre inférieur droit

Muscle long fléchisseur des orteils II à V   :   80 UI
Muscle long fléchisseur de l'hallux   :   40 UI
Muscle court fléchisseur des orteils II à V   :   20 UI

Dosage total   : **350 UI**

Date of interview : 20.11.12

DOB : 21.12.1941

TOBI ID : HE21ER

Sex : male

☒ BCI training   ☒ Prototype(s) : WP4 hybrid

Diagnosis : Stroke, 11.07.2011 with right hemiplegia

1. Comment vous êtes-vous retrouvé(e) impliqué(e) dans l'étude BCI ?

   Par l'intermédiaire de ma physiothérapeute à la Suva.

2. Quel type de technologie d'assistance utilisez-vous actuellement

   Actuellement, en technologie d'assistance, j'utilise mon ordinateur et c'est tout. J'avais déjà l'ordinateur avant l'AVC. Ce n'est pas un moyen auxiliaire effectivement.

3. Cette technologie vous est-elle pratique ?

   C'est la seule qui me permettait de m'exprimer physiquement après l'accident.

4. Aviez-vous déjà eu recours à la technologie BCI ?

   Non, pas jusqu'à ce jour.

5. Que saviez-vous à propos de la technologie BCI ?

   Quand on m'a proposé de faire ce type de thérapie, je me suis un petit peu informé sur le déroulement du système.

6. Vous êtes-vous senti(e) bien informé(e) quand vous avez commencé à participer aux essais BCI ?

90

   Excellemment bien informé.

7. Qu'attendiez-vous de cette technologie ?

   J'attendais des résultats spectaculaires.

8. Une fois sollicité(e) pour participer, quelles ont été vos motivations pour répondre favorablement à cette demande ? Pour quelles raisons êtes-vous devenu(e) un(e) participant(e) à l'étude BCI ?

   Parce que j'étais très très impliqué dans le, comment il faut que je m'exprime, j'étais persuadé que cela m'aiderait à quelque chose et que cela ferait avancer mon handicap.

9. Comment avez-vous vécu toute la procédure d'utilisation d'un dispositif BCI impliquant toute cette préparation obligatoire et tous ces efforts ?

Avec énormément de plaisir et je me suis impliqué à fond.

10. Selon vous, la technologie est-elle utile et apporte-t-elle une aide ? Si oui : quel bénéfice vous a apporté l'utilisation de la BCI ? Si non : quels sont les types de problèmes auxquels vous avez dû faire face ?

   Effectivement je n'ai été confronté à aucun problème, je n'ai eu que des solutions aux erreurs tels que l'usage de mes doigts et la mobilité de mes mains. La mobilité de ma jambe, paradoxalement, qui n'avait rien à être impliquée dedans, qui allait bien ensuite en fin de l'exercice, la capacité de me concentrer sur mon esprit.

11. Êtes-vous plutôt satisfait(e) de vos expériences ou êtes-vous déçu(e) ? Veuillez préciser dans quelle mesure vos attentes ont été satisfaites ou insatisfaites ?

   Mes expériences ont été satisfaisantes, pleinement satisfaisantes, parce qu'à chaque séance, j'ai remarqué que je pouvais faire des efforts de concentration, des efforts de mémorisation et des efforts physiques tels que les doigts de la main, le bras, la jambe qui ne faisait pas du tout partie de cette étude.

12. S'agit-il d'une performance spéciale que vous avez été capable d'entreprendre et qui vous a surpris ou étonné ?

Cette expérience m'a étonné et m'étonne encore, bien que l'on soit arrivé à la fin de cette expérience, c'était quelque chose de fabuleux.

13. Avez-vous ressenti une différence entre l'utilisation du dispositif BCI et l'utilisation d'outils ou de dispositifs plus traditionnels ? Si oui, comment avez-vous vécu la différence ?

Enorme différence, en ce sens que la physio c'est vraiment musculaire et cette étude, c'était vraiment cérébral.

14. Pouvez-vous décrire à quoi ressemble l'utilisation d'un dispositif BCI ?

Comment expliquer ça ? C'est la concentration extrême qu'il faut avoir pour réussir ce type d'opération.

15. Comment avez-vous vécu le rôle de votre cerveau lors de l'utilisation d'un dispositif s'appuyant sur la BCI ?

Cela m'a apporté des connaissances supplémentaires parce que je me suis informé au fur et à mesure des thérapies.

16. Avez-vous eu l'impression que le dispositif BCI et vous-même formiez ensemble une sorte d'unité fonctionnelle ? ou en d'autres termes, avez-vous appréhendé le dispositif BCI, au moment de son utilisation, comme une partie de vous-même, dans tous les sens du terme ?

Alors ça c'est clair. Il est clair c'est la coordination cerveau-ordinateur qui m'a été bénéfique.

17. Lors de l'utilisation de la BCI, étiez-vous capable de vous concentrer directement sur le travail que vous tentiez d'accomplir ? Je veux dire par là : avez-vous pu faire abstraction de la technologie et des stratégies d'utilisation apprises pour l'utiliser, et faire uniquement ce que vous souhaitiez faire ?

Effectivement, j'ai entre autre une petite anecdote, c'est que dans les thérapies j'ai eu un début de lumbago qui, à ce moment-là, a empêché ma concentration extrême et cela s'est remarqué sur mes performances.

18. Imaginez que le dispositif que vous avez testé devienne une solution standard largement employée dans la vie de tous les jours. Pouvez-vous en envisager certains problèmes spécifiques provenant d'une telle utilisation ?

Alors écoutez, c'est très difficile de dire. Mais je n'ai pas connu de problème spécifique durant toute cette thérapie. Il n'y a pas de raison que cela ne puisse pas aller de l'avant.

19. Selon vous, faudrait-il mettre en place des dispositions formelles spécifiques réglementant l'utilisation de la technologie BCI en général ou du dispositif que vous utilisez en particulier ?

Je ne pense pas nécessaire de réglementer étant donné que sa propriété intellectuelle est vraiment intellectuelle.

20. Si vous revenez sur votre participation, de quelle manière évalueriez-vous votre contribution à ce projet ? Avez-vous le sentiment que votre participation a été utile ?

Ma participation a été terriblement utile, dans le sens qu'elle m'a permis de progresser sans contrainte.

21. Si une personne vous demandait si elle devait participer à une étude similaire, quelle serait votre réponse ?

Il faut le faire, il faut profiter de cette opportunité.

22. Aujourd'hui que les études sont terminées, vous sentez-vous soulagé(e) ? Ou regrettez-vous qu'elles le soient ? (ou : vous sentirez-vous mieux une fois les études terminées? ou regretterez-vous qu'elles le soient ?

Je suis très triste que cela soit fini.

23. Si vous revenez sur votre participation, quels sont vos conclusions et commentaires personnels ?

J'ai eu énormément de plaisir à participer avec tout le personnel qui s'en est occupé et je souhaite que tout le monde puisse avoir cette chance-là.

93

Merci beaucoup de votre participation !

A.2 Media Coverage

When the mind controls the machines (EPFL Mediacom, **full text availabel here.**)

 23.01.13 - More than a hundred patients suffering from severe motor impairments have voluntarily participated in the development of non-invasive brain-machine interfaces. The main purpose of these machines is to allow the patients either regain some of their mobility or improve their social relationships. Today, three presentations took place in Sion during the closing seminar of the TOBI European research program (www.tobi-project.org), which has been coordinated by EPFL for approximately four years.

Stroke survivors, as well as patients suffering from other serious conditions, may have to deal with the partial or complete inability to move one or more of their limbs. In the most severe cases, the sufferer may become fully paralyzed and in need of permanent assistance.

The TOBI project (Tools for brain-computer interaction) is financed by the European Commission under the Seventh Framework Programme for Research (FP7) and is coordinated by EPFL. Since 2008 it has focused on the use of the signals transmitted by the brain. The electrical activity that takes place in the brain when the patient focuses on a particular task such as lifting an arm is detected by electroencephalography (EEG) through electrodes placed in a cap worn by the patient. Subsequently, a computer reads the signals and turns them into concrete actions as, for instance, moving a cursor on a screen.

Tests involving more than 100 patients
Based on this idea, researchers from thirteen institutions together with TOBI project partners have developed various technologies aimed at either obtaining better signal quality, making them clearer, or translating them into useful and functional applications. During the research, more than 100 patients or handicapped users had the opportunity to test the devices. Three of the technologies developed within the framework of TOBI were publicly presented at the closing seminar of the research program that took place in Sion from 23 to 25 January 2013.

1. **Robotino, for helping rebuild social ties when bedridden.** Combining EEG, signal recognition, obstacle sensors and the internet, researchers have been able to develop a small robot equipped with a camera and a screen that can be controlled remotely by physically disabled people. Thanks to this device, the patient can take a virtual walk in a familiar environment, meet her/his relatives and talk to them, even if they are thousands of miles away from each other.

2. **Braintree, for writing texts and internet surfing.** Researchers have also developed a graphical interface specially adapted for web browsing by severely disabled people. By thinking, the patient is able to move a cursor in a tree structure in order to type a character or choose a command. Depending on the specific situation, the sensors can

Figure A.1: **EPFL News - When the mind controls the machines.** Youtube video describing the basic functioning of the BCI-aided NMES system presented in this Thesis. Link to video content here.

also detect residual muscular activity to complement the management of the device.

3. **Functional electrical stimulation**, to restore some basic mobility. Coupling EEG with electrical muscle stimulation can allow a patient to voluntarily control the movement of a paralyzed limb. In some cases, intensive training using this system has allowed the patients to regain control of the limb and keep it without assistance. A report on this technique can be seen in the video above.

The results of the TOBI research program have restored patients' hope. They will constitute the basis of subsequent developments to be conducted among the research partners or at industrial level. As for EPFL, such results will be the core of its health research chairs at the new EPFL Valais Wallis academic cluster, which can also count on the participation and support of the SuvaCare rehabilitation clinic in Sion.

"Our results are already very promising," says José del R. Millán, professor at the Centre for Neuroprosthetics (CNP) at EPFL, holder of the Defitech Foundation Chair in Non-Invasive Brain-Machine Interface and TOBI project coordinator. Nevertheless, he adds: "The road is still long before the "turnkey" product is made available to physicians and patients. Each brain has its own way of transmitting its signals and the devices' calibration requires the investment of significant resources. However, we have paved the way for a new critical approach to the physical and social rehabilitation of patients."

EPFL implantée à la Suva: les chercheurs sont déjà actifs (Canal9 en continu, **full text availabel here.**)

Ils sont cinq et travaillent dans le domaine de la rééducation des personnes cérébro-lésées. Ce sont les premiers chercheurs installés en Valais dans le cadre du projet d'implantation de

95

Figure A.2: **Canal 9.** .Link to video content here.

l'EPFL à la clinique SUVA. Sur quoi travaillent-ils et avec qui? C'est le sujet de notre reportage.

Bibliography

[1] Ackery, A., Tator, C., Krassioukov, A. (2004) "A global perspective on spinal cord injury epidemiology." Journal of Neurotrauma 21 (10): 1355–1370.

[2] Ang, K.K., Cuntai G. (2013) "Brain-Computer Interface in Stroke Rehabilitation." Journal of Computing Science and Engineering 7 (2): 139–146.

[3] Ang, K.K., Cuntai G., Kok S.P., Chuanchu W., Longjiang Z., Ka Y.T., Ephraim J., Gopal J., Keong C.W., Sui, K., Geok C. (2014) "Brain-Computer Interface-based robotic end effector system for wrist and hand rehabilitation: results of a three-armed randomized controlled trial for chronic stroke." Frontiers in Neuroengineering 7: 30.

[4] Marcia, A., Jerome, P. Kassirer, A., Relman, S. (2000) "Looking back on the millennium in medicine." New Englamd Journal of Medicine 342: 42–49.

[5] Ang, K.K., Guan, C., Phua, K.S., Wang, C., Teh, I., Chen, C.W., Chew, E. (2012) "Transcranial direct current stimulation and EEG-based motor imagery BCI for upper limb stroke rehabilitation". In Annual International Conference of the IEEE Engineering in Medicine and Biology Society (EMBC): 4128–4131.

[6] Ang, K.K., Guan, C., Phua, K.S., Wang, C., Zhao, L., Teo, W.P., Chew, E. (2013) "Facilitating effects of transcranial direct current stimulation on EEG-based motor imagery BCI for stroke rehabilitation." In Proceedings of the Fifth International Brain-Computer Interface Meeting: 76.

[7] Bates, J. A. V. (1951) "Electrical Activity of the Cortex Accompanying Movement." Journal of Physiology 113: 240–257.

[8] Berger, H. (1929) "Über das Elektroenkephalogramm des Menschen." Archiv fur Psychiatrie und Nervenkrankheiten 87: 527–570.

[9] Biasiucci, A., Chavarriaga, R., Hamner, B., Leeb, R., Pichiorri, F., De Vico Fallani, F., Mattia, D., Millán, J.d.R. (2011) "Combining discriminant and topographic information in BCI: preliminary results on stroke patients." 5th International IEEE/EMBS Conference on Neural Engineering (NER): 290-293.

Bibliography

[10] Biasiucci, A., Chavarriaga, R., Leeb, R., Murray, M.M., Mattia, D., Millán, J.d.R. (2014) "Decoding single-trial topographic EEG correlates of motor engagement and rest reveals subject-independent organization" In preparation.

[11] Biasiucci, A., Leeb, R., Al-Khodairy, A., Zhang, H., Schnider, A., Schmidlin, T., Vuadens, P., Guggisberg, A., Millán, J.d.R. (2014) "Brain-Controlled Neuromuscular Electrical Stimulation Promotes Permanent Upper Limb Functional Recovery after Stroke" In review.

[12] Birbaumer, N., Ghanayim, M., Hinterberger, T., Iversen, I., Kotchoubey, B., Kübler, A., Perelmouter, J., Taub, E., Flor, H. (1999) "A spelling device for the paralysed." Nature 398 (6725): 297–298.

[13] Birbaumer, N., Cohen. L.G. (2007) "Brain–computer interfaces: communication and restoration of movement in paralysis." The Journal of physiology 579 (3): 621–636.

[14] Blankertz, B., Tomioka, R., Lemm, S., Kawanabe, M., Muller, K. R. (2008) "Optimizing spatial filters for robust EEG single-trial analysis." IEEE Signal Processing Magazine, 25(1), 41–56.

[15] Blankertz, B., Lemm, S., Treder, M., Haufe, S., Müller, K.R. (2011) "Single-trial analysis and classification of ERP components — A tutorial." NeuroImage 56: 814–825.

[16] Borton, D., Micera, S., Millán, J.d.R., Courtine. G. (2013) "Personalized Neuroprosthetics." Science Translational Medicine 5 (210): 210.

[17] Britz, J., Van De Ville, D., Michel, C. M. (2010) "BOLD correlates of EEG topography reveal rapid resting-state network dynamics." Neuroimage, 52(4), 1162–1170.

[18] Broetz, D., Braun, C., Weber, C., Soekadar, S.R., Caria, A., Birbaumer, N. (2010) "Combination of brain-computer interface training and goal-directed physical therapy in chronic stroke: a case report." Neurorehabilitation and Neural Repair 24 (7): 674–679.

[19] Buch, E., Weber, C., Cohen, L. G., Braun, C., Dimyan, M. A., Ard, T., Mellinger, J., Birbaumer, N. (2008) "Think to move: a neuromagnetic brain-computer interface (BCI) system for chronic stroke." Stroke, 39(3): 910–917.

[20] Bullmore, E. T., Suckling, J., Overmeyer, S., Rabe-Hesketh, S., Taylor, E., Brammer, M. J. (1999) "Global, voxel, and cluster tests, by theory and permutation, for a difference between two groups of structural MR images of the brain." IEEE Transactions on Medical Imaging 18(1): 32–42.

[21] Caldara, R., Deiber, M. P., Andrey, C., Michel, C. M., Thut, G., Hauert, C. A. (2004) "Actual and mental motor preparation and execution: a spatiotemporal ERP study." Experimental Brain Research 159(3): 389–399.

[22] Caria, A., Weber, C., Brötz, D., Ramos, A., Ticini, L. F., Gharabaghi, A., Birbaumer, N. (2011). "Chronic stroke recovery after combined BCI training and physiotherapy: a case report." Psychophysiology 48(4): 578–582.

[23] Carlson, T., Millán, J.d.R. (2013) "Brain-controlled wheelchairs: a robotic architecture." IEEE Robotics and Automation Magazine 20: 65–73.

[24] Cassim, F., Szurhaj, W., Sediri, H., Devos, D., Bourriez, J. L., Poirot, I., Derambure, P., Defebvre, L., Guieu, J. D. (2000) "Brief and sustained movements: differences in event-related (de) synchronization (ERD/ERS) patterns." Clinical Neurophysiology 111 (11): 2032–2039.

[25] Chae, J., Sheffler, L.R., Knutson, J.S. (2008) "Neuromuscular electrical stimulation for motor restoration in hemiplegia." Topics in stroke rehabilitation 15 (5): 412-426.

[26] Chavarriaga, R., Biasiucci, A., Molina, A., Leeb, R., León, V. S., Campolo, M., Millán, J.d.R. (2013) "tDCS Modulates Motor Imagery-Related BCI Features." In Converging Clinical and Engineering Research on Neurorehabilitation: 647–651, Springer Berlin Heidelberg.

[27] Chavarriaga, R., Biasiucci, A., Creatura, M., Carrasco C., León, V. S., Campolo, M., Oliviero, A., Millán, J.d.R. (2014) "Selective Enhancement of Sensorimotor Rhythms for Brain Computer Interaction by Means of tDCS." In preparation.

[28] Chavarriaga, R., Sobolewski, A., Millán, J.d.R. (2014) "Errare machinale est: the use of error-related potentials in brain-machine interfaces." Frontiers in Neuroscience 8.

[29] Clark, V. P., Coffman, B. A., Mayer, A. R., Weisend, M. P., Lane, T. D., Calhoun, V. D., Wassermann, E. M. (2012) "TDCS guided using fMRI significantly accelerates learning to identify concealed objects". Neuroimage 59(1): 117–128.

[30] Clark, V. P., Parasuraman, R. (2014) "Neuroenhancement: enhancing brain and mind in health and in disease." Neuroimage 85: 889–894.

[31] Coffman, B. A., Trumbo, M. C., Clark, V. P. (2012) "Enhancement of object detection with transcranial direct current stimulation is associated with increased attention." BMC Neuroscience 13(1): 108.

[32] Grégoire, C., Micera, S. Di Giovanna, J., Millán, J.d.R. (2012) "Brain-machine interface: closer to therapeutic reality?" The Lancet 381 (9866): 515–517.

[33] Daly, J.J., Wolpaw, J.R. (2008) "Brain-computer interfaces in neurological rehabilitation." The Lancet Neurology 7 (11): 1032–43.

[34] Daly JJ, Cheng R, Rogers J, Litinas K, Hrovat K, Dohring M. (2009) "Feasibility of a new application of noninvasive Brain Computer Interface (BCI): a case study of training for

recovery of volitional motor control after stroke." Journal of Neurology and Physical Therapy 33(4): 203–211.

[35] Damoiseaux, J.S., Rombouts, S.A.R.B, Barkhof, F., Scheltens, P. Stam, C.J., Smith, S.M., Beckmann, C.F. (2006) "Consistent resting-state networks across healthy subject." Proceedings of the National Academy of Sciences 103 (37): 13848–13853.

[36] Dimyan, M. A. and Cohen, L. G. (2011) "Neuroplasticity in the context of motor rehabilitation after stroke." Nature Reviews Neurology 7: 76–85.

[37] Dobkin, B.H. (2003) "Do electrically stimulated sensory inputs and movements lead to long-term plasticity and rehabilitation gains?" Current Opinion in Neurology 16 (6): 685–691.

[38] Dobkin, B.H. (2004) "Strategies for stroke rehabilitation." The Lancet Neurology 3 (9): 528-536.

[39] Dobkin, Bruce H. (2005) "Rehabilitation after stroke." New England Journal of Medicine 356 (16): 1677-1684.

[40] Dobkin, B. (2007) "Brain-computer interface technology as a tool to augment plasticity and outcomes for neurological rehabilitation." The Journal of Physiology 579 (3): 637–42.

[41] Dobkin BH. (2009) "Progressive Staging Of Pilot Studies To Improve Phase iii Trials For Motor Interventions." Neurorehabil Neural Repair 23: 197—206.

[42] Duda, R.O., Hart, P. E., Stork, D.G. (2012) "Pattern classification." New York: John Wiley & Sons.

[43] Elbert, T., Rockstroh, B., Lutzenberger, W., Birbaumer, N. (1980) "Biofeedback of slow cortical potentials. I." Electroencephalography and Clinical Neurophysiology 48(3): 293–301.

[44] Elbert, T. (1993) "Slow cortical potentials reflect the regulation of cortical excitability." Springer US.

[45] Falcone, B., Coffman, B. A., Clark, V. P., Parasuraman, R. (2012) "Transcranial direct current stimulation augments perceptual sensitivity and 24-hour retention in a complex threat detection task". PloS one 7 (4): e34993.

[46] Famm, K., Litt, B., Tracey, K. J., Boyden, E. S., Slaoui, M. (2013) "Drug discovery: a jump-start for electroceuticals". Nature 496 (7444): 159–161.

[47] Farwell, L.A., Donchin, E. (1988) "Talking off the top of your head: toward a mental prosthesis utilizing event-related brain potentials." Electroencephalography and Clinical Neurophysiology 70 (6): 510–523.

[48] Fawcett, T. (2006) "An introduction to ROC analysis." Pattern Recognition Letters, 27 (8): 861–874.

[49] Feigin, V. L., Forouzanfar, M. H., Krishnamurthi, R., Mensah, G. A., Connor, M., Bennett, D. A., Murray, C. (2014) "Global and regional burden of stroke during 1990–2010: findings from the Global Burden of Disease Study 2010." The Lancet 383 (9913): 245–255.

[50] Fiedler, I. G., Laud, P. W., Maiman, D. J., Apple, D. F. (1999) "Economics of managed care in spinal cord injury." Archives of physical medicine and rehabilitation 80(11): 1441–1449.

[51] Förster, K., Biasiucci, A., Chavarriaga, R., Millán, J.d.R., Roggen, D., Tröster, G. (2010) "On the use of brain decoded signals for online user adaptive gesture recognition systems." In Pervasive Computing: 427-444, Springer Berlin Heidelberg.

[52] Fregni, F., Pascual-Leone, A. (2007) "Technology insight: noninvasive brain stimulation in neurology—perspectives on the therapeutic potential of rTMS and tDCS." Nature Clinical Practice Neurology 3(7): 383–393.

[53] Fuentes, B., Tejedor, E. D. (2014) "Stroke: The worldwide burden of stroke – a blurred photograph." Nature Reviews Neurology 10(3): 127–128.

[54] Fugl-Meyer, A.R., Jääskö, L., Ley man, I., Olsson, S., Steglind, S. (1975) "The post-stroke hemiplegic patient 1: a method for evaluation of physical performance." Scandinavian Journal of Rehabilitation Medicine 7: 13–31.

[55] Galán, F., Ferrez, P., Oliva, F., Guardia, J., Millán, J.d.R. (2007) "Feature extraction for multi-class BCI using canonical variates analysis." In IEEE International Symposium on Intelligent Signal Processing.

[56] Galán, F., Nuttin, M., Lew, E., Ferrez, P. W., Vanacker, G., Philips, J., Millán, J.d.R. (2008) "A brain-actuated wheelchair: asynchronous and non-invasive brain–computer interfaces for continuous control of robots." Clinical Neurophysiology 119 (9): 2159–2169.

[57] Gandiga, P. C., Hummel, F. C., Cohen, L. G. (2006) "Transcranial DC stimulation (tDCS): a tool for double-blind sham-controlled clinical studies in brain stimulation." Clinical Neurophysiology 117 (4): 845–850.

[58] Garipelli, G., Chavarriaga, R., Millán, J.d.R. (2013) "Single trial analysis of slow cortical potentials: a study on anticipation related potentials." Journal of Neural Engineering 10 (3).

[59] Go, A. S., Mozaffarian, D., Roger, V. L., Benjamin, E. J., Berry, J. D., Blaha, M. (2014). "Heart disease and stroke statistics–2014 update: a report from the American Heart Association." Circulation 129 (3): e28.

Bibliography

[60] Guggenmos, D.J., Azin, M., Barbay, S., Mahnken, J.D., Dunham, C., Mohseni, P., Nudo, R.J. (2013) "Restoration of function after brain damage using a neural prosthesis." Proceedings of the National Academy of Sciences 110 (52): 21177–21182.

[61] Hallett, M. (2001) "Plasticity of the human motor cortex and recovery from stroke." Brain Research Reviews 36 (2): 169–174.

[62] He, B., Liu, Z. (2008) "Multimodal functional neuroimaging: integrating functional MRI and EEG/MEG". IEEE Reviews in Biomedical Engineering 1: 23–40.

[63] Honda, M., Nagamine, T., Fukuyama, H., Yonekura, Y., Kimura, J., Shibasaki, H. (1997) "Movement-related cortical potentials and regional cerebral blood flow change in patients with stroke after motor recovery." Journal of the Neurological Sciences 146 (2): 117–126.

[64] Horst, R.L., Donchin, E. (1980) "Beyond averaging. II. Single-trial classification of exogenous event-related potentials using stepwise discriminant analysis." Electroencephalography and Clinical Neurophysiology 48 (2): 113—126.

[65] Hummel, F., Cohen, L. G. (2005) "Improvement of motor function with noninvasive cortical stimulation in a patient with chronic stroke". Neurorehabilitation and neural repair, 19 (1), 14–19.

[66] Jasper, H., Penfield, W. (1949) "Electrocorticograms in man: effect of voluntary movement upon the electrical activity of the precentral gyrus." Archiv für Psychiatrie und Nervenkrankheiten, 183 (1-2), 163–174.

[67] Jazwinski, A. H. (1970) Stochastic Processes and Filtering Theory. New York: Academic Press.

[68] M. Jeannerod, (2001) "Neural simulation of action: A unifying mechanism for motor cognition" NeuroImage 14: S104–S109.

[69] Kaiser, V., Daly, I., Pichiorri, F., Mattia, D., Müller-Putz, G. R., Neuper, C. (2012) Relationship between electrical brain responses to motor imagery and motor impairment in stroke. Stroke 43(10): 2735–2740.

[70] M. Kamiski, M. Ding, W. A. Truccolo, and S. L. Bressler (2001) "Evaluating causal relations in neural systems: Granger causality, directed transfer function and statistical assessment of significance." Biological Cybernetics 85 (2): 145–157.

[71] Kaplan, Alexander Ya., Andrew A. Fingelkurts, Alexander A. Fingelkurts, Sergei V. Borisov, and Boris S. Darkhovsky (2005) "Nonstationary nature of the brain activity as revealed by EEG/MEG: Methodological, practical and conceptual challenges." Signal processing 85 (11): 2190–2212.

[72] Kapur, Narinder (1996) "Paradoxical functional facilitation in brain-behaviour research A critical review." Brain 119 (5): 1775–1790.

[73] Klamroth-Marganska, V., Blanco, J., Campen, K., Curt, A., Dietz, V., Ettlin, T., Felder, V., Riener, R. (2014). "Three-dimensional, task-specific robot therapy of the arm after stroke: a multicentre, parallel-group randomised trial." The Lancet Neurology 13 (2): 159–166.

[74] T. Koenig, F. Marti-Lopez and P. Valdes-Sosa (2001) "Topographic time-frequency decomposition of the EEG" Neuroimage 14 (2).

[75] Koenig, T., Prichep, L., Lehmann, D., Sosa, P. V., Braeker, E., Kleinlogel, H., John, E. R. (2002) "Millisecond by millisecond, year by year: normative EEG microstates and developmental stages." Neuroimage 16 (1): 41–48.

[76] Korzeniewska, A., Mańczak, M., Kamiński, M., Blinowska, K. J., Kasicki, S. (2003) "Determination of information flow direction among brain structures by a modified directed transfer function (dDTF) method." Journal of Neuroscience Methods 125 (1-2): 195–207.

[77] Kuncheva, L.I. (2007) "A stability index for feature selection." In IASTED Multi-Conference: artificial intelligence and applications.

[78] Laganaro, M., Stéphanie M., Michel, C.M., Spinelli, L., Schnider, A. (2011) "ERP correlates of word production before and after stroke in an aphasic patient." Journal of Cognitive Neuroscience 1(8).

[79] Langhorne, P., Coupar, F., Pollock, A. (2009) "Motor recovery after stroke: a systematic review." The Lancet Neurology 8 (8): 741–754.

[80] Lang, N., Nitsche, M.A., Paulus, W., Rothwell, J.C., Lemon, R.N. (2004) "Effects of transcranial direct current stimulation over the human motor cortex on corticospinal and transcallosal excitability." Exp Brain Res, 156 (4):439–443.

[81] Lapenta, O.M., Minati, L., Fregni, F., Boggio, P.S. (2013) "Je pense donc je fais: transcranial direct current stimulation modulates brain oscillations associated with motor imagery and movement observation." Frontiers in Human Neuroscience 7: 256.

[82] Leeb, R., Perdikis, S., Tonin, L., Biasiucci, A., Tavella, M., Creatura, M., Millán, J.d.R. (2013) "Transferring brain–computer interfaces beyond the laboratory: Successful application control for motor-disabled users." Artificial intelligence in medicine 59 (2): 121–132.

[83] Lehmann, D. (1971) "Multichannel Topography of Human Alpha EEG Fields." Electroencephalography and Clinical Neurophysiology 31: 439–449.

[84] Lehmann, D., Skrandies, W. (1980) "Reference-free identification of components of checkerboard-evoked multichannel potential fields." Electroencephalography and Clinical Neurophysiology 48 (6): 609–621.

[85] D. Lehmann, (1971) "Multichannel topography of human alpha EEG fields", Electroencephalography and Clinical Neurophysiology 31 (5).

[86] Lehmann, D., Faber, P.L. Galderisi, S. Herrmann, W.H., Kinoshita, T., Koukkou, M., Mucci, A., Koenig, T. (2005) "EEG microstate duration and syntax in acute, medication-naive, first-episode schizophrenia: a multi-center study." Psychiatry Research: Neuroimaging 138 (2): 141–156.

[87] Lemm, S., Blankertz, B., Dickhaus, T., Muller K.R. (2011) "Introduction to machine learning for brain imaging." NeuroImage 56 (2): 387–399.

[88] Lew, E. Y. L., Chavarriaga, R., Silvoni, S., Millán, J.d.R. (2014) "Single trial prediction of self-paced reaching directions from EEG signals." Fontiers in Neuroprosthetics (8) 222.

[89] Lopes da Silva, F. (2004) "EEG analysis: theory and practice." In Electroencephalography: Basic Principles, Clinical Applications and Related Fields": 1199–1232, Williams & Wilkins.

[90] Lynch, Z. (2004) "Neurotechnology and society (2010–2060)". Annals of the New York Academy of Sciences 1013(1): 229-233.

[91] MacMahon, S. (2002) "Introduction: The global burden of stroke", Clinician's Manual on Blood Pressure and Stroke Prevention: 1-6, J. Chalmers Science Press London.

[92] Mantini, D., Perrucci, M.G., Del Gratta, C., Romani, G.L., Corbetta, M. (2007) "Electrophysiological signatures of resting state networks in the human brain." Proceedings of the National Academy of Sciences 104 (32): 13170–13175.

[93] Matsumoto, J., Fujiwara, T., Takahashi, O., Liu, M., Kimura, A., Ushiba, J. (2010) "Modulation of mu rhythm desynchronization during motor imagery by transcranial direct current stimulation." J Neuroeng Rehabil 7: 27.

[94] Menken, M., Munsat, T. L., Toole, J. F. (2000) "The global burden of disease study: implications for neurology." Archives of Neurology 57 (3): 418–420.

[95] Michel, C.M., Murray, M.M. (2012) "Towards the utilization of EEG as a brain imaging tool." NeuroImage 61: 371–385.

[96] Millan, J.d.R., Renkens, F., Mouriño, J., Gerstner, W. (2004) " Noninvasive brain-actuated control of a mobile robot by human EEG." IEEE Transactions on Biomedical Engineering 51 (6): 1026–1033.

[97] Millán, J.d.R., Rupp, R., Müller-Putz, G.R., Murray-Smith, R., Giugliemma, C., Tangermann, M., Vidaurre, C., Mattia, D. (2010) "Combining brain–computer interfaces and assistive technologies: state-of-the-art and challenges." Frontiers in Neuroscience 4.

[98] Mjolsness, E., DeCoste, D. (2001) "Machine learning for science: state of the art and future prospects." Science 293 (5537): 2051–2055.

[99] Moon, T.K. (1996) "The expectation-maximization algorithm." IEEE Signal processing magazine 13 (6): 47–60.

[100] Mordillo-Mateos, L., Turpin-Fenoll, L., Millán-Pascual, J., Núñez-Pérez, N., Panyavin, I., Gómez-Argüelles, J.M., Botia-Paniagua, E., Foffani, G., Lang, N., Oliviero, A. (2011) "Effects of simultaneous bilateral tDCS of the human motor cortex." Brain Stimulation.

[101] Morris, P., Perkins, A. (2012) "Diagnostic imaging." The Lancet 379 (9825): 1525–1533.

[102] Müller-Putz, G., Scherer, R., Brunner, C., Leeb, R., Pfurtscheller, G. (2008) "Better than random: A closer look on BCI results". International Journal of Bioelectromagnetism 10: 52–55.

[103] Muller, K.R., Tangermann, M., Dornhege, G., Krauledat, M., Curio, G., Blankertz, B. (2008) "Machine learning for real-time single-trial EEG-analysis: from brain-computer interfacing to mental state monitoring." Journal of Neuroscience Methods 167 (1): 82–90.

[104] Murase, N., Duque, J., Mazzocchio, R., Cohen, L.G. (2004) "Influence of interhemispheric interactions on motor function in chronic stroke." Annals of Neurology 55 (3) : 400–409.

[105] Murray, C. J., Lopez, A. D. (1997) "Alternative projections of mortality and disability by cause 1990–2020: Global Burden of Disease Study." The Lancet 349 (9064): 1498–1504.

[106] Murray, M.M., Brunet, D., Michel, C.M. (2008) "Topographic ERP analyses: a step-by-step tutorial review." Brain Topography 20(4): 249-264.

[107] Musso, F., Brinkmeyer, J., Mobascher, A., Warbrick, T., Winterer, G. (2010) "Spontaneous brain activity and EEG microstates. A novel EEG/fMRI analysis approach to explore resting-state networks." NeuroImage 52 (4): 1149–1161.

[108] Neuper, C., Wörtz, M., Pfurtscheller, G. (2006) "ERD/ERS patterns reflecting sensorimotor activation and deactivation." Progress in Brain Research 159: 211–222.

[109] Nilsen, D.M., Gillen, G., Gordon, A.M. (2010) "Use of mental practice to improve upper-limb recovery after stroke: A systematic review", The American Journal of Occupational Therapy 64 (5).

Bibliography

[110] Nitsche, M. A., Paulus, W. (2000) "Excitability changes induced in the human motor cortex by weak transcranial direct current stimulation." The Journal of Physiology 527(3): 633–639.

[111] O'Shea, J., Boudrias, M. H., Stagg, C. J., Bachtiar, V., Kischka, U., Blicher, J. U., Johansen-Berg, H. (2014) "Predicting behavioural response to TDCS in chronic motor stroke." Neuroimage 85: 924–933.

[112] Page, S.J., Fulk, G.D., Boyne, P. (2012) "Clinically important differences for the upper-extremity Fugl-Meyer Scale in people with minimal to moderate impairment due to chronic stroke." Physical Therapy 92: 791—98.

[113] Pascual-Marqui, R.D., Michel, C.M., Lehmann, D. (1995) "Segmentation of brain electrical activity into microstates: model estimation and validation." IEEE Transactions on Biomedical Engineering 42 (7): 658–665.

[114] Peckham, P.H., Knutson, J.S. (2005) "Functional Electrical Stimulation for Neuromuscular Applications" Annual Reviews in Biomedical Engineering 7: 327–360.

[115] Perrin, F., Pernier, J.,Bertrand, O., Giard, M.H., Echallier, J.F. (1987) "Mapping of scalp potentials by surface spline interpolation." Electroencephalography and Clinical Neurophysiology 66: 75—81.

[116] Pfurtscheller, G. (1989) "Functional topography during sensorimotor activation studied with event-related desynchronization mapping." Journal of Clinical Neurophysiology 6 (1): 75–84.

[117] Pfurtscheller, G., Pregenzer, M., Neuper, C. (1994) "Visualization of sensorimotor areas involved in preparation for hand movement based on classification of μ and central β rhythms in single EEG trials in man." Neuroscience letters (181): 43–46.

[118] Pfurtscheller, G., Lopes da Silva, F.H. (1999) "Event-related EEG/MEG synchronization and desynchronization: basic principles." Clinical Neurophysiology (110): 1842–1857.

[119] Pfurtscheller, G., Brunner, C., Schlögl, A., Lopes da Silva, F.H. (2006) "Mu rhythm (de) synchronization and EEG single-trial classification of different motor imagery tasks" Neuroimage 31 (1).

[120] Pichiorri, F., F. De Vico Fallani, F. Cincotti, F. Babiloni, M. Molinari, S.C. Kleih, C. Neuper, A. Kübler, D. Mattia (2011) "Sensorimotor rhythm-based brain–computer interface training: the impact on motor cortical responsiveness." Journal of Neural Engineering 8 (2)

[121] Poldrack, R. A. (2000) "Imaging brain plasticity: conceptual and methodological issues—a theoretical review." Neuroimage 12(1): 1-13.

[122] Pollock, A., St George, B., Fenton, M., Firkins, L. (2012) "Top ten research priorities relating to life after stroke." The Lancet Neurology 11 (3): 209.

[123] Powell, J., Pandyan, A. D., Granat, M., Cameron, M., Stott, D. J. (1999). "Electrical stimulation of wrist extensors in poststroke hemiplegia." Stroke 30 (7): 1384–1389.

[124] Prasad, G., Herman, P., Coyle, D., McDonough, S., Crosbie, J. (2010) "Applying a brain-computer interface to support motor imagery practice in people with stroke for upper limb recovery: a feasibility study." Journal of Neuroengineering and Rehabilitation 7 (1): 60.

[125] Quartarone, A., Morgante, F., Bagnato, S., Rizzo, V., Sant'Angelo, A., Aiello, E., Reggio, E., Battaglia, F., Messina, C., Girlanda, P. (2004) "Long lasting effects of transcranial direct current stimulation on motor imagery." Neuroreport 15 (8): 1287–1291.

[126] Ramos-Murguialday, A., Broetz, D., Rea, M., Läer, L., Yilmaz, Ö., Brasil, F., Birbaumer, N. (2013). "Brain–machine interface in chronic stroke rehabilitation: A controlled study." Annals of neurology 74 (1): 100–108.

[127] Ramoser, H., Muller-Gerking, J., Pfurtscheller, G. (2000) "Optimal spatial filtering of single trial EEG during imagined hand movement." IEEE Transactions on Rehabilitation Engineering, 8(4), 441–446.

[128] The Intercollegiate Working Party for Stroke, Royal College of Physicians (2008) "National clinical guidelines for stroke." 3rd edn. London: Royal College of Physicians.

[129] Reis, J., Schambra, H.M., Cohen, L.G., Buch, E.R., Fritsch, B., Zarahn, E., Celnik, P.A., Krakauer, J.W. (2009) "Noninvasive cortical stimulation enhances motor skill acquisition over multiple days through an effect on consolidation." Proceedings of the National Academy of Sciences 106 (5): 1590–1595.

[130] Schlaug, G., Renga, V., Nair, D. (2008) "Transcranial direct current stimulation in stroke recovery." Archives of Neurology 65 (12): 1571–1576.

[131] Schwartz, A. B., Cui, X. T., Weber, D. J., Moran, D. W. (2006). "Brain-controlled interfaces: movement restoration with neural prosthetics." Neuron 52 (1): 205–220.

[132] Sharma, N., Pomeroy, V.M., Baron, J.C. (2006) "Motor imagery: A backdoor to the motor system after stroke?" Stroke 77 (7): 1941–1952.

[133] Scherer, R., Mohapp, A., Grieshofer, P., Pfurtscheller, G., Neuper, C. (2007). "Sensorimotor EEG patterns during motor imagery in hemiparetic stroke patients." Int. J. Bioelectromagn. 9: 155–162.

Bibliography

[134] Duncan, P. W., Propst, M., and Nelson, S. G. (1983) "Reliability of the Fugl-Meyer assessment of sensorimotor recovery following cerebrovascular accident." Physical therapy 63 (10) 1606-1610.

[135] Shibasaki, H., Barrett, G., Halliday, E., Halliday, A.M. (1980) "Components of the movement-related cortical potential and their scalp topography." Electroencephalography and Clinical Neurophysiology 49 (3): 213–226.

[136] Shimizu, T., Hosaki, A., Hino, T., Sato, M., Komori, T., Hirai, S., Rossini, P.M. (2002) "Motor cortical disinhibition in the unaffected hemisphere after unilateral cortical stroke." Brain 125 (8): 1896–1907.

[137] Silvoni, S., Ramos-Murguialday, A., Cavinato, M., Volpato, C., Cisotto, G., Turolla, A., Piccione, F., Birbaumer, N. (2011) "Brain-computer interface in stroke: a review of progress." Clinical EEG and Neuroscience 42 (4): 245–252.

[138] Small, Steven L., Giovanni Buccino, and Ana Solodkin. (2013) "Brain repair after stroke—a novel neurological model." Nature Reviews Neurology 9 (12): 698–707.

[139] Sridharan, D., Levitin, D. J., Menon, V. (2008). "A critical role for the right fronto-insular cortex in switching between central-executive and default-mode networks." Proceedings of the National Academy of Sciences 105 (34): 12569–12574.

[140] Sur, M., Rubenstein, J.L.R. (2005) "Patterning and plasticity of the cerebral cortex." Science 310 (5749): 805–810.

[141] Taub, E., Crago, J. E., Burgio, L. D., Groomes, T. E., Cook, E. W., DeLuca, S. C., Miller, N. E. (1994) "An operant approach to rehabilitation medicine: overcoming learned nonuse by shaping." Journal of the experimental analysis of behavior 61 (2): 281–293.

[142] Tibshirani, R., Walther, G. (2005) "Cluster validation by prediction strength." Journal of Computational and Graphical Statistics 14 (3): 511–528.

[143] Tzovara, A., Murray, M. M., Bourdaud, N., Chavarriaga, R., Millán, J.d.R., De Lucia, M. (2012) "The timing of exploratory decision-making revealed by single-trial topographic EEGanalyses." Neuroimage 60 (4): 1959–1969.

[144] Tzovara, A., Murray, M. M., Plomp, G., Herzog, M. H., Michel, C. M., De Lucia, M. (2012) "Decoding stimulus-related information from single-trial EEG responses based on voltage topographies." Pattern Recognition 45 (6): 2109–2122.

[145] Utz, K. S., Dimova, V., Oppenländer, K., Kerkhoff, G. (2010) "Electrified minds: transcranial direct current stimulation (tDCS) and galvanic vestibular stimulation (GVS) as methods of non-invasive brain stimulation in neuropsychology—a review of current data and future implications." Neuropsychologia 48 (10): 2789–2810.

[146] Van de Ville, D., Britz, J., Michel, C. M. (2010) "EEG microstate sequences in healthy humans at rest reveal scale-free dynamics." Proceedings of the National Academy of Sciences 107 (42): 18179–18184.

[147] Varkuti, B., Guan, C., Pan, Y., Phua, K. S., Ang, K. K., Kuah, C. W. K., Sitaram, R. (2013) "Resting state changes in functional connectivity correlate with movement recovery for BCI and robot-assisted upper-extremity training after stroke." Neurorehabilitation and neural repair 27(1): 53–62.

[148] Vidal, J.J. (1973) "Toward direct brain-computer communication." Annual Review in Biophysics and Bioengineering 157–180.

[149] Wagner, J.M., Rhodes, J.A., Patten, C. (2008) "Reproducibility and minimal detectable change of three-dimensional kinematic analysis of reaching tasks in people with hemiparesis after stroke." Physical Therapy 88: 652–63.

[150] Wei, P., He, W., Zhou, Y., Wang, L. (2013) "Performance of motor imagery brain-computer interface based on anodal transcranial direct current stimulation modulation." IEEE Transactions on Neural Systems and Rehabilitation Engineering 21 (3): 404–415.

[151] Wolpaw, J.R., McFarland, D.J., Neat, G.W., Forneris, C.A. (1991) "An EEG-based brain-computer interface for cursorcontrol." Electroencephalography and Clinical Neurophysiology 78 (3): 252–59.

[152] Wolpaw, J.R., Birbaumer, N., McFarland, D.J. Pfurtscheller, G., Vaughan, T.M. (2002) "Brain–computer interfaces for communication and control." Clinical neurophysiology 113 (6): 767–791.

[153] Young, B. M., Nigogosyan, Z., Remsik, A., Walton, L. M., Song, J., Nair, V. A., Prabhakaran, V. (2014) "Changes in functional connectivity correlate with behavioral gains in stroke patients after therapy using a brain-computer interface device." Frontiers in Neuroengineering 7.

[154] Yuan, H., Zotev, V., Phillips, R., Drevets, W. C., Bodurka, J. (2012) "Spatiotemporal dynamics of the brain at rest—exploring EEG microstates as electrophysiological signatures of BOLD resting state networks." Neuroimage 60 (4): 2062–2072.

[155] Zeiler, S. R. and Krakauer, J. W. (2013) "The interaction between training and plasticity in the poststroke brain" Current Opinion in Neurology 26: 609–616.

BCI   Brain–Computer Interface

BCIs   Brain–Computer Interfaces

BMI   Brain–Machine Interface

CAR   Common Average Reference

CVA   Canonical Variate Analysis

EEG   electroencephalographic

ECoG   Electrocorticogram

LDA   Linear Discriminant Analysis

GMM   Gaussian Mixture Model

MI   Motor Imagery

PSD   Power Spectrum Density

tDCS   Transcranial Direct Current Stimulation

TMS   Transcranial Magnetic Stimulation

SMR   Sensorimotor Rhythms

ERD/ERS Event-related Synchronization/Desynchronization

ERD   Event-related Desynchronization

MEP   Motor Evoked Potential

MEPs   Motor Evoked Potentials

FES   Functional Electrical Stimulation

NMES   neuromuscular electrical stimulation

TBI   Traumatic Brain Injury

SCI   Spinal Cord Injury

Andrea Biasiucci

Curriculum Vitae

Rue Du Simplon 26, 1006 Lausanne (Switzerland)
Date of Birth: November 21, 1984
Citizenship: Italian
Marital status: Single, no children

http://people.epfl.ch/andrea.biasiucci
<andrea.biasiucci@epfl.ch>
Mobile: (+41) 76 219 3472
Office: (+41) 21 693 6989

Professional Profile

Highly motivated Biomedical Engineer specialized in Neural Interfaces and Rehabilitation. Strong team spirit, he worked on pioneering translational research on Brain-Machine Interfaces at the École Polytechnique Fédérale de Lausanne (EPFL), in cooperation with Clinical Sites in Switzerland, Italy, Spain, and Germany.

Education

2014 (expected) **Ph.D. in Manufacturing Systems and Robotics**, EPFL (Switzerland)

Selected topics: Brain Computer interfaces, Neuromuscular electrical stimulation, Brain stimulation, Neuroimaging
Thesis title: "*Neurotechnology for Brain Repair: Imaging, Enhancing and Restoring Human Motor Function*"
Supervisor: Prof. José del R. Millán; Co-supervisor: Prof. Micah M. Murray

2010 **M.Sc. in BioEngineering**, University of Genua (Italy)

Selected topics: Machine learning, Neurophysiology, neuroscience, robotics
Included 6 months of Final Project at EPFL (Switzerland)
Thesis title: "*Human in the Loop: Mental State Recognition to Increase Performances of External Systems*"
Final Grade: *110/110* with Honors.

2006 **B.Sc. in Electronic Engineering**, Third University of Rome (Italy)

Selected topics: Analog & digital electronics, signal processing
Included 12 months of **Erasmus Scolarship** at University of Bergen, Norway
Thesis title: "*Digital Watermarking of Stereoscopic Images*".

Work Experience

Scientific and Clinical Investigation

2012-2014   Designed and followed an **early stage multicenter clinical trial on brain controlled electrical stimulation** for stroke rehabilitation involving SUVA Care Rehabilitation Clinic, Sion (Switzerland) and Beau-Séjour Hospital Geneva (Switzerland)

2009-2013   Responsible of the "Motor Recovery" work package for **EU-ICT Project TOBI – Tools for Brain Computer Interaction** at EPFL

2012-2013   Teaching Assistant for the course of "**Data Analysis and Model Classific**ation" at EPFL

111

Innovation and Technology Transfer
- **Co-inventor of 2 patents**
  1. **A. Biasiucci***, A. Maesani* and S. Varricchio, "System For Fabricating Non-Invasive Electrodes Directly On The Skin",2014, *Equal Contributions
  2. **A. Biasiucci***, A. Maesani* and H. Dimassi, "Neuroprosthetic System Restoring Upper Limb Function Through Coordinated Electrical Stimulation", 2013, *Equal Contributions
- 2013 **Venture Challenge**, Swiss Center for Technological Innovation (CTI) Training Program: 6 months course for members of universities with business ideas who aspire to set up a company.
- 2012 **PreSeed Workshop**: intensive workshop that simulates the work of a start-up company by collaborating with a team of experts on selected projects. My application was sponsored by NCCR Chemical Biology
- 2012 **Master of Innovation and Technology Transfer**, Swiss Federal Institute of Technology Lausanne (EPFL): intensive course on invention management and start-up option evaluation.

Skills

Programming: C, C++, Java, Matlab, SPSS;   **Electronics**: PSpice, EAGLE, Atmel ASF;
Statistics, Machine Learning, Signal Processing, Problem Solving, Design of Experiment

Selected Publications

A. Biasiucci et al. "Closed-loop Neuroprosthetic Electrical Stimulation Boosts Motor Recovery After Stroke", i*n prep*

A. Biasiucci et al. "Decoding single-trial topographic EEG signatures of motor preparation, action, and rest reveals subject-independent organization", *in prep*

R.Chavarriaga*, **A. Biasiucci*** et al., "Selective Enhancement of Sensorimotor EEG Features for Brain Computer interaction by means of tDCS", in prep, *Equal Contributions

Chavarriaga R., **A. Biasiucci**, A. Molina, R. Leeb, V. Soto León, M. Campolo, A. Oliviero and J. del R. Millán. "tDCS Modulates Motor Imagery-Related BCI Features." In *Biosystems & Biorobotics* (2013)

A. Biasiucci, R. Leeb, A. Al-Khodairy, V. Buhlmann and J. del R. Millán, "Motor Recovery After Stroke by Means of BCI-Guided Functional Electrical Stimulation." In *Proceedings of the 5th International BCI Meeting* (2013)

R. Leeb, S. Perdikis, L. Tonin, **A. Biasiucci**, M. Tavella, M. Creatura, A. Molina, A. Al-Khodairy, T. Carlson and J. del R. Millán. "Transferring brain–computer interfaces beyond the laboratory: Successful application control for motor-disabled users." In *Artificial intelligence in* (2013)

A. Biasiucci et al. "Combining discriminant and topographic information in BCI: Preliminary results on stroke patients." In *Proceedings of the 5th International IEEE/EMBS Conference on Neural Engineering (NER)* (2011)

A. Biasiucci et al. "EEG Microstates for BCI Therapist Feedback: Preliminary Results on a Stroke Patient." International Journal of Bioelectromagnetism (2011)

Languages

Italian	Native language
Spanish	Native language
English	Proficient user (C2)
French	Independent user (B1)

Interests

Amateur acoustic and bass guitar player
Enthusiastic football fan, discrete snowboarder
Travels, design and innovation
Voracious reader